NUMERICAL MODELLING TO PREDICT THE IMPACT OF MINING ACTIVITIES ON WATER RESOURCES IN THE VICINITY OF KAROWE DIAMOND MINE

Mpho Kejeleng

Submitted in fulfilment of the requirements for the degree.

Magister Scientiae in Geohydrology

in the

Faculty of Natural and Agricultural Sciences

(Institute for Groundwater Studies)

at the

University of the Free State

Supervisor: Professor Francois Fourie

November 2024

DECLARATION

I, Mpho KEJELENG, hereby declare that the dissertation hereby submitted by me to the Institute for Groundwater Studies in the Faculty of Natural and Agricultural Sciences at the University of the Free State, in fulfilment of the degree of Magister Scientiae, is my own independent work. It has not previously been submitted by me to any other institution of higher education. In addition, I declare that all sources cited have been acknowledged by means of a list of references.

I furthermore cede copyright of the dissertation and its contents in favour of the University of the Free State.

Mpho KEJELENG

30 November 2024

ACKNOWLEDGEMENTS

I would hereby like to express my sincere gratitude to all who have motivated and helped me in the completion of this dissertation:

Special thanks to my supervisor Professor Francois Fourie for his invaluable advice, encouragement, academic guidance, and support throughout the period of my research. I would also like to acknowledge, Ms Anneke Rossouw, for the support she gave me during my time as a student at IGS. Thanks to all academic staff at IGS for their technical input and advice during my research period.

TABLE OF CONTENTS

LIST OF FIGURES

LIST OF TABLES

LIST OF UNITS, SYMBOLS AND ABBREVIATIONS

AK6	Kimberlite now called KDM
AMD	acid mine drainage
ASM	artisinal small mining
BCL	Botswana Concession Limited
DRC	Democratic Republic of Congo
EC	electrical conductivity
EIA	environmental impact assessment
EMP	environmental management plan
EPA	Environmental Protection Authority
FTF	fine tailings facility
GL/year	gigaliters per year
HDPE	high density polyethylene
km^2	square kilometer
KDM	Karowe Diamond Mine
KPCSC	Kimberley Process Civil SocietyCoalition
LPE	low pumping elevation
m	meter
MAE	mean absolute error
MAP	mean annual precipitation
MCDF	Maluti Community Development Forum
ME	mean error
mm/year	miilimetre per year
Mm^3/year	mega cubic meter per year
MSE	mean square error
m/d	meter per day
m^2/d	square meter per day
m^3	cubic meter

m^3/d	cubic meter per day
m^3/hr	cubic meter per hour
mbgl	meter below ground level
mg/L	milligram per liter
ppm	parts per million
SCADA	supervisory control and data acquisition
RMSE	root mean squared error
TDS	total dissolved solids
VSD	variable speed drive
WAB	Water Apportionment Board
WF6	Wellfield 6
WHO	World Health Organization
WRSA	waste rock storage area

CHAPTER 1:
INTRODUCTION

1.1 GENERAL INTRODUCTION

The mining industry in Botswana is heavily reliant on groundwater for ore processing and other activities. Groundwater exploration in the Boteti region of Central Botswana started in the 1970s when mining in the area began (JDS, 2019). As more mineral exploration occurred and mining developments increased, the population in the Boteti region expanded and more than 100 boreholes were drilled to meet the water needs (KLMCS, 2010). Substantial hydrogeological data has been collected, improving the understanding of the local and regional hydrogeological regime.

Lucara Botswana operates Karowe Diamond Mine (KDM, formerly known as the AK6 kimberlite pipe) which occurs in the Boteti region. The mine is situated within an agricultural zone where livestock farming averages 173,768 cattle with daily water requirements of 45 L/animal (Statistics Botswana, 2017). The mine was commissioned in July 2012 as an open pit mine (JDS, 2019). The life of mine for the open pit is expected to extend to 2025 upon which underground operations will start. The underground mining has an expected lifespan until 2050.

Open pit mining excavations at KDM have extended below the groundwater table. Groundwater is removed through dewatering boreholes to lower the phreatic surface to allow for a safe mining environment. The large volumes of water extracted are pumped for use in ore processing, while the slimes from the process plant are deposited in a tailings facility. Chemical constituents used in mining are also deposited in the tailings facility.

The main existing and potential impacts from mining are therefore twofold: 1) impacts on groundwater quantity because of depletion of the aquifer system due to mine dewatering, and 2) impacts on groundwater quality from the open pit, waste rock dump, plant, and tailings facility.

Groundwater is the main source of water supply for industrial, mining, agriculture, and household use in the Boteti region. While mining operations abstract water from deeper saline aquifer system, private farmers tap the shallow fresh basalt waters. The sustainable use and management of the scarce water resource is critical for the livelihoods of people in Boteti. Research into the possible impacts of mining on the water resources is needed for the following reasons:

- Groundwater in the Boteti region is a shared and scarce resource needed for mining, agriculture, and domestic use. It is the only naturally available water source in the region and its understanding and management is vital for economic development of the region.

- Diamond mining in Botswana was started in the late 1970s and its economic importance to the country is well documented. However, the impact of mining activities on the environment have not been studied in detail (Geoflux, 2007).
- Previous studies at KDM (prior to 2010) were done when there were limited data, before mining excavations extended below the water table. Large quantities of data on the behaviour of the aquifer system at the mine have since been collected. The current research will assist in gaining a better understanding of the impacts that mining activities could have on the water resources.

This study aims to investigate the impacts that open pit mining will have on the water resources in the vicinity of KDM. The research project will assess current and possible future changes in the aquifer system. Based on the results of the research, mitigation measures will be proposed.

1.2 AIMS AND OBJECTIVES

The main aims of the research are to predict the impacts of mining activities on the water resources in the vicinity of KDM and to propose mitigatory actions. To reach these aims, the following objectives are identified:

- To investigate the current groundwater levels at and around the mine to allow evaluation of the impact of dewatering on the aquifer system,
- To obtain baseline information on the surface and groundwater quality against which the presence and severity of contaminant impacts can be assessed,
- To establish a database for abstraction rates from the dewatering boreholes and measured water levels around the open pit,
- To develop a conceptual hydrogeological model of the aquifer system in the vicinity of the mine,
- To develop a three-dimensional (3D) numerical model of the aquifer system based on the conceptual model,
- To use the numerical model to investigate the potential impacts of mining activities on the aquifer system in terms of groundwater quantity,
- To assess the vulnerability of groundwater resources in the vicinity of KDM to depletion due to mine dewatering,
- To identify gaps in the current groundwater monitoring programme, and,

- To propose mitigatory actions to prevent or reduce detrimental impacts on the aquifer system.

1.3 RESEARCH METHODOLOGY

To achieve the aims and objectives of the study, the following research methodology will be followed:

1.3.1 Data collection

During the data collection phase, the following actions will be taken:

- A literature review will be conducted with emphasis on studies whose contents are relevant to current project.
- A hydrocensus survey will be conducted to map all private wells within a 10 km radius of KDM. The following data will be recorded where available:
  - Borehole ID,
  - Owner,
  - Date drilled,
  - Depth,
  - Depths of water strikes,
  - Volumes currently abstracted and planned future abstraction rates,
  - Groundwater level,
  - Current and planned future use, and,
  - Geology intersected.
- A comprehensive database of the information collected during the hydrocensus survey will be developed.
- The Botswana Geological Institute and the Department of Water Affairs will be visited to collect hydrogeological, geophysics and geological data pertaining to the study area.
- All available reports on geological, geophysical and hydrogeological investigations will be reviewed to extract information relevant to the current study.
- Groundwater sampling will be done from boreholes at the mine as well as from private boreholes on properties surrounding the mine. During sampling, water levels will also be recorded,
- Groundwater samples will be submitted to a recognised laboratory for chemical analyses.

1.3.2 Data analysis

Data analysis will comprise the following actions:

- Groundwater level data will be analysed to determine the impact that mine dewatering has had on the groundwater table,
- Water level and pumping rate data will be evaluated to estimate the hydraulic parameters of the aquifer system,
- The data on groundwater chemistry will be used to assess the current groundwater quality and to identify possible contaminant sources, and,
- The results of previous geophysics surveys will be analysed to map possible contaminant plumes around the different mining activities.

1.3.3 Numerical modelling

For the development and utilisation of a numerical model, the following activities are foreseen:

- A conceptual hydrogeological model will be developed based on knowledge of the geological and hydrogeological conditions at the mine.
- A numerical groundwater model will be constructed based on the conceptual model. This model will be calibrated using the available information in groundwater levels and qualities.
- The numerical model will be used to run different scenarios to predict the impacts of mining on the groundwater system, in terms of both quantity and quality,
- The numerical model will be used to estimate the cone of depression every five years until end of life of the underground mine,
- The possible migration of contaminant plumes from the different mining activities will be investigated through transport modelling,
- The results of the flow and transport modelling will be used to predict the potential future impacts of mining activities on groundwater users in the vicinity of the mine, and,
- Based on the results of the study, recommendations will be made to prevent or mitigate against the impacts of mining.

1.4 LIMITATIONS OF THE RESEARCH PROJECT

Several limitations exist which may affect the results of the current study, including:

- Private boreholes may not have all the records and data needed for the research. Farmers do not typically conduct water level monitoring and often do not keep records of abstraction rates.
- There may not be an adequate distribution of private boreholes around the mine. Farms seem to be concentrated to the north, north-west and north-east of the mine with only a few boreholes to the west and south of the mine. This lack of a good distribution and density of boreholes will limit the data available for modelling purposes.
- Pre-mining water quality and water level data may not be available for establishing baseline conditions.
- Numerical modelling predictions are inherently associated with uncertainties because models are constrained by the quality and quantity of the available data. The capacity of numerical models to represent real world complexity is therefore limited.
- No mass transport modelling will be done in the current study to investigate the potential impacts of contaminants from mining infrastructure and activities on the groundwater quality. Only the impact of mine dewatering on the groundwater quantity during the time of active dewatering will be investigated by means of a flow model. The hydraulic gradient created by mine dewatering will cause flow to be towards the mine, thereby reducing the potential impacts of mining-related contaminants on the groundwater resources. However, in the post-closure phase of the mine, the natural groundwater gradient will be reestablished, and any remaining contaminants could then potentially be transported away from the mine, affecting the groundwater quality at positions down-gradient from the mine.

1.5 STRUCTURE OF DISSERTATION

The dissertation will be structured as follows:

Chapter 1 will introduce the research subject by providing a brief background and justification for the project. The aims and objectives of the project will be stated, as well as the research methodology to be followed to achieve these aims and objectives.

Chapter 2 will cover all literature review and present relevant research studies that were done in the past. The chapter will discuss content on previous studies related to impact mining activities have on groundwater resources.

Chapter 3 will describe the study area in terms of its regional setting, geological setting, topography and drainage, climatic conditions, and land use. The mining history, infrastructure, and current and future mining activities of KDM will also be discussed.

Chapter 4 will focus on hydrogeological investigations that have been performed at KDM. Aspects such as the aquifers present at the mine, borehole yields, the hydraulic properties of the aquifers, the borehole networks at the mine, the results of baseline and ongoing groundwater monitoring will be discussed.

In **Chapter 5**, a conceptual hydrogeological model will be developed for the aquifer system at the mine and surrounding areas by incorporating existing geological and hydrogeological data. Groundwater occurrence and movement, the different hydrogeological units and their hydraulic parameters will be described in this chapter.

Chapter 6 will discuss the development of the numerical groundwater flow model, and calibration processes for both steady state and transient conditions. The chapter will also present the results of simulations performed to establish the expansion of cone of the depression between 2009 – 2025.

In **Chapter 7**, conclusions will be drawn from the results of the research project and recommendations will be presented here.

CHAPTER 2:
LITERATURE REVIEW

2.1 INTRODUCTION

It is beneficial for scientists to refer to the lessons learned from history for continuous improvements in the water resources investigations of today. Hydrogeological work already started in biblical times when ancient people in Asia dug wells for agricultural and domestic use (Robins, 2013).

Literature review is an opportunity for evaluating previous research works relevant to the current study. It provides researchers with current information on the topic, offers insight into research methods that may be applied, and identifies existing data gaps and possible future research topics.

This chapter evaluates some of the most relevant recent literature, both international and regional, on the impacts of mining activities with emphasis on groundwater abstraction and water quality.

2.2 IMPACTS OF DIAMOND MINING ON WATER RESOURCES

There are five major diamond producers in the world, namely: Russia, Botswana, Canada, Angola and South Africa (Figure 2.1) (Oluleye, 2021). Diamonds are also mined in other countries such as Namibia, Lesotho, Zimbabwe, Liberia, Australia, and the Democratic Republic of Congo. Groundwater research studies have been carried in these countries, some with the objective of understanding the impacts of mining on the natural environment.

The impact of mining on groundwater resources includes the following (Karmakar and Das, 2012):

- Lowering of the phreatic surface,
- Groundwater contamination,
- Ground subsidence, and,
- Reduction of moisture content in the soil.

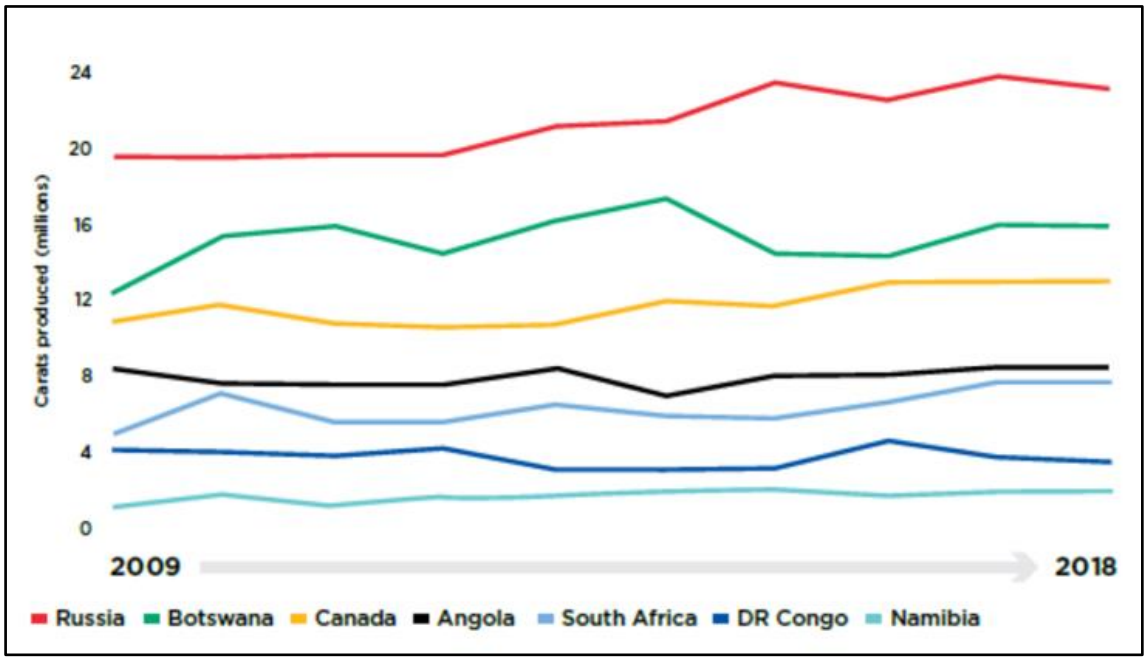

Figure 2.1: Major diamond producers in the World (Oluleye, 2021)

2.2.1 International case studies

2.2.1.1 Introduction

Although diamond mining is crucial to the world economy, excavation of minerals cause irreversible damage to the natural environment, such as soil erosion, deforestation, pollution, and depletion of water resources (Oluleye, 2021). Governments and non-governmental organisations are concerned about the impacts of mining on the environment. The solution to this problem requires consultation of all stakeholders, government, private and community of interest (Yakovleva *et al*., 2000).

Diamond mining is a water-intensive operation that requires diamonds to be liberated from the host rock. Trucost (2019) compared the environmental impacts of diamond mining to the impacts associated with the mining of other commodities. The results of this investigation are presented in Figure 2.2. The environmental impact of diamond mining per million dollars of revenue are 52% less than the costs of mining lead and 89% less than the costs of mining cerium (Trucost, 2019). Although every mining activity is harmful to the environment irrespective of the mineral being excavated, diamond mining is less harmful to the environment compared to the other mineral operations investigated (Trucost, 2019).

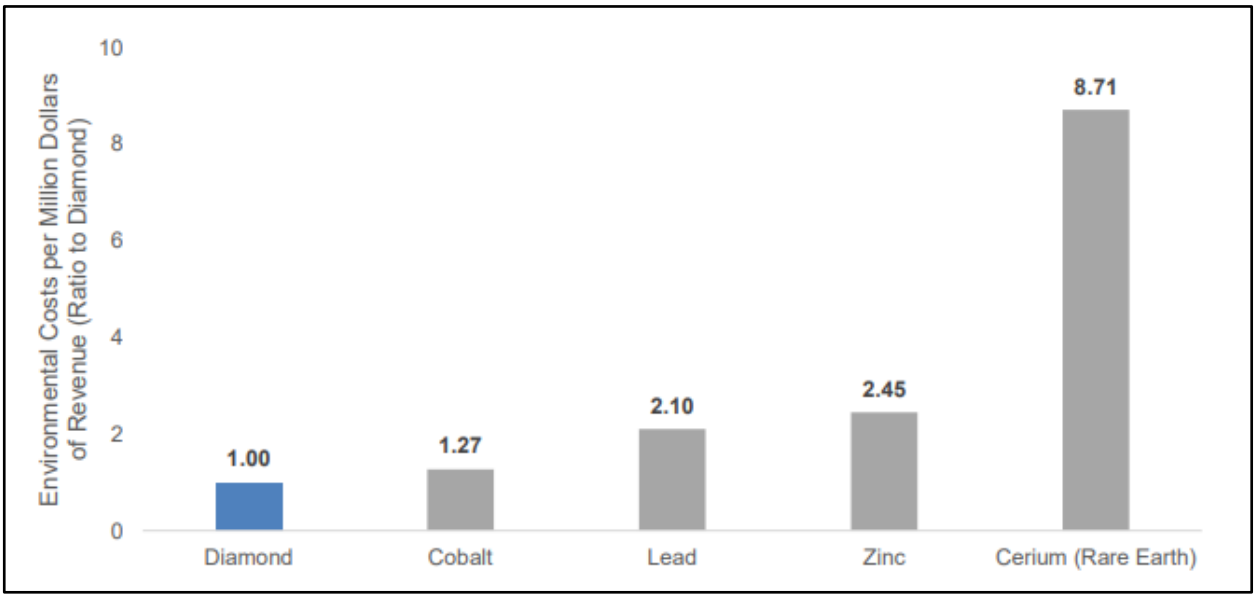

Figure 2.2: Environmental performance of various commodities (adapted from Trucost, 2019).

2.2.1.2 Ekati Diamond Mine

Ekati Diamond Mine is in the north-west of Canada. The mine is located within several watersheds (Figure 2.3). One third of the Ekati Mining licence area is covered with water and that makes groundwater monitoring a key aspect of the operation (Dominion Diamonds, 2019). Ekati Diamond Mine operates Panda, Koala, Koala North, Fox and Beartooth pits and two underground excavations. The licence regulates water use and the quality of water that can be released back into the environment. Mine water from operation is disposed of in several ways depending on water quality and approval from the Inspector (Dominion Diamonds, 2019).

The environmental impacts of mining diamonds vary from one country to the other such that in the Ekati Diamond Mine in Canada, the major concern is loss of land-based habitat for wildlife (Oleluye, 2021). Other communities are concerned about the creation of dust, and generation of gases which destroy the ozone layer. This section will, however, focus on the impacts of diamond mining on groundwater resources in terms of availability and pollution.

Waste rock and kimberlite material from the mining process is deposited in waste rock storage areas (WRSA) and 90% of waste rock at Ekati Mine is granite. Dominion Diamonds has been monitoring the potential for pollution from the waste rock since 2018. The 2019 monitoring programme indicated that the granite has a low potential for acid generation. However, the metasediments found in other operations at the Misery and Pigeon WRSAs, have potential for acid generation (Dominion Diamonds, 2019). Additionally, explosives used for blasting kimberlites pipes introduce nitrogen, ammonia and nitrate into waste rock (IEMA, 2005).

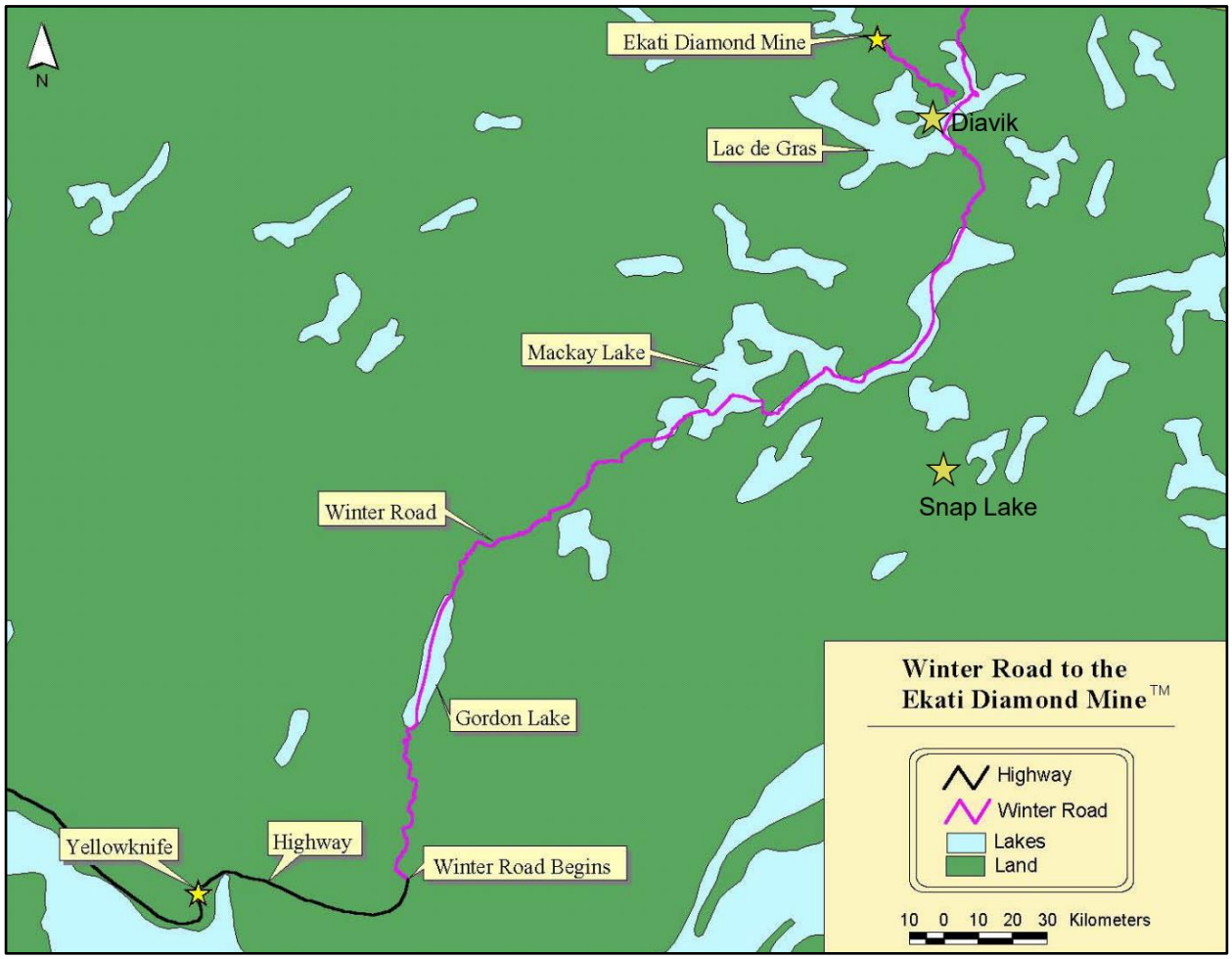

Figure 2.3: Location of Ekati Mine (Dominion Diamonds, 2019).

The 2019 water monitoring programme evaluated 21 water quality variables (Dominion Diamonds, 2019). The monitoring program focused on areas likely to be affected by effluent from the mines. Two major watersheds were monitored for potential effects by mine effluent, and these are King-Cujo Watershed or Lac du Sauvage. The results indicate that concentrations for 17 parameters were above baseline values due to mine effluent (Figure 2.4) (Dominion Diamonds, 2019).

Environmental impacts caused by mining vary depending on location and, as such, each operation should conduct environmental impact assessments (EIAs) that will advise on the best way of protecting the environment. The EIA conducted at Koala pit recommended separation of diamonds from ore using physical means instead of using chemicals (Couch, 2002). The potential for polluting the water resources was thus reduced. Monitoring programmes were put in place to assist with monitoring of water resources and other high-risk areas.

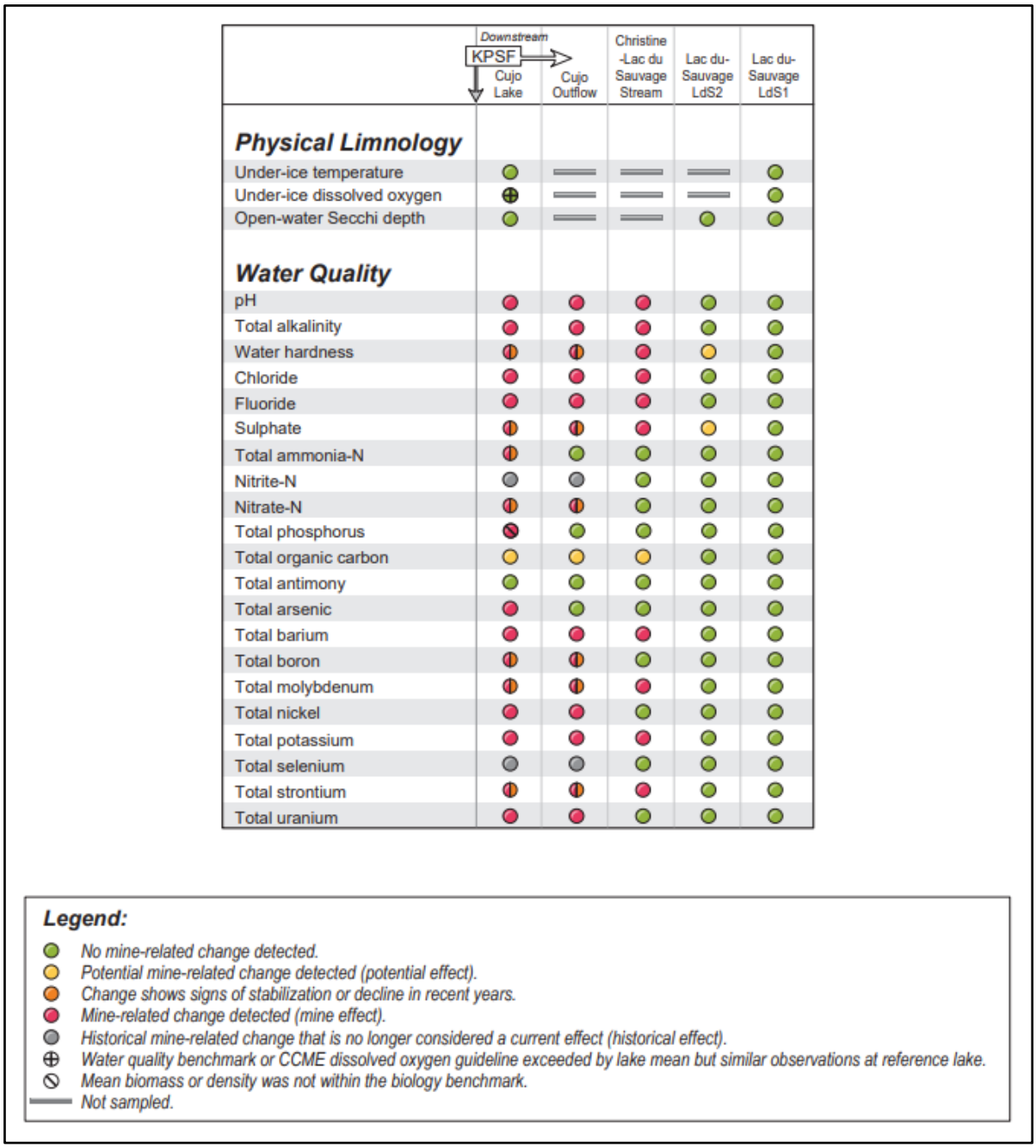

Figure 2.4: Water changes in the King-Cujo Watershed and Lac du Sauvage (Dominion Diamonds, 2019)

2.2.1.3 Diavik Diamond Mine

Diavik Diamond Mine is an open pit operation in the Northwest Territories of Canada. The water supply of the mine is from the *Lac de Gras* Lake and an approximate volume of 1.05 GL/year was withdrawn from the lake in 2021 (Rio Tinto, 2023). The Diavik site has a water licence that allows withdrawal of up to 1.28 GL/year and the average catchment rainfall runoff of 197 GL/year. Annual runoff replenishes what the site removes from the system. This means that the Diavik Diamond Mine is compliant with its water licence and withdraws 0.5 GL/year less than the allocated amount. Table

2.1 and Figure 2.5 summarise the volumes of water pumped monthly from the Diavik Open Pit during 2021.

Table 2.1: Monthly dewatering volumes at Diavik Diamond Mine (2021).

Month	Volume pumped (m^3)
January	270 285
February	276 748
March	312 520
April	278 147
May	322 472
June	631 619
July	317 977
August	234 927
September	208 229
October	320 559
November	452 094
December	314 882

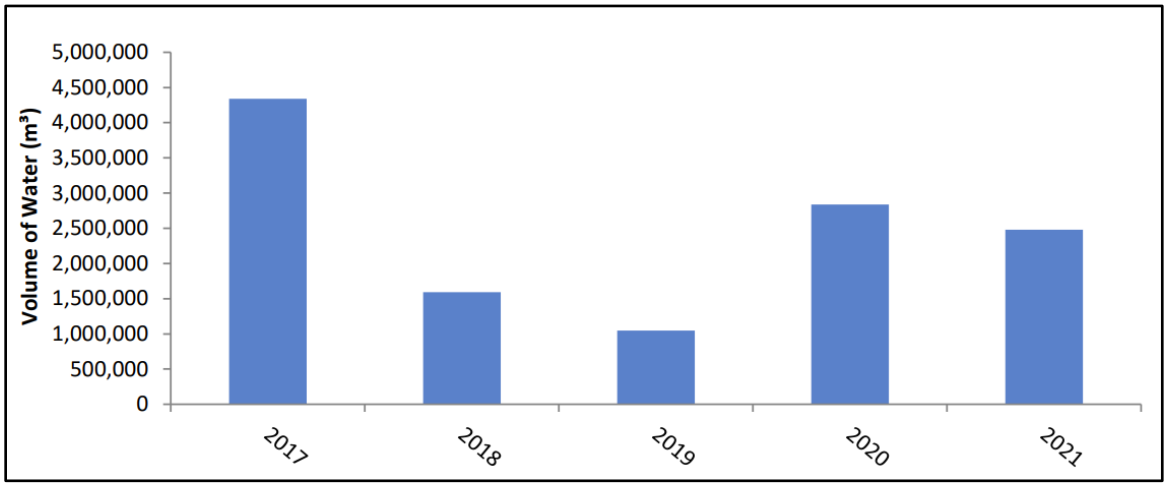

Figure 2.5: Annual dewatering volumes at Diavik Diamond Mine (2017 – 2021).

Before Diavik Diamond Mine releases water into the environment, the quality is determined to confirm compliance to the water licence. If the water quality does not conform to the licence, it is not released into the environment.

Baseline water chemistry conditions at the Diavik sites were defined for a pH, TDS, hardness, alkalinity, total aluminium, iron, and strontium. Other parameters such as chloride and total metals were undefined (Rio Tinto, 2023). Examination of spatial differences in post baseline water chemistry indicated an increasing trend in conductivity, total hardness, chloride, and sulphate (Deton' Cho Stantec, 2015). Measurements and water chemistry analyses from selected monitoring points indicate that there has been a cumulative effect of mine discharge on the lake resulting in oligotrophic conditions in the lake.

2.2.1.4 Argyle Diamond Mine

The Argyle Mine is in the regions of Miriuwung, Gija, Malgnin and Wularr in Western Australia. It used to be one of the largest diamond mines in the world, responsible for approximately 40% of total global production (Borden *et al*., 2022). The operation is within the Ord River Catchment and upstream from Lake Argyle (EPA, 2005).

Diamond-bearing rocks such as lamproite and kimberlite generally pose a much lower environmental risk than base metals and precious minerals (Borden *et al*., 2022). The depth to groundwater at Argyle Mine averages 15 m from surface. Dewatering activities at the mine is expected to abstract 4 ML/day and 10 ML/day for open pit and underground operations, respectively (EPA, 2005). Groundwater model predictions showed declining heads caused by dewatering activities. The model also predicted drawdowns to extend over distances between 4 km and 7 km from the centre of the pit. The nearby Devil Spring no longer flows, and dewatering has been pointed out as the main cause (EPA, 2005).

Acid mine drainage (AMD) was identified as a potential environmental impact for the project. During the wet season, runoff and seepage containing sulphides enter the environment and ultimately reach the local water table altering the chemical composition of groundwater resources. To mitigate against AMD, Argyle Mine endeavours to control the flow of oxygen and water passing through the waste rock dump. Rocks with potential for forming AMD are to be isolated and isolated from rainfall and erosion (EPA, 2005).

After 15 years of open pit production, localised acidification and high sulphate concentrations were detected at some monitoring points. Increasing concentrations of nickel, magnesium, nitrate, and sulphate were observed over the 20-year groundwater monitoring program. However, nitrate concentrations have declined after open pit blasting was stopped in 2013 (Borden *et al*., 2022).

In the Lake Argyle catchment area in Australia, diamond mining was thought to have altered the quality of water as sediments were released into streams (DAA, 2017). To understand the impacts of diamond mining on the water quality, researchers in Australia compared fish diets between different streams using stable isotope mixing models. However, the results of the model were not conclusive and could not be used to attribute changes in water quality to mining. Further research was recommended because the changes in water quality could have been caused by other biological and environmental activities.

2.2.1.5 Yakutia in Russia

Yakutia in eastern Siberia is the largest territorial unit in the Russian Federation. Yakutia is also the largest producer of diamonds in Russia. Between 1974 and 1987, underground nuclear explosions

were caused. One of these explosions was done to support diamond mining in the area. However, due to the nuclear explosion, radionuclides were released into the environment, thus polluting the surface.

River systems are the main sources of potable water for the diamond province. In the early years of diamond exploration, water resources were contaminated because of drainage from waste dumps and dispersion of water from kimberlite pipes (Yakovleva *et al*., 2000). High concentrations of heavy metals were disposed in rivers, affecting the water quality. Slack implementation of environmental laws led to river systems being contaminated (Yakovleva *et al.*, 2000).

When diamond mining started booming in northern Russia, it attracted other industries such as the hydro-electric power industry. A hydroelectric power station was built along the river supplying villages with water. The Vilyuy River flooded in 1969 which caused pollution of the river system, changing the hydrological and hydro-chemical status of the flooded area (Yakovleva *et al.*, 2000).

In 1990, a movement was formed that advocated for improvement and reduction of mining impacts on the environment. An all-inclusive stakeholder engagement was adopted to fight impacts of mining activities on water resources and other social ills. The public was to be involved in environmental awareness campaigns and government was to draft environmental laws in support of environmental protection (Yakovleva *et al.*, 2000).

2.2.1.6 Diamond Mining in China

China started exploring for diamonds in the 1960s and has developed and operated diamond mines in six districts (Keller and Guo-dong., 1986). Four of the districts, Yuan River, Changde County, Yingcheng, Linshu and Tancheng were alluvial deposits (Keller and Guo-dong., 1986). Changma and Binhai were mined as kimberlite intrusions (Keller and Guo-dong., 1986).

Once the ore reaches the plant, it is crushed and relayed through various sections of the plant via a conveyor belt into a series of trommels, and screens of various sizes (Keller and Guo-dong., 1986). The ore is washed using water and the concentrate is passed through a grease belt where diamonds are trapped by the grease on the belt. The grease belt is boiled in water to separate the diamonds from grease. During the process of diamond liberation, hydrocarbons are introduced in water and if disposed into the environment may contribute to water quality degradation.

Dingjigang Mine is located 25.4 km NE of Changde in Dingcheng District, China (Mindat, 2024). It operated between 1960 and 1980 and was closed as the operation posed danger to agricultural land (Diamant-Gems, undated). China’s large scale mining industry has contributed to water pollution (Olson, 2023).

The government of China responded to the impact caused by mining activities on the environment by promoting sustainable mining practices. Once the Chinese diamond industry closed, the focus shifted to lab grown diamonds which is environmentally friendly (Rentmeesters, 2021).

2.2.1.7 Submarine Tailings/Rock Waste Disposal

Mining is a fundamental industry for development of all economies around the world as it produces the much-needed raw materials for our daily needs. It is also a fact that mining will continue to impact the environment as high grade ores diminish and low grades are mined out. As more low-grade ore is mined, the volume of waste generated from mining will increase as will the associated environmental impacts (Dold, 2014). Waste rock from diamond mining usually contains minerals such as silica, magnesia, and iron oxide. Deposition of waste and mine tailings on land has several environmental concerns. Sulphide minerals have been reported in the country rock associated with diamond mining. The sulphide minerals are the main drivers for the formation of AMD (Dold, 2014). In the past, some countries used to deposit mine tailings in natural depression, lakes, shorelines, and rivers and this negatively affected the water resources in these countries. The coastal areas that were affected by deposition of tailings are shown in Figure 2.6.

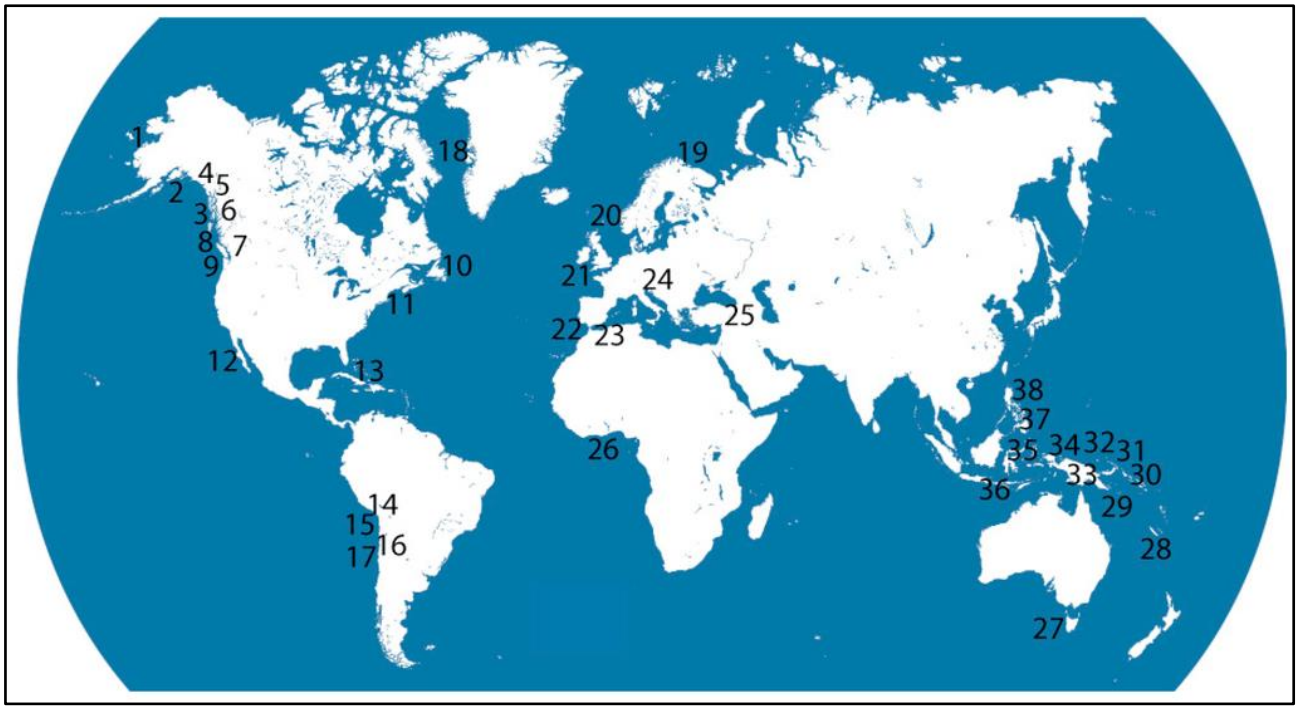

Figure 2.6: Locations of coastal areas impacted by tailings deposition (Dold, 2014 after Koski, 2012).

Chañaral in Chile and Ite Bay in Perú used to deposit tailings along the shoreline until the practice was stopped for environmental reasons. Freeport-Grasberg in Indonesia still deposits tailings in the rivers and shoreline (Dold, 2014).

Therefore, some countries with access to the sea, have resorted to depositing waste and tailings into the deep ocean. This is seen as a more secure and environmentally friendly option as sulphide minerals are geochemically stable under the reducing conditions associated with the deep-sea environment. However, tailings deposited close to water bodies end up reaching the shoreline of the sea. Chemical alteration resulting from sulphide oxidation and AMD end up damaging water sources (Dold, 2014).

2.2.2 Regional case studies

Africa produces 65% of the global diamond output (GGF, 2017). Diamond mining in Africa is known to be associated with severe environmental impacts, mainly because of the lack of policies governing the conservation of natural resources.

2.2.2.1 Marange Diamond Fields

Zimbabwe is one of the diamond producers on the African continent. The Marange Diamond Fields in Chiadzwa, Zimbabwe, is a small-scale diamond operation. There are four diamond companies operating in the area (Mac, 2012). The Save River passes through the Marange Diamond fields and the river has become muddy because of diamond mining operations (Maguwu, 2019). People and livestock have experienced complications and even death after drinking water from their boreholes or river (Chenjerai, 2017). This happened after diamond operations started in Marange, a sign that water quality has changed because of pollution. Since the start of mining in Marange area, people have also found it difficult to get access to water (GGF, 2017).

A study was conducted by the Zimbabwe Environmental Law Association in 2012. Ten sites were sampled, and the results indicated siltation, and chemical and heavy metal pollution of water resources (Mac, 2012). High concentrations of iron, chromium and nickel were detected in water; these elements come from ferrosilicon – a compound used in kimberlite processing (ZELA, 2012). The results of the hydrochemical analyses performed on the water samples from the 10 sites are presented in Table 2.2. All elements evaluated showed elevated concentrations compared to samples further from mining sites. Many of the 10 sites exhibited iron, chromium and nickel concentrations exceeding the WHO drinking water standards. Chromium and nickel are known carcinogens and their presence in drinking water is a major concern.

Table 2.2: Heavy metal concentrations in water samples from the Maranga Diamond Fields.

Parameter	Site										WHO standard
	1	2	3	4	5	6	7	8	9	10	
Iron	18.8	37.45	11.25	34.1	0.16	0.007	0.05	77.85	44.65	not detected	0.3
Chromium	0.07	0.04	0.04	0.05	0.001	<0.001	0.01	0.08	0.05	<0.001	0.05
Nickel	0.01	0.03	0.03	0.01	<0.001	<0.001	<0.001	0.04	<0.001	<0.001	0.07

Values in ppm

High levels of bacteria, of faecal origin, were detected in drinking water (Table 2.3). The total coliform counts were greater than 1100 at all sites and faecal coliform and salmonella were present at all sites. The measurements were all above the WHO drinking water standards, a sign of poor water quality.

The assessment of the quality of water samples from the Odzi and Save Rivers, the National Science Foundation Water Quality Index (WQI) was used (ZELA, 2012 after Ott,1978). The values of the WQI are based on physical, chemical, and biological factors that are combined into a single value ranging from 0 – 100 (Chidiac *et al*., 2023). The parameters used for assessing water quality were dissolved oxygen, faecal coliforms, pH, biological oxygen demand (BOD), total phosphorus, nitrates and total solids (ZELA, 2012). The different classes of the WQI are described as follows (ZELA, 2012):

- 90 – 100: Excellent
- 70 – 90: Good
- 50 – 70: Medium
- 25 – 50: Poor
- 0 – 25: Very Poor

According to the WQI standard, Sites 1, 2, 3, 4, 8 and 9 contained water of poor quality and these sites were probably affected by discharges from the mining operations (ZELA, 2012). Sites 5, 6, 7 and 10 were of medium quality and required immediate attention to reverse the problem of water quality deterioration.

Table 2.3: Water Quality Index values for the sampled sites.

Parameter	Sites									
	1	**2**	**3**	**4**	**5**	**6**	**7**	**8**	**9**	**10**
Dissolved oxygen	79	89	99	46	85	98	94	41	46	76
Faecal coliform	22	22	22	22	22	22	22	22	22	22
pH	57	37	62	61	91	92	65	45	52	91
Biological oxygen	50	50	64	62	66	64	51	51	53	58
Total phosphorus	20	21	30	46	90	97	96	69	87	57
Nitrates	96	97	97	97	97	96	97	96	96	97
Turbidity	29	5	5	5	89	94	71	5	5	71
Total solids	44	67	20	20	82	80	81	20	20	86
WQI	45.7	45.1	48.7	41.0	66.8	69.8	62.9	39.4	43.0	59.9

Parameter values in mg/L

Water quality changes were attributed to poor mining practices in the Marange region. Mining operations have not developed a proper plan or mitigation measures for the impacts caused by mining activities on water resources (GGF, 2017). However, local environmental groups have developed a groundwater monitoring programme for collecting data to provide evidence for impacts caused by diamond mining. The scientific research by the Zimbabwe Environmental Law Association recommended that infrastructure should be put in place to rehabilitate all polluted water sources (ZELA, 2012).

2.2.2.2 Diamond Mining in the Democratic Republic of Congo

In the DRC, artisanal and small-scale mining (ASM) is prevalent, and miners dig the ground using their hands due to the lack of machinery (O'Connell, 2022). Alluvial diamond mining in the DRC occurs along riverbeds and floodplains. Mining in these areas requires removal of large volumes of earth material. Sand aquifers are removed, and rivers are destroyed, resulting in pollution and exploitation of water resources (Galli *et al*., 2020).

Between 2004 and 2018, the diamond mining industry in DRC has used average annual volumes of water of approximately 0.311 km^3 (Figure 2.7). The water use is directly proportional to the production of diamonds, as measured in (million) carats (Mcts), but is negligible compared to the annual renewable water resources of the equatorial DRC which averages approximately 900 km^3 (Galli *et al*., 2020).

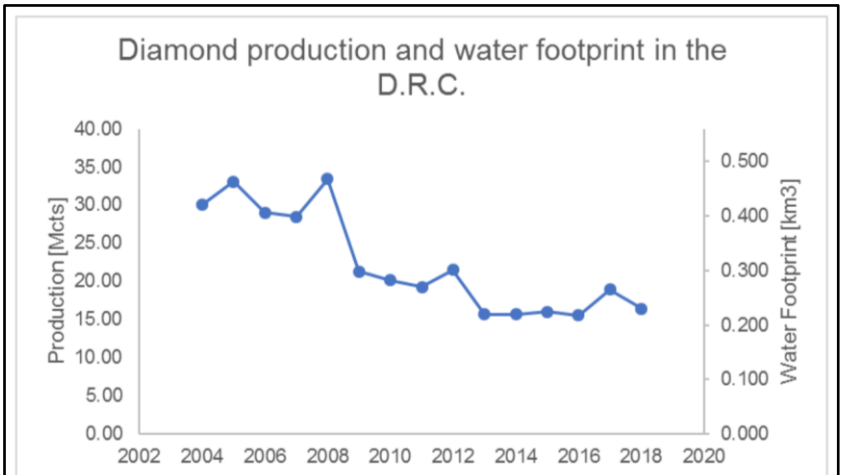

Average over the period	0.311 km³
Yearly total internal renewable water resources (IRWR)	900 km³

Figure 2.7: Diamond production and water footprint in the DRC (Galli *et al.*, 2020).

Maydan (2015) warned of acute water shortage and pollution of water resources because of unethical mining practices in the DRC. This action will leave 51 million people without potable water. It has been difficult to quantify the impacts of diamond mining in the DRC because of political instability in the country (UNEP, 2017). There is also a lack of data on water level changes since mining started in DRC. The United Nations is doing some assessments that will help the DRC adopt a more sustainable approach to environmental issues.

2.2.2.3 Diamond Mining in Cameroon

Diamond mining in Cameroon is mainly artisanal and with no machinery for excavation (RELUFA, 2022). RELUFA (2020) conducted a mapping exercise to determine the location of artisanal diamond sites in Cameroon. The other aim of the exercise was to quantify the impact of mining on the environment. The exercise noted the high number of illegal mining sites and lack of environmental monitoring. The Kimberley Process Civil Society Coalition (KPCSC) advised that government policies should be revised to ensure operations commit to responsible mining practices. It was recommended that each mining site should have a detailed and approved water resources monitoring programme.

2.2.2.4 Tswapong Diamond Mine

Tswapong Diamond Mine is in Central District of Botswana and was first operated by De Beers between 1997 and 2000 (WCS, 2001). The major environmental issue was the use of water resources.

DiamondEx reopened the mine in 2006 and drilled groundwater production boreholes targeting the quartzite units of the Palapye Group, the scree aquifers at the foot of Tswapong Hills and the basement complex. The targeted units also supplied neighbouring villages with water and, as such, was not deemed a sustainable source of water.

The tailings and slimes dam were not to be lined because the FeSi and flocculants used in the diamond recovery process were considered environmentally inert and not toxic (WCS, 2001). An integrated groundwater monitoring programme was developed to collect data on water quality, drawdowns, and abstraction and build a database. Unfortunately, the operation was shut down within a year of operation when market prices slumped during the economic recession.

2.2.2.5 Diamond Mining in Lesotho

The Maluti Community Development Forum (MCDF) in Lesotho investigated the impacts of diamond mining in 19 villages. The results of a survey on negative impacts due to diamond mining at Letseng Mine are shown in Figure 2.8.

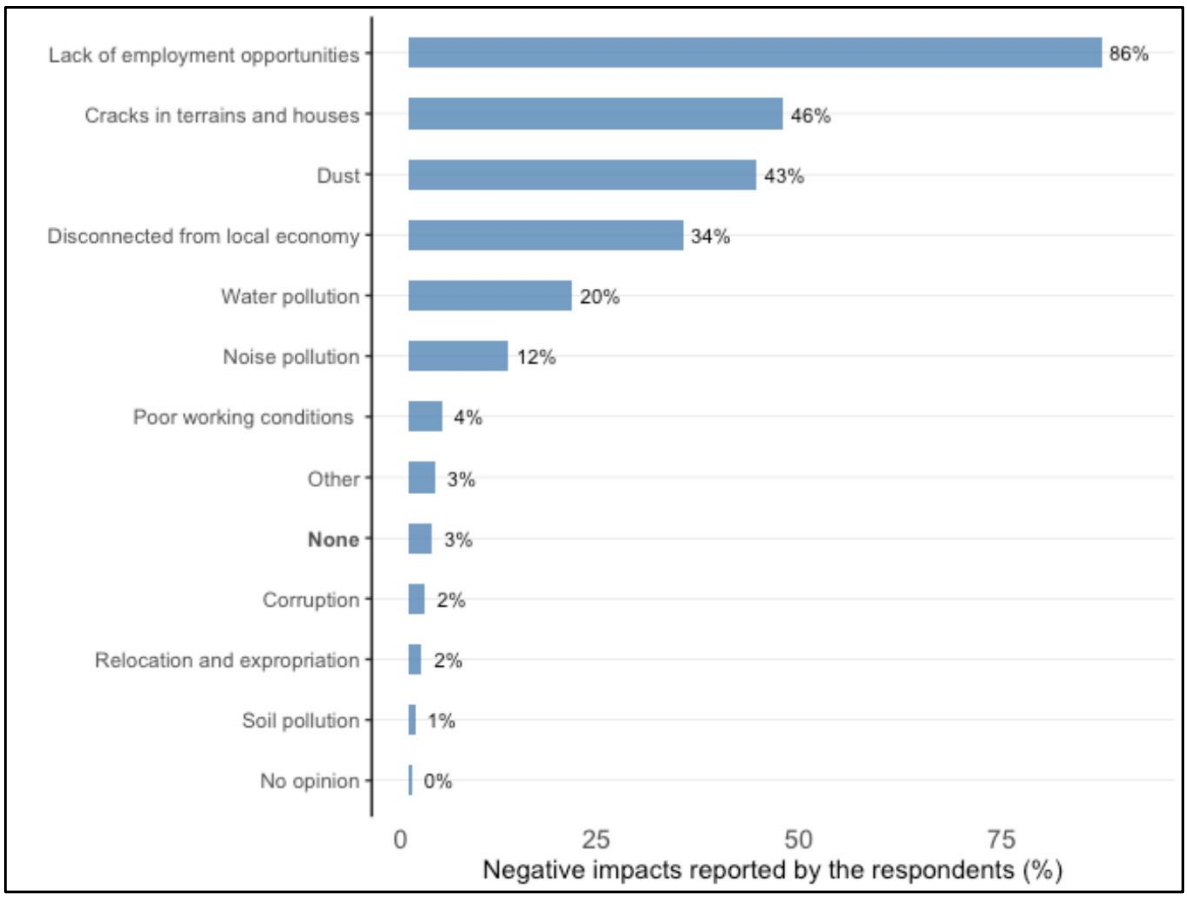

Figure 2.8: Reported negative impacts of diamond mining at Letseng Mine (MCDF, 2021).

The investigation reported poor water quality, and high levels of nitrate were recorded from samples taken near the Letseng Mine (MCDF, 2021). As many as 40% of people complained about

discoloration of their water, and the tailings facility was identified as the source of pollution. Wetlands were also reportedly destroyed by mining activities. Two deaths in the Maloraneng and Patising areas were attributed to water pollution (MCDF, 2021).

In 2019, eight locations were sampled for water quality analysis. High concentrations of nitrates were reported in samples taken near the tailing facility at Letseng and Maloraneng villages (MCDF,2021). The MCDF recommended an all-inclusive and collaborative action plan to be drawn where all stakeholders will be consulted to enable proper regulations to be put in place.

2.2.2.6 Diamond Mining in Central African Republic

CCRAG (2021) conducted a study in the Central African Republic (CAR) with the aim of understanding the impacts of artisanal diamond mining on the environment. The study visited 42 sites, and the main environmental issue was found to be water pollution coming from waste rocks and washed into water sources. Waste rock and other chemicals from the mine are discharged into watercourses, polluting the water resources. CCRAG advised the CAR government and artisanal miners to avoid dumping waste rock and other chemical in the rivers to reduce pollution of the water sources. There was no environmental monitoring at any of the sites visited and as such the impact of mining on water resources could not be quantified.

2.2.2.7 Diamond Mining in the Republic of Guinea

Thirty-eight mining sites were assessed to study the impact of artisanal diamond mining on the environment in the Republic of Guinea. Water resources were identified to be at risk of pollution from waste rock dumped in the river (Amines and Cecide, 2021). The miners in Guinea do not conduct water resources monitoring and this made it difficult to determine the impact of mining on the water resources.

2.2.2.8 Diamond Mining in Sierra Leone

Artisanal diamond mining in Sierra Leone has always been conducted by illegal miners (Figure 2.9). The challenges of illegal mining range from tax dodging, unsafe mine working conditions and environmental degradation. These challenges led to a study conducted by NMJD (2021). The study by NMJD visited 25 artisanal diamond sites in the Kono and Kenema districts.

Water is crucial in diamond mining for washing of gravel and diamonds. Fifteen of the investigated mining operations were located along water sources. Villagers in neighbouring settlements indicated that the water had turned muddy and brown because of miners washing gravels in the water (NMJD, 2021). There were no records of water resources monitoring, primarily because the artisanal sector was informal and without regulation.

Figure 2.9: Unregulated artisanal mining in Sierra Leone (adapted from NMJD, 2021).

Once artisanal diamond miners reach the water table, they either abandon the site or improvise by pumping water out of the excavation hole These unregulated mining and dewatering schemes expose water resources to pollution. The government was advised by NMJD to formalise artisanal mining and develop policies that will force miners to monitor environmental impacts.

2.2.2.9 Diamond Mining in South Africa

South Africa occupies the southern tip of the African continent and is classified as having an arid to semi-arid climate. Since large volumes of water are used for diamond mining and processing, the country has put in place laws and policies to manage and monitor water usage by all stakeholders (Minerals Council, 2022). The water usage per mine for the major diamond mines in South Africa is listed in Table 2.4. The Helam, Sedibeng, and Star operations rely entirely on groundwater abstraction for their water demand, withdrawing a combined total of more than 1,250,000 m^3 per annum. The Kimberley, Koffiefontein and Cullinan Mines get additional water from municipalities.

Apart from the problem of the availability of water in a water-scarce country, pollution of the water resource is another problem to consider. Matthews (undated) indicated that river pollution caused by diamond mining had increased by 36% between 1956 and 2003.

Table 2.4: Water consumption at South African diamond mines (source: Imperial College London).

Mine	Water consumption (m^3)			% Recycled
	Municipal	Groundwater	Total	
Cullinan	391 833	319 518	711 351	99
Koffiefontein	51 200	1 034 835	1 086 035	99
Kimberly Underground	39 780	1 175 852	1 215 632	0
Helam	0	250 000	250 000	95
Sedibeng	0	750 000	750 000	95
Star	0	250 000	250 000	95

2.2.2.9.1 Venetia Diamond Mine

Venetia Mine occurs in the Limpopo Province and is the largest producer of diamonds in South Africa (De Beers, undated). Venetia Mine operates on the principle that early collection of hydrogeological data is the key to understanding the groundwater regime (Morton and Muller, 2003).

Pre-mining water levels at the mine ranged between 2.84 mbgl and 14.25 mbgl with the boreholes at the mine yielding a total volume of less than 5 m^3/hr (Morton and Muller, 2003). The background shallow water chemistry was found to be of sodium bicarbonate type, whereas that of the kimberlite was of sodium chloride type.

Venetia Mine uses approximately 3.55 million m^3/annum and groundwater abstraction is governed keeping the water level at a 4 mbgl baseline. Water usage in at the operation is presented in Figure 2.10. On average, the operation uses between 0.6 and 0.7 m^3 of water per ton of ore mined. The company has also installed a 35 km long water pipeline for supply of water to the operation (Mining Technology, 2013).

Catchment drains have been developed along the tailing facilities at the mine to prevent contaminated water from reaching the aquifer at the open pit. This was done to control and reduce pollution of water sources. As part of developing the underground mine, Venetia will construct a storm water dam that will contain runoff from coarse residue deposits and overflow from upstream water containment facility (Concor, 2023). The dam will be lined with HDPE geomembrane to prevent seepage from reaching the water table.

Mining operations are surrounded by waste dumps, tailings and stockpiles containing pulverised material. These facilities contain large concentrations of silica, alumina, iron oxide and magnesia and these minerals may increase the total suspended solids in groundwater.

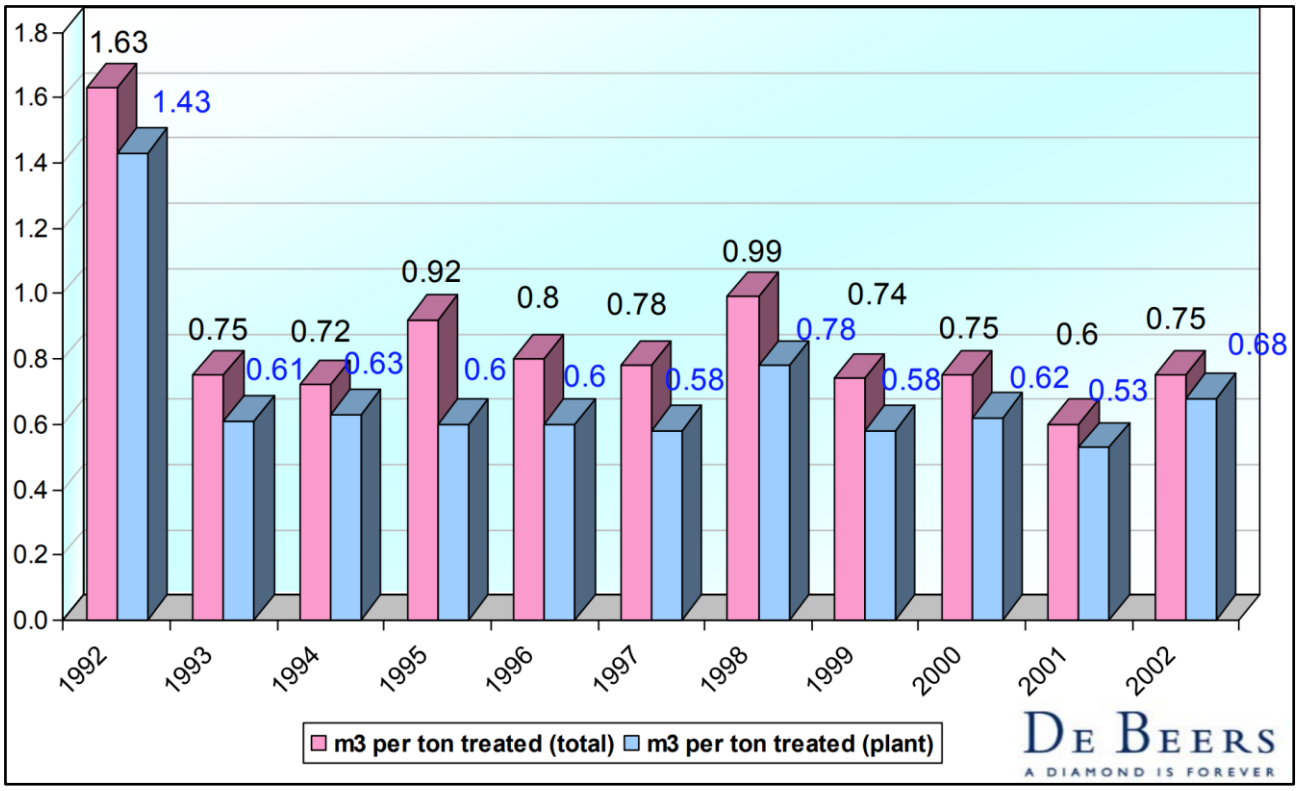

Figure 2.10: Water usage at the Venetia Mine between 1992 and 2002 (De Beers, undated).

2.2.2.9.2 Petra Diamonds

Petra Diamonds operates in several countries, namely: South Africa, Botswana, Tanzania, Namibia, and Lesotho. Diamond mining in all these countries requires large volumes of water which makes water resource management and pollution a key part of their operations. In South Africa, Petra Diamonds operates Cullinan, Kimberley Underground, Koffiefontein and Williamson Mines. Water is mainly abstracted as part of operational dewatering requirements. Groundwater thus abstracted is then used for ore processing.

A potential pollution source is the crushing of kimberlite ore which generates dust or suspended solids in water. Iron silicate is used during processing and will likely act as a water contaminant if not reclaimed (Petra Diamonds, 2009).

Excess water generated at Petra Diamonds' Kimberley Underground operations is sold to neighbouring De Beers Mine instead of disposing it into the environment. Water usage at the operations of the company is monitored twice a year and a water resources management report is produced annually (Petra Diamonds, 2009).

Petra Diamonds is obliged by South African environmental laws and regulations to limit negative environmental impact likely to emanate from its mining processes at all its operations. The mining company has developed an environmental management plan (EMP) as required by South African

legislation. The EMP is used to put in place mitigation measures to counteract the impacts of diamond mining on the water resources.

2.2.2.10 Diamond Mining in Botswana

The Botswana mining industry accounts for 10–15% of water use in Botswana and three quarters of the use comes from the diamond mining industry (DWA, 2014). Debswana operates four open pit diamond mines and relies heavily on groundwater for mining and ore processing activities. Jwaneng Mine is in the southern part of Botswana and three mines (Orapa, Damtshaa and Letlhakane) are on the eastern margins of Central Kalahari Game Reserve. The company carried out a comprehensive groundwater modelling exercise of the areas where it operates and on average 15 projects are annually conducted in the field of water resources management (Brook, 2011). Diamond mining operations are shown in Figure 2.11. The BK11 Kimberlite Mine (mined by Firestone Diamonds) is no longer operational but is located 5 km northeast of KDM. Lerala Mine is in eastern Botswana and is no longer operational. Most of its water demands of these mines were met by abstraction from the Limpopo River system.

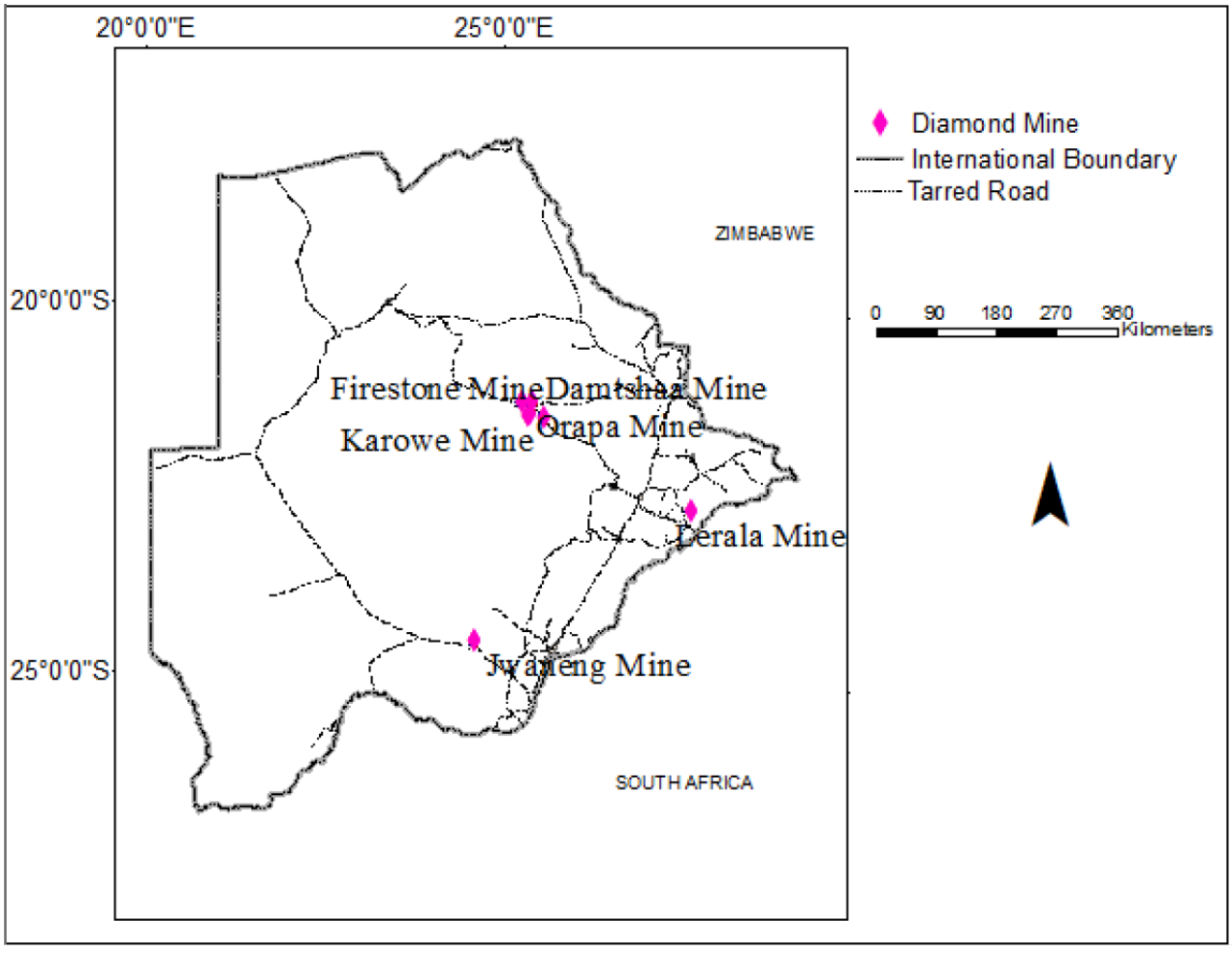

Figure 2.11 Mining Operations in Botswana (Brook, 2012).

Lerala Diamond Mine ceased operations in 2000 and its water demand were met from the sand aquifer system along the Limpopo River, which forms the eastern border between Botswana and South Africa. The local community relies on the alluvial and scree aquifers and access the groundwater through hand-dug wells. These aquifers have an average yield of 10 m^3/hr and an average TDS concentration of 100 mg/L. Other aquifer systems are the fractured quarzitic environment at >200 m depth (WCS, 2013). Groundwater from the two aquifer systems fall within the WHO limits for potable water, and the nitrate content in water is thought to come from wellhead pollution.

WCS (2013) conducted an EIA for the reopening of the mine and identified two major concerns that may lead to pollution of groundwater resources. The slimes dams, and coarse tailings facilities were identified as two areas requiring close monitoring. WCS (2013) recommended recycling of process water to reduce groundwater abstraction by the operation and to reduce leakages into the subsurface. A monitoring program was also recommended to quantify water abstraction, drawdown, and water quality. WCS (2013) suggested that slimes dams would not need to be lined since the FeSi, and flocculants used in diamond processing are environmentally inert and bear no toxicity. The operation has remained closed since 2000.

Firestone Mine closed operations in 2012 and has been on care and maintenance since then owing to economic recession (Jeffay, 2021). The operation was sold in 2021, and the sale conditions required the new owner to inherit the environmental liabilities that come with operating a diamond mine. Firestone sits on an area that has similar hydrogeological and geological properties KDM. Information on the impact of mining at Firestone Mine is not available in public space, however environmental impacts caused by diamond mining are well understood, and it was recommended that a comprehensive EIA would be required to mitigate adverse impacts on groundwater resources should Firestone reopen (World Bank, 2010).

Orapa Mine, Damtshaa and Letlhakane Mines share similar geological setting with KDM. These operations utilise water from sandstone and granite aquifers. Jwaneng Mine is in the south of Botswana where the host rock is metasediments and quartzites. The mine has developed a wellfield in the sandstone aquifer to meet its water needs.

Borehole yields from Debswana's wellfields generally range between 10 – 40 m^3/hr with TDS concentrations of >2000 mg/L (WSB, 2013). Two types of water are currently abstracted from the Orapa, Damtshaa and Letlhakane Mines: Na-HCO_3 and Na-Cl (WSB, 2013). The high TDS water is used for ore processing and portable water use, Debswana uses reverse osmosis plant to reduce TDS to within BOS32:2015 drinking water standards (WSB,2013).

The impact of pumping on water levels at the Orapa and Letlhakane Mines was modelled by Debswana (WSB, 2013). Figure 2.11 shows localised depression around the mining and wellfield

areas, respectively, as simulated with the numerical model. The model predicted drawdowns ranging between 10 to 40 m between 2013 to 2023 (WSB, 2013).

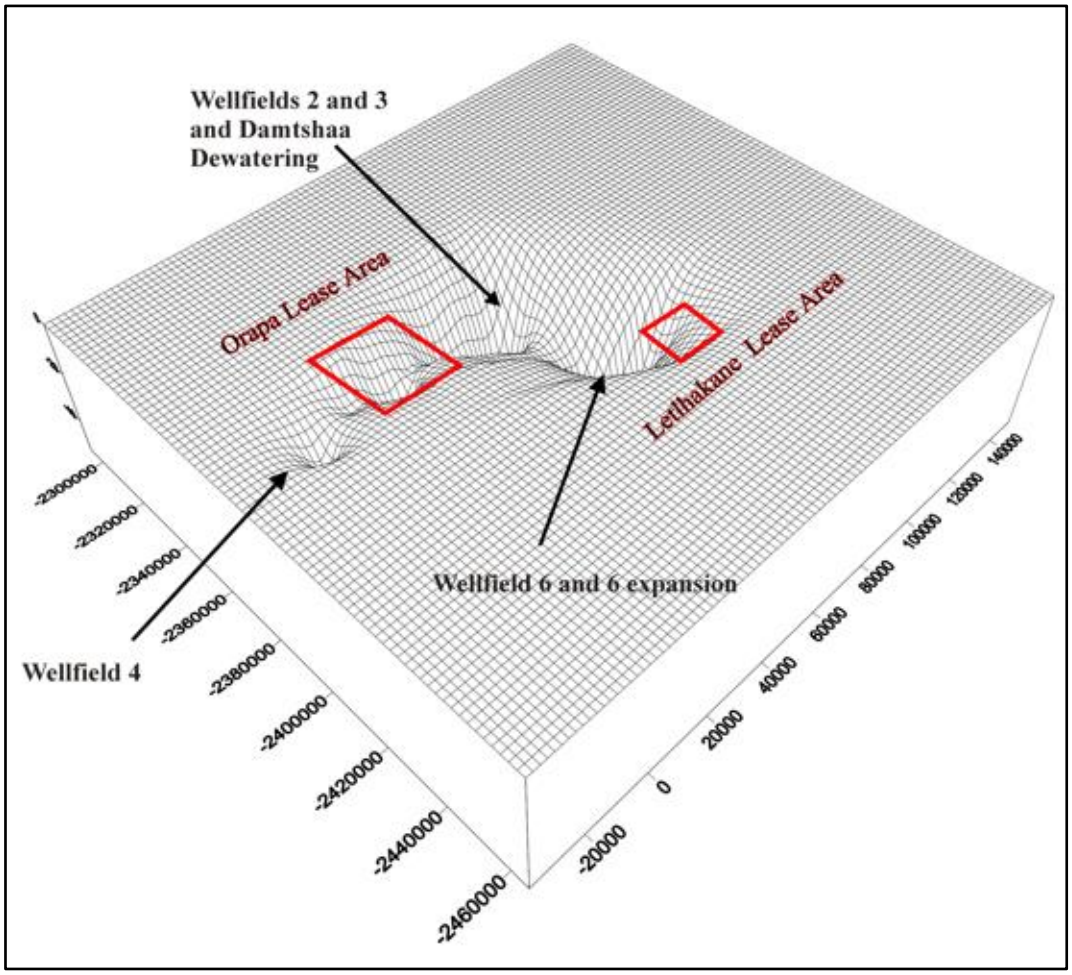

Figure 2.11: Groundwater depressions around Orapa and Letlhakane Mines (Brook, 2011).

Orapa mine constructed a 1 Mm^3 storm water dam with the objective of harvesting runoff from rainfall and reducing the use of groundwater (Brook, 2011). Debswana is also exploring the possibility of using deep-seated saline groundwater at all its operations (Brook, 2011).

CHAPTER 3:
DESCRIPTION OF THE STUDY AREA

3.1 REGIONAL SETTING

The study area is located on the eastern margins of the Kalahari Desert in the Boteti District in the central parts of Botswana. It lies between latitudes 25°16′30″E and 25°48′0″E, and longitudes 21°40′0″S and 21°20′0″S (Figure 3.1). The nearest town is Letlhakane, situated approximately 15 km north-east of KDM. The project area can be accessed along various sandy roads. The district has five mining operations, of which four are currently active.

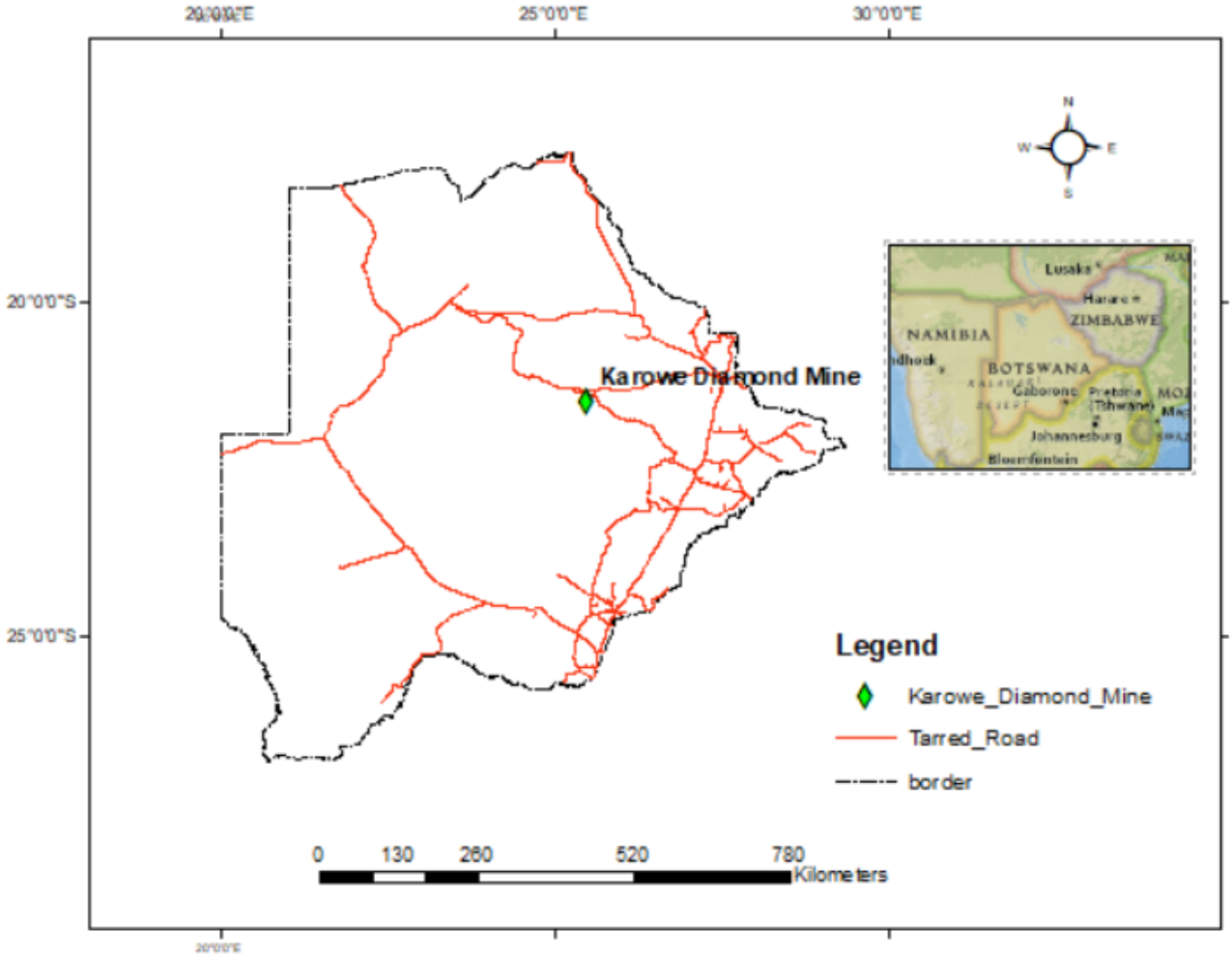

Figure 3.1: Location of Karowe Diamond Mine (KDM) within Botswana.

3.2 GEOLOGICAL SETTING

The principal rocks within the research area belong to the Karoo Supergroup, in particular the Stormberg Lava Group, and the Lebung Group which includes the Ntane and Mosolotsane Sandstone Formations. The Stormberg basalts underlie Kalahari sands and are in turn underlain by a sequence

of sedimentary rocks. Below the sedimentary rocks, consisting of sandstones and mudstones, the Mea-arkose and basement granitic gneiss occur. The surface geology (below the Kalahari sand cover) and stratigraphic sequence of the study area are presented in Figure 3.2 and Table 3.1.

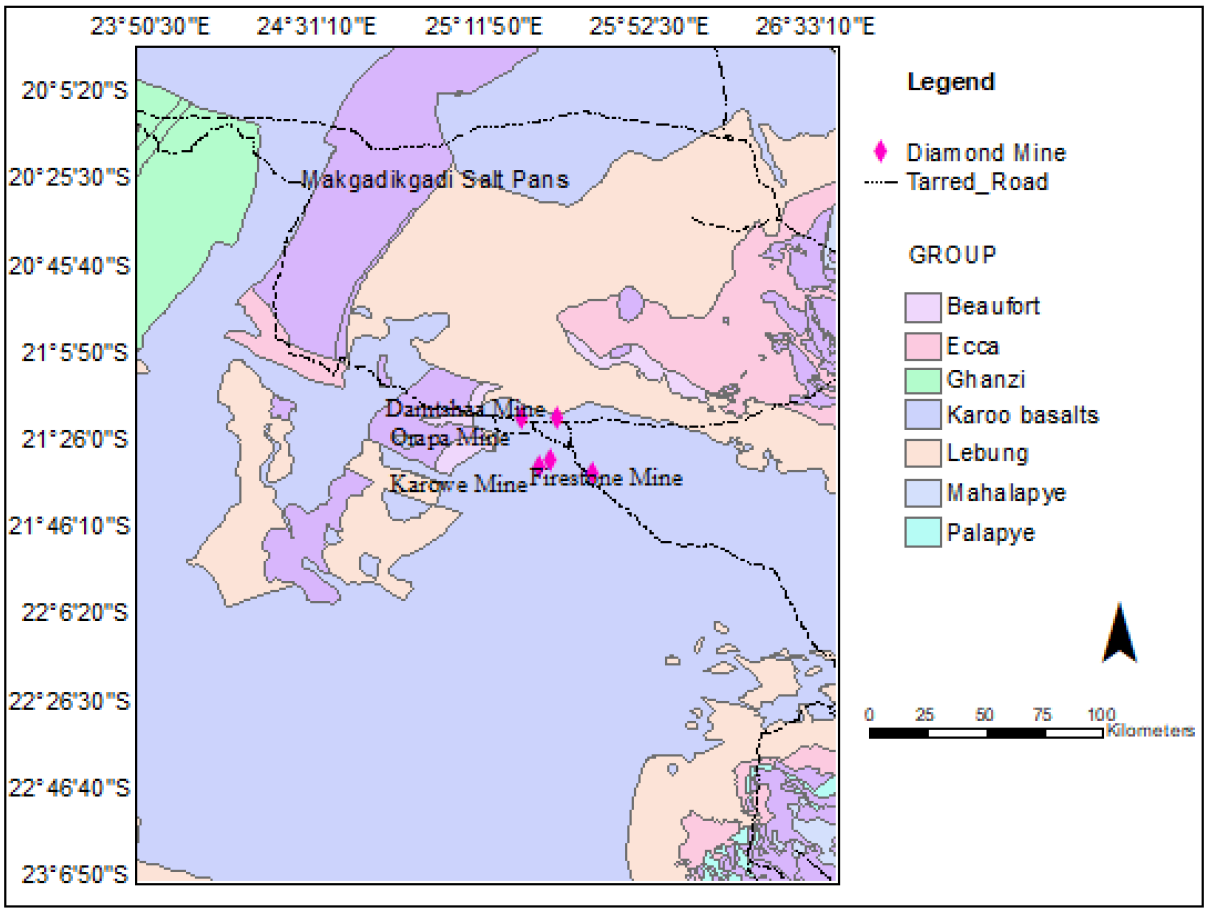

Figure 3.2: Surface geology in the vicinity of the KDM.

Table 3.1: Stratigraphic sequence (after Carney *et al.*, 1994).

Age	Supergroup	Group	Formation	Lithological Description
Cainozoic		Kalahari	Kalahari Beds	Soil, sand, calcrete, silcrete and clay
			Tuli Dyke Swarm	Dolerite dykes and sill intrusion
Mesozoic	Karoo	Stormberg Lava	Serwe Pan	Massive amygdaloidal flood basalt extrusion
		Lebung	Ntane Sandstone	Aeolian sandstone, Medium- to fine-grained with minor mudstone intercalations becoming fluvial to base
			Mosolotsane	Fluvial red beds, siltstones and fine-grained sandstones
		Beaufort	Tlhabala	Non carbonaceous shales
		Ecca	Tlapana	Carbonaceous shales and dull coal seams with minor sandstones
			Mea Arkose	Coarse clastic fluvio-deltaic sediments
Archaen	Basement			Metamorphic gneisses with intruded granite

3.2.1 Kalahari Sediments

Kalahari beds consist of sand, silcrete and calcrete, varying in thickness between 10 m and 20 m. The sediments are mostly dry and do not play any significant role in groundwater flow. There has been no recorded borehole in the vicinity of KDM that taps water from the Kalahari beds. However, AquiSim (2020) recorded perched aquifers in the Kalahari sediments at locations more than 10 km away from KDM. Calcrete limits vertical flow from the perched aquifer and, as such, the Kalahari sediments do not contribute to dewatering flows.

3.2.2 Stormberg Basalt

The basalt occurs as a series of layered, jointed lava flows with a total thickness in the vicinity of the pit ranging from about 80 m in the south to almost 120 m in the north. The first 20 m to 30 m of basalt is highly weathered and this is where the first water strike was intersected by farmers. The basalt is grey black in colour and is characterised by the presence of thin calcite veins.

3.2.3 Ntane Sandstone

The unit is characterized by fine- to medium-grained sandstones of primarily aeolian origin that unconformably underlie the basalt. The thickness of the Ntane rocks varies between approximately 20 m and 60 m in the pit area. WSB (2007) divided the Ntane Sandstone into three sub-units:

- an upper, relatively permeable layer with an average thickness of 12 m,
- a less permeable middle layer with an average thickness of 33 m, and,
- a basal layer with an average thickness of 8 m and a hydraulic conductivity intermediate to the two overlying layers.

3.2.4 Mosolotsane Formation

The Mosolotsane Formation is a sequence of fine - to coarse-grained sandstones, siltstones, and mudstones that were water deposited and vary in thickness from about 80 m to 100 m in the pit area. The formation has been subdivided into two units (AquiSim, 2020):

- an upper mudstone unit consisting of interbedded mudstones, siltstones, and fine- to medium grained sandstones with an average thickness of 62 m, and,
- a basal coarse-grained, locally conglomeratic, arkosic sandstone with an average thickness of 31 m.

3.2.5 Tlhabala Mudstone

The Tlhabala Formation belongs to the Beaufort Group and comprises a 100- to 120-m-thick sequence of shells and non-carbonaceous mudstones and siltstones with minor sandstone (WSB, 2007).

3.2.6 Tlapana Mudstone

The Tlapana Formation belongs to Ecca Group and comprises a 50-m-thick sequence of primarily carbonaceous mudstones with some thin coal seams and sandstone lenses (WSB, 2007).

3.2.7 Mea-arkose

The Mea-arkose belongs to the Ecca Group, and this is a fine-grained to granular and pebbly arkosic sandstone with a bit of weathering where fracturing has occurred. Its thickness in the research area, as determined from four boreholes that intersected the granite, ranges between 6 m and 9 m, while at the Letlhakane Mine, its thickness ranges between 25 m and 110 m (WSB, 2007).

3.2.8 Granite

The basement rocks comprise a family of granitoid rocks, gneiss, and ultramafic schists. Drill logs from boreholes at the mine indicate that the granites occur at a depth of 450 m below ground level (WSB, 2007). Opencast mining at KDM has not intersected the granites, but the granites are expected to be intersected in 2026 when underground excavations come into operation.

3.2.9 Kimberlite

The AK6 kimberlite at KDM has three pipes of varying geological parameters. The South Lobe is distinctly different from the North and Centre Lobes which are similar in terms of their geological characteristics. The South Lobe is broadly massive and more homogeneous and ultramafic than the North and Centre Lobes which exhibit greater textural complexity and are more variable and contain higher proportions of internal country rock dilution (JDS, 2019)

3.3 STRUCTURAL FEATURES

Five known kimberlite pipes intruded the research area in late to post-Karoo times (Barnett, 2006). The kimberlite intrusions influenced the current structural pattern in the research area (Barnett, 2006). Two dykes traverse the research area, one running east/west between the pit and the tailings facility, and the other dyke having a south-east/north-west azimuth (Figure 3.3). The dykes were intersected during drilling programs in 2007 and 2019 (KDM, 2023). The dolerite dykes dip at 88^{o} to the north

and have an average depth of 35 m and a width of 44 to 88 m (GMS, 2019). Faults and joints mapped within the open pit are also predominantly south-east trending (GMS, 2019).

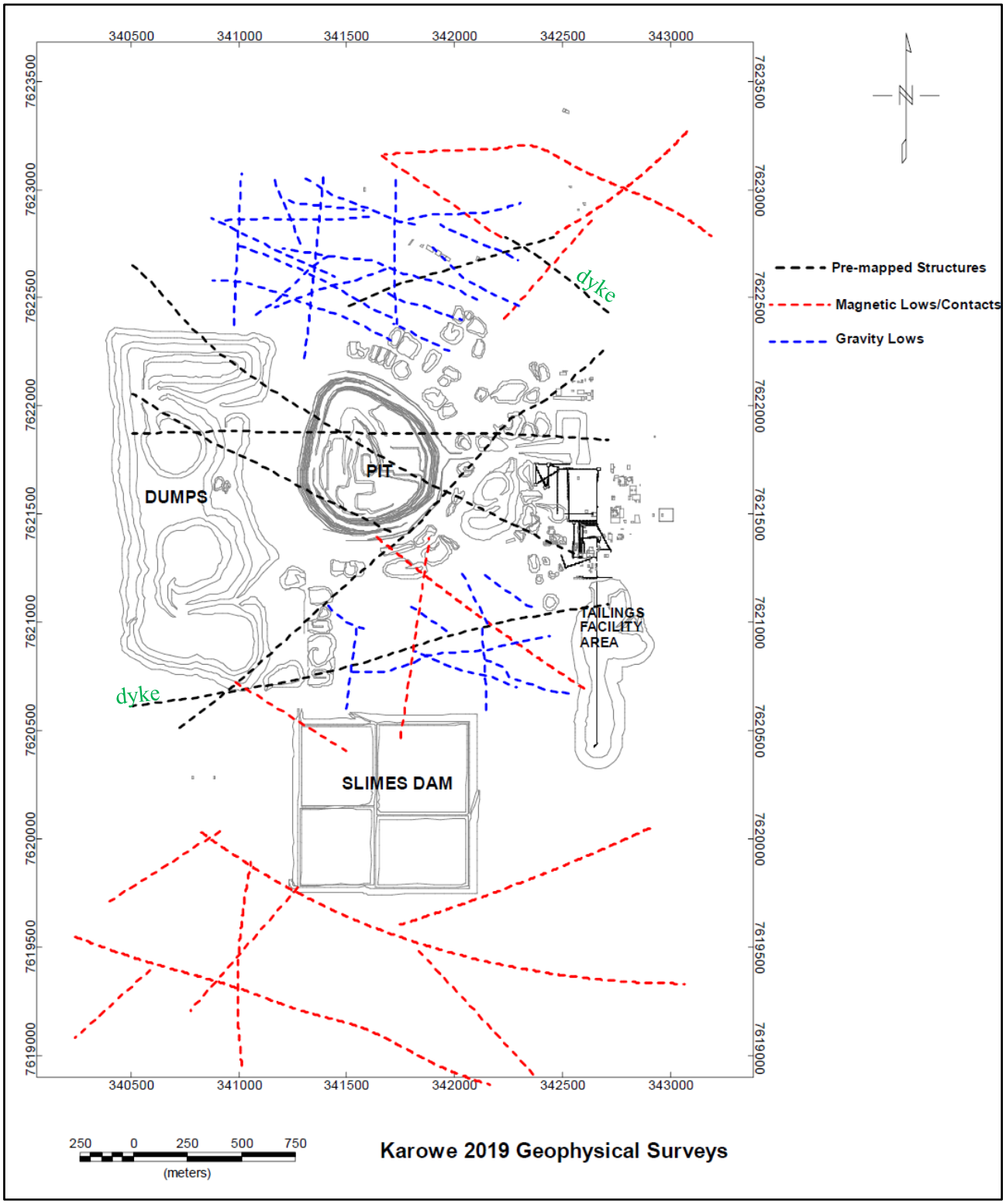

Figure 3.3: Gravity and magnetic survey (GMS, 2019).

Apart from the mapped structures, other linear features in the vicinity of the mine were identified from geophysical surveys. WSB (2008) interpreted airborne magnetic data and identified linear

magnetic structures in the vicinity of KDM. These structures predominantly trend south-east/north-west and south-west/north-east in the vicinity of the pit (Figure 3.3, red dashed lines). Gravity surveys conducted north and south of the pit also revealed linear zones of gravity lows (Figure 3.3, blue dashed lines).

The different structural sets are responsible for water movement through the study area. Dolerite dykes act as groundwater barriers and impede movement of water, resulting in waters of different quality on either side of the dyke (WSB, 2008). These dykes form barriers throughout the full thickness of the Ntane aquifer, and thus they may control groundwater at local or regional scale. However, past numerical modelling of the groundwater response to pumping suggested that the aquifers are not completely compartmentalised (AquiSim, 2020).

3.4 TOPOGRAPHY AND DRAINAGE

The regional topography is generally flat with a slight topographical fall towards the Makgadikgadi Pans. The regional topography near KDM slopes north-westwards from an average elevation of 1012 mamsl to about 900 mamsl at the edge of Makgadikgadi Pans, north of Orapa (Figure 3.4). The local topographic gradient at the mine is towards the south-east, in the direction of the Letlhakane River. Large drainage channels or rivers are almost non-existent with the Letlhakane River the only significant drainage feature, occurring approximately 15 km east of the research area. The Letlhakane River is seasonal and only flows during the rainy season. The Makgadikgadi Pans to the north form a flat depression in which the aquifer system and storm water discharge.

3.5 CLIMATE AND RAINFALL

The climate in the Boteti area is semi-arid, with variable annual rainfall events that occur as high intensity storms, which cause occasional flooding. Rainfall occurs mainly between October and March and is measured at the KDM Rain Gauge Station (Figure 3.5). Winter rainfall occurs but is as low as 5 to 20 mm/month. Temperatures can be as high as 30^{o}C to 40^{o}C during summer, whilst during winter they may go as low as 10^{o}C to 15^{o}C (KDM, 2019). The potential evapotranspiration is high due to high temperatures and low humidity. Evaporation from open water bodies is in the range of 2 m/year (Lekula and Lubczynski, 2019).

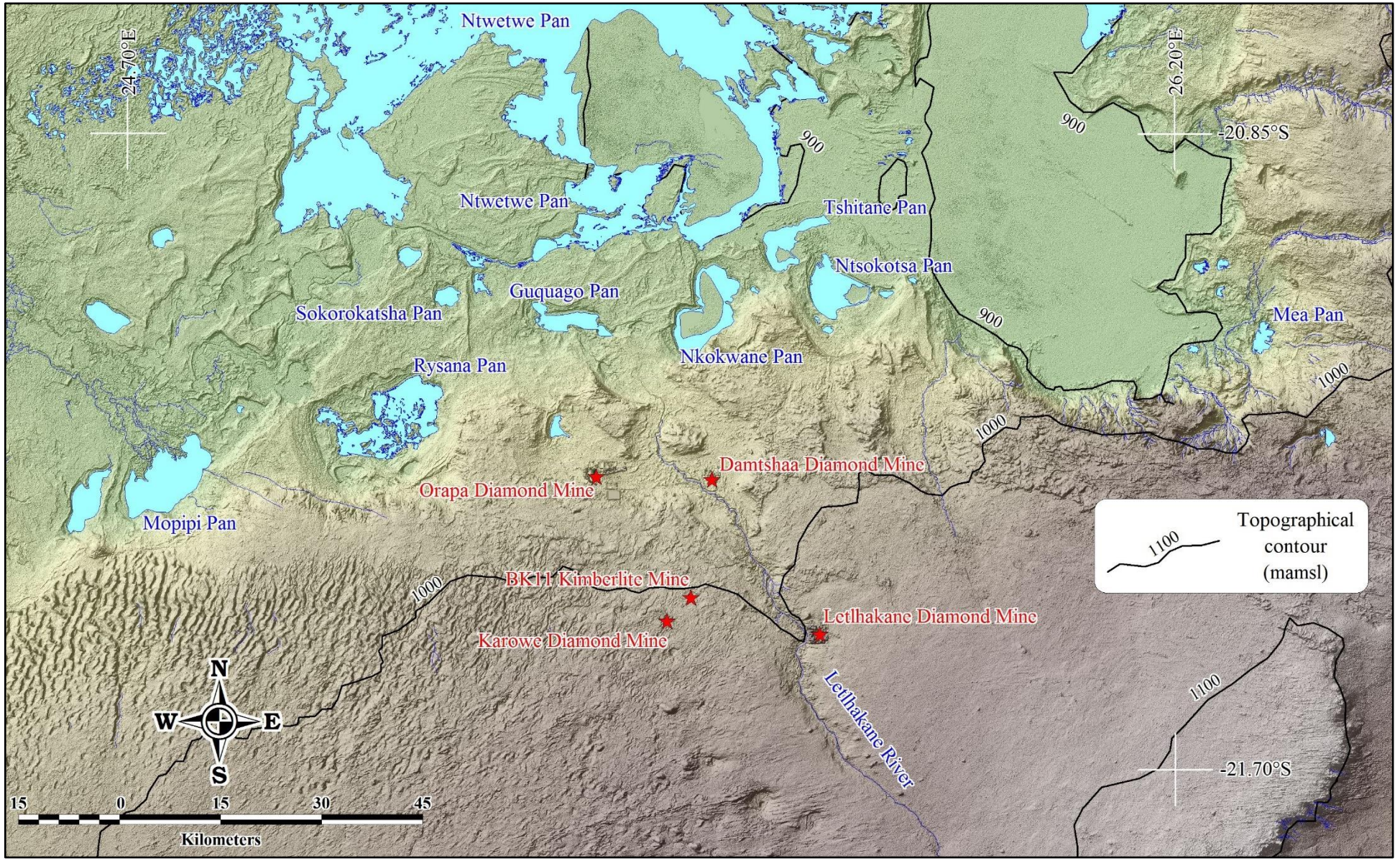

Figure 3.4: Topography and drainage towards the Makgadikgadi Pans.

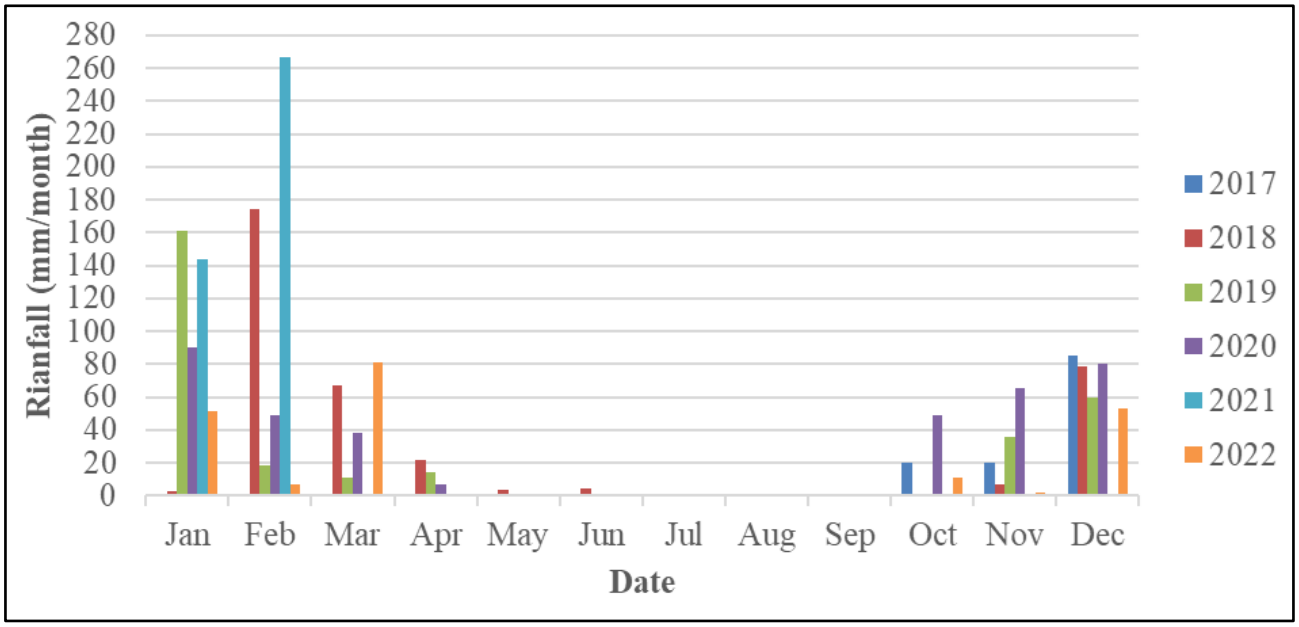

Figure 3.5: Rainfall record from 2017 to 2022 at the KDM rain gauge station.

3.6 LAND USE

The land use types of the study area are the same across the Boteti Region and is predominantly agricultural (crops and livestock), residential, wildlife and mining. Letlhakane is the main village in the area and has a population of 20 841 (Statistics Botswana, 2022). Water demand for irrigation; domestic and industrial use is met from the groundwater resource.

3.7 MINING ACTIVITIES AND SITE INFRASTRUCTURE

KDM is one of four active diamond mines in the Boteti region of Botswana. Orapa Diamond Mine and Damtshaa Diamond Mine occur approximately 24 km north-north-west and 22 km north-north-east of KDM, respectively (Figure 3.6). Letlhakane Diamond Mine is situated 23 km east of KDM. In the past, Firestone Diamonds operated the BK11 Kimberlite Mine approximately 5 km north-east of KDM. Mining operations at this mine started in 2010, but the mine is no longer operational.

The mining infrastructure at KDM is shown in Figure 3.7. Mining at KDM is carried out by blasting in the open pit. The blasted waste rock is transported and deposited to the west of the pit while the kimberlite ore is strategically placed to the east of the pit and closer to the plant.

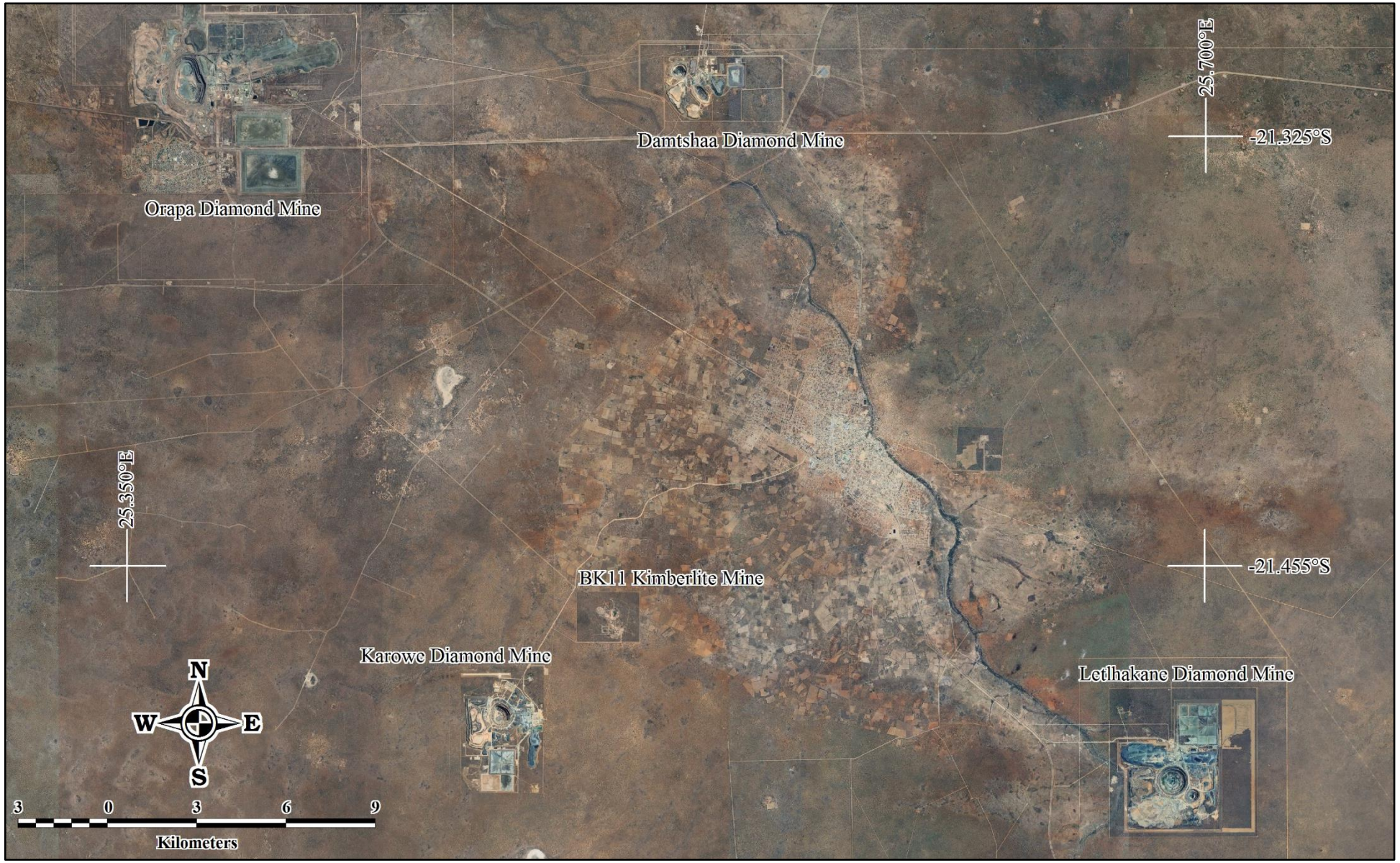

Figure 3.6: Diamond mines in the Boteti region of Botswana.

Figure 3.7: Mining activities and infrastructure of KDM.

Once the ore is broken, it is loaded into haul trucks and taken to the plant where it passes through various stages of crushing and separation to liberate diamonds. The broken ore is first taken to the primary crusher to reduce it into smaller and more manageable sizes. The reduced pieces are then taken through the dense media separation where ore is mixed with a solution of ferrosilicon and water (Mills, 2019). At the dense media separation, material of high density settles to the bottom forming a layer of diamond rich concentrate.

The concentrate is relayed to the recovery circuit of the plant and passes through various stages of processing, x-ray luminescence, laser and magnetic machines (JDS, 2019). At this stage, diamonds are separated from high density material. The residue from recovery is separated into two fractions, fine and coarse tailings. The fine residue is pumped together with water to the slimes dam and after settling, water is pumped back for re-use at the plant. The coarse residue is deposited separately as coarse tailings. The process dam is placed further to the east of the plant and is used for storing water coming from pit dewatering boreholes, sump and return water from slimes. The stormwater dam is used for collecting and storing runoff water. Runoff water is used for dust suppression and drilling and to supplement plant water demand when needed.

3.8 HYDROGEOLOGICAL SETTING

3.8.1 Aquifer system

The aquifer systems in the research area are fractured/weathered basalt, Ntane sandstone, Mosolotsane sedimentary rocks, Mea-arkose sandstone, and the weathered/fractured basement granites (Exigo3, 2019). Dolerite dykes partition the study area into distinct aquifer units, and it is assumed that little movement of water takes place between the different compartments. Groundwater connection between the compartments only occurs through surface and near-surface drainage.

The basalt aquifer system is fractured and exhibits only secondary porosity. The Ntane sandstone exhibits both primary and secondary porosity, with less cementation. However, yields are encountered where fracturing is enhanced and well developed. The Mosolotsane sandstone is made up of fine to coarse sandstones with lenses of red mudstone within the unit. These lenses form aquitards and impede flow in the vertical direction.

Underlying Mosolotsane, are the Tlhabala and Tlapana Formations. These are a sequence of siltstones, shales and carbonaceous mudstones. These form aquitards and impede flow between the Mosolotsane sandstones and the granites. There are thin lenses of sandstone with the Tlhabala and Tlapana units and these have produced groundwater yields of <1 m^3/hr (Exigo3, 2019).

3.8.2 Water strikes and borehole yields

Private boreholes belonging to farmers abstract fresh waters from the shallow basalt aquifer while dewatering boreholes at the mine were drilled to the base of Mosolotsane sandstone. Most water strikes occur at or below the contact of the Ntane sandstone and the overlying basalt (KDM, 2023). A noticeable water strike and usually a change in groundwater quality occurs at the base of the Mosolotsane Formation where a horizon of coarse-grained arkosic sandstone occurs below red mudstone and siltstone. Deep water strikes occur in the granites at depths >400 mbgl (KDM, 2023).

Borehole yields are influenced by structures within the rock mass. Kalahari sediments have not yielded any water in the project area (WSB, 2008). Water abstraction from the basalts has not been recorded within the KDM lease area. However, a perched aquifer system noted around the slimes dam was caused by seepage water coming from the dams.

The agricultural sector in the research area relies on low TDS water from the fractured and weathered basalt. Accurate pumping rates from this formation have not been recorded but an average of 5 m^3/hr was reported (Boteti Mining, 2012).

3.8.3 Regional and local groundwater flow

Regional groundwater level monitoring was started in 2009. Regionally, groundwater flows from south-east to north-west, draining into the Makgadikgadi Pans (Connelly and Gibson, 1985). The pre-mining groundwater levels near KDM indicate a local hydraulic gradient to the south-east in the direction of the Letlhakane River. However, this gradient may be partly due to groundwater abstraction from boreholes in a wellfield (Wellfield 6) located east and south-east of KDM.

3.8.4 Hydrochemical characteristics

The waters from the fractured and weathered basalts have a TDS below 1000 mg/L. The sandstones, on the other hand, have a brackish chemistry with a natural TDS concentration ranging between 2000 mg/L and 4000 mg/L (KLMCS, 2013). Water quality deteriorates with depth, with TDS concentrations of more than 10 000 mg/L reported from the granite waters.

Generally, the groundwater is slightly alkaline with a pH ranging between 7.8 and 8. Groundwater from the sandstone aquifers in the area is dominated by sodium, chloride, and sulphate ions. The Na-Cl content indicates that the groundwater has had a long residence time to interact with country rock resulting in the following evolution process:

- bicarbonate→bicarbonate-chloride→chloride-bicarbonate→chloride-sulphate→chloride

Stiff diagrams of the two dominant water types in the study are presented in Figure 3.8. The presence of Ca and HCO_3 in water indicates the presence of fresh water from shallow basalt aquifers (Figure 3.8, left) while Na-Cl dominance typically represents the deeper sandstone and granite aquifer systems receiving little or no recharge from rainfall (Figure 3.8, right).

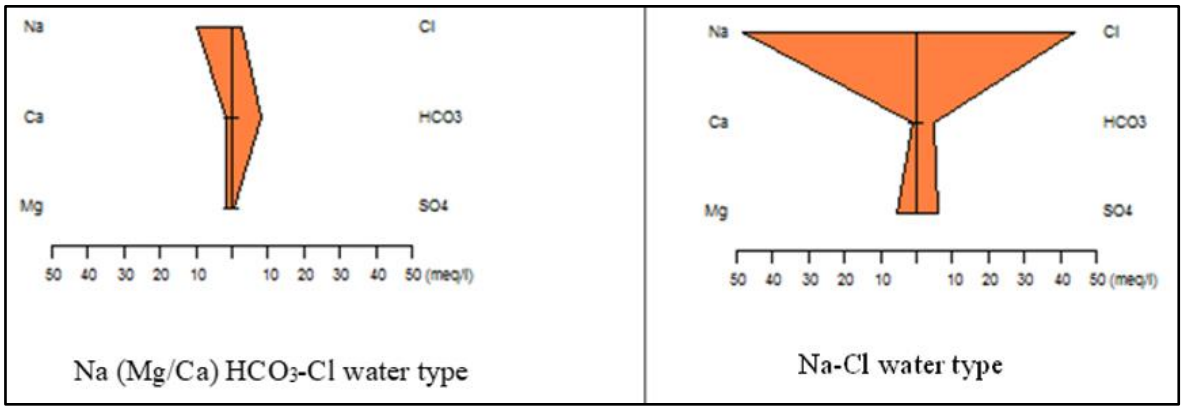

Figure 3.8: Stiff diagrams showing the two dominant water types in the study area (KLMCS, 2010).

Figure 3.9 is a Piper plot of the groundwater chemistry recorded at boreholes in the vicinity of KDM prior to the commencement of mining. The KDM monitoring boreholes form a cluster with Na-Cl as the dominant water type, while the private boreholes are more scattered in the diagram but indicate that the dominant water type is Na-HCO_3.

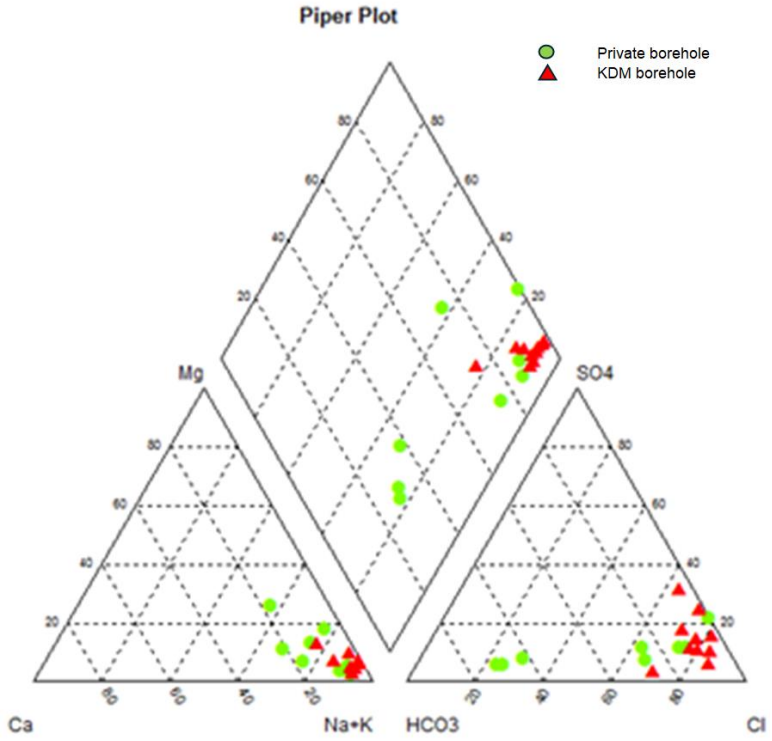

Figure 3.9: Piper diagram of pre-mining groundwater samples collected from monitroing boreholes at KDM and from farm boreholes in the area (KLMCS, 2010).

3.8.5 Groundwater recharge

The average annual precipitation in the project area, based on data collected on site, is approximately 400 mm (KDM, 2019). Recharge was estimated at <1% of annual rainfall (i.e., <4 mm/year) (Obakeng, 2007) with aquifer replenishment occurring in an area 200 km south-east of the study area where outcrops of the Ntane sandstone occur (Figure 3.10) (Selaolo,1998?). HCI (2007) indicated that natural recharge from precipitation contributes >1 mm/year.

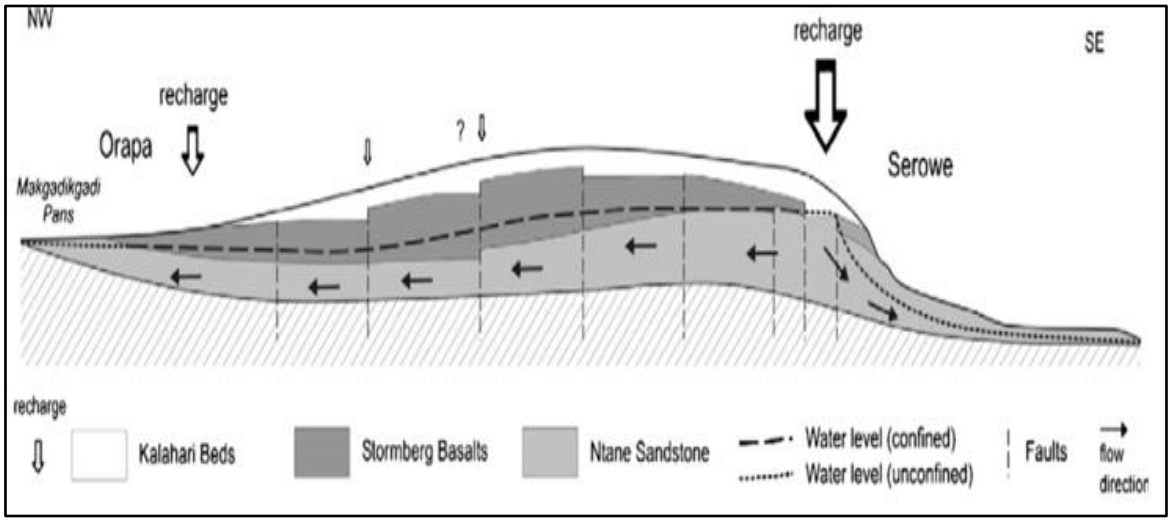

Figure 3.10: Recharge of the aquifer system in the Eastern Fringe of Kalahari, Botswana (Selaolo, 1998)

AquiSim (2020) suggested a recharge of <1 mm/year across the research area. However, recharge values >1 mm/year had been used for groundwater modelling work around the Letlhakane River (HCI, 2007). A recharge of 0.5 mm/year was used for a numerical groundwater model developed for KDM (KP, 2021). Water Surveys (2007) concluded that recharge in the study area was as low as <0.5 mm and could be ignored. Previous models for Orapa, Damtshaa and Letlhakane were calibrated with recharge values of 0.5 to 0.02 mm/year.

Enhanced recharge from mining facilities and operations may occur. This may come in the form of seepage from surface water ponds. Evidence of enhanced recharge is present in the slimes dam monitoring boreholes, where water levels have been steadily increasing since mining began.

The silicified calcrete and thick basalt layers in the vicinity of KDM act as aquitards that prevent recharge of the deep sandstone and granite aquifers. The high TDS in both these aquifers have been used as evidence of limited natural recharge.

Recharge is high and uniform in areas north of the research area where the thickness of basalt is thin with outcrops of calcrete increasing the opportunity for groundwater recharge (AquiSim, 2020).

CHAPTER 4:
HYDROGEOLOGICAL INVESTIGATIONS AT KDM

4.1 OVERVIEW

Since 2006, several hydrogeological investigations have been conducted at KDM. These studies include the development of conceptual hydrogeological models, dewatering studies, wellfield investigations, environmental impact assessments, the development of numerical groundwater flow models, and geochemical investigations. Table 4.1 lists all known investigations completed in the study area up to 2023.

An environmental impact assessment (EIA) study was carried out prior to the start of mining of the AK06 kimberlite. One of the aims of the study was to document all impacts that mining would likely have on the environment (Geoflux, 2007). A key impact identified was depletion of groundwater resources because of pit dewatering activities. Possible sources of groundwater contamination were identified as sewage ponds, tailings facilities, explosives, workshops, and magazine storage. The problem of water depletion and contamination was to be addressed through a monitoring programme and use of an integrated water resource management scheme (Geoflux, 2007).

Water Surveys Botswana (WSB, 2007) developed a wellfield for AK6 mine. The project included groundwater modelling of the water resource and assessment of the impact of groundwater abstraction on private boreholes close to the mine. This was a regional aquifer model extending from Boteti in the west to Serowe in the east. The model was based on limited data from before mining began at KDM; however, the model predicted a drawdown of 100 m by 2020 around the open pit. The model also predicted very little interference between mining activities and the private farms. In 2019, KDM recorded complaints from farmers who believed that their boreholes were losing their yield, and an investigation was launched to put in place short- and long-term measures to address the problem. As part of the long-term solutions, KDM intensified groundwater monitoring in the areas surrounding private wells.

Various groundwater models have been developed over the years to better define dewatering requirements for the AK6 kimberlite pipe (WSB, 2007; KLMCS, 2017). The latest model was generated in 2019 when Lucara Botswana (Pty) Ltd and Debswana Diamond Company (Pty) Ltd appointed AquiSim Consulting Services (Pty) Ltd to conduct a groundwater flow modelling study for the aquifers from which the diamond mines of Karowe, Orapa, Letlhakane and Damtshaa abstract groundwater (AquiSim, 2020). A three-dimensional (3D) groundwater flow model was constructed using long periods of historical data (44 years) and the latest abstraction and water level data (KDM,

2019). However, not much work was done to quantify the impacts of mining activities on private boreholes.

Table 4.1: Hydrogeological investigations at KDM (formerly AK6) since 2006

Date	Project Name	Reference
2006	AK6 Project: Preliminary Hydrogeological Conceptual Model	KLMCS (2006)
2006	AK6 Structural geology interpretation	Barnett (2006)
2007	AK6 Dewatering Project Pre-Feasibility Study	KLMCS (2007a)
2007	Initial Groundwater Flow Model of AK6 Pit and Recommendations for Dewatering	KLMCS (2007b)
2007	AK6 Country Rock Model - De Beers	Barnett (2007)
2007	AK6 Wellfield Investigation Study	WSB (2007)
2007	Environmental Impact Assessment for the Proposed AK06 Diamond Mine	Geoflux (2007)
2007	Initial 3D Groundwater Flow Model	HCI (2007)
2008	AK6 Wellfield Investigation Study	WSB (2008)
2010	AK6 Mine Feasibility Study Project	KLMCS (2010)
2011	AK6 Drilling and Aquifer Testing Report	KLMCS (2011)
2014	Karowe Mine Groundwater Modelling Review	KLMCS (2014)
2015	Karowe Diamond Mine Groundwater Flow Model	Itasca (2015)
2017	Karowe Mine Conceptual Model to 720 mbgl	KLMCS (2017)
2018	Karowe Mine Numerical Modelling Report	KLMCS (2018)
2019	Annual Groundwater Monitoring Report	KDM (2019)
2019	Geochemical Study for Karowe Diamond Mine	Mills (2019)
2019	Karowe Mine Underground Feasibility Study	JDS (2019)
2019	Groundwater Numerical Modelling	Exigo3 (2019)
2019	Borehole Geophysics Siting for Dewatering	GMS (2019)
2019	Update of the AK6 geological model in support of a mineral update for the 2019 Karowe Underground Feasibility Study	SRK (2019b)
2020	Karowe/Orapa - 2020 Groundwater Flow Model Update	Aquism(2020)
2021	Karowe Groundwater Model	Itasca (2020)
2023	Annual Groundwater Monitoring Report	KDM (2023)

4.2 AQUIFERS AND BOREHOLE YIELDS

Drilling data has revealed that the Mosolotsane sandstone aquifer is a major and significant aquifer at KDM, contributing 20% to 100% of the total borehole yield (AquiSim, 2020). However, the Ntane sandstone has produced yields exceeding 20 m^3/hr from boreholes drilled more than 2 km away from the pit perimeter. On the other hand, boreholes that were drilled after commencement of pit dewatering show that groundwater resources in the Ntane aquifer have been depleted and the Mosolotsane aquifer remains the source of water, contributing >90% of the borehole yield (KDM, 2023). The basalt in the pit area has not yielded any water, an indication that basalt only holds water where fractures exist.

WSB (2007) found that borehole yields around AK6 were generally higher than the average for the area: >40 m^3/hr as opposed to 10-20 m^3/hr.

4.3 HYDRAULIC PROPERTIES

The hydraulic parameters of the different rock formations forming the aquifer system at KDM have been estimated during various studies using pumping and packer tests (WSB, 2007; HCI, 2007; KLMCS 2017; Exigo3, 2019). The different hydraulic parameters controlling the storage and movement of water through the various formations are presented in Table 4.2.

Table 4.2: Aquifer hydraulic parameters (KLMCS, 2017).

Geological Formation	Thickness (m)	Depth of test (mbgl)	Horizontal *K* (m/d)	Vertical *K* (m/d)	Specific storage (/m)	Specific yield (-)
Basalt	130	130	0.05	0.01	2×10^{-6}	1×10^{-3}
Ntane sandstone	70	200	0.25	0.15	2×10^{-6}	2×10^{-2}
Lower Mosolotsane	12	252	0.1	0.1	2×10^{-6}	5×10^{-3}
Tlhabala mudstone	90	342	0.0005	0.0005	3×10^{-5}	1×10^{-3}
Tlapana mudstone	45	387	0.0005	0.0005	3×10^{-5}	1×10^{-3}
Upper granite	>300	487	0.05	0.05	2×10^{-6}	1×10^{-3}

The average vertical and horizontal hydraulic conductivities (*K*) for the basalt formation were found to be 0.01 m/d and 0.05 m/d, respectively (KLMCS, 2017). The specific storage (S_s) and specific yield (S_y) for basalt were estimated to be 2×10^{-6} $m^{-1}$and 1×10^{-3}, respectively. The basalt has a low *K* and S_y because of a low primary porosity.

The hydraulic conductivity of the Ntane Formation was estimated in different studies and found to range between 0.15 m/d and 0.25 m/d (WSB, 2007). However, AquiSim (2020) recorded values of 0.05 m/d to 0.16 m/d at Orapa Mine. These values were recorded for boreholes with fractures that are

not fully interconnected. The high *K*-values of this unit are because the rocks exhibit both primary and secondary porosity. The hydraulic conductivity increases where fracturing is more enhanced and at the contact with the overlying basalts. Taking the thickness of the formation (~70 m) into account, the transmissivity (*T*) of the Ntane Sandstone was estimated at 3.5 m^2/d to 42 m^2/d (WSB, 2007). A transmissivity of 37 m^2/d to 42 m^2/d was estimated during a constant rate test (CRT) and 50 m^2/d to 58 m^2/d was estimated for recovery test using the Jacob-Cooper method (KLMCS, 2014). Because groundwater drawdown in the vicinity of the pit exceeds the depth of the lower boundary of the confining basalt layer, the hydraulic conditions in the Ntane sandstone aquifer are unconfined. Under these conditions, the specific yield of the aquifer is the parameter to consider when investigating groundwater storage and flow.

The basal part of the Mosolotsane Formation is also coarse and highly permeable. This unit also displays both primary and secondary porosity. The *K*-value of the Mosolotsane Formation ranges between 0.05 m/d and 0.1 m/d based on reported transmissivities (KLMCS 2011, 2017).

The grey mudstone of the Tlhabala and Tlapana Formations were found to have very low *K*-values because of the low permeabilities of these formations. Their hydraulic conductivities are 5×10^{-5} m/d to 5×10^{-4} m/d and 5×10^{-4} m/d to 3×10^{-2} m/d, respectively (KLMCS, 2014). These units are not considered for water supply.

The Mea-arkose aquifer system is not well established in the project area. The aquifer occurs as isolated lenses where present, and its thickness ranges between 5 and 9 m. Thickness of more than 10 m were reported in Letlhakane Mine (HCL, 2007). Packer testing exercise at KDM estimated the hydraulic conductivity of this unit at 3.66×10^{-2} m/d (Exigo, 2019).

The *K*- and *T*-values of the granites forming the basement rocks were estimated at 5.78×10^{-3} m/d and 1.30×10^{-3} m^2/d, respectively (Exigo, 2019), although a higher *K*-value of 0.05 m/d was found for weathered and fractured zones. Underground mining operations will terminate in the basement granite at approximately 700 mbgl. The granites will be dewatered during mining operations for safe mine working conditions.

4.4 BOREHOLE NETWORKS

4.4.1 Pre-mining hydrocensus boreholes

In 2007, a request for accessing farm boreholes was sent out to all stakeholders with boreholes within a 10 km radius of the planned AK6 development. A total of 23 boreholes were mapped within the farmland. The boreholes were surveyed using a handheld global positioning system. The owners and coordinates of the boreholes are listed in Table 4.3 while their positions are indicated in Figure

4.1.Groundwater levels could not be measured from the boreholes because farmers did not make provision for access of the water level dipper. Eight boreholes were not accessible during the research duration and no information could be collected from the boreholes. Some of the boreholes identified during the hydrocensus were included in the groundwater monitoring network of KDM. Water samples were collected on a quarterly basis from these boreholes.

Table 4.3: Farm boreholes and owners.

Borehole ID	Easting	Northing	Owner
PR001	346316	7624998	Tiroyamodimo
PR002	346314	7621182	Nawe
PR003	350336	7622469	Gabontime
PR004	351369	7623728	Nyepi
PR005	350704	7618899	Otsile
PR006	343139	7615768	Ramotlhala
PR007	340430	7610975	Keboswedtse
PR008	334008	7623906	Modiragale
PR009	335603	7620239	Nkalolang
PR010	335065	7627003	Moremi
PR011	338354	7631051	Kabakae
PR012	341032	7620659	Mokgalo
PR013	346716	7628716	Lebala
PR014	339317	7631605	Unknown
PR015	346748	7624591	Moutlwatsi
PR016	346315	7621188	Keopasitse
PR017	343143	7615791	Moreri
PR018	337925	7621701	Motheo
PR019	341528	7628284	Binang
PR021	343596	7627118	Nkwane
PR022	343887	7626256	Katholo
PR023	343883	7626893	Bright
PR024	344690	7626945	Israel

4.4.2 Wellfield boreholes

The wellfield boreholes were used for water supply to the mine between 2014 and 2019. Most of them occur more than a kilometre from the pit perimeter. While they were operational, there was no impact on the groundwater levels close to the pit. Although boreholes Z18429 and Z18436 were initially part of the wellfield, they were low yielding compared to the other boreholes and were converted to monitoring points. The wellfield boreholes were put on standby in 2019 when in-pit boreholes were drilled to accelerate the pit dewatering process.

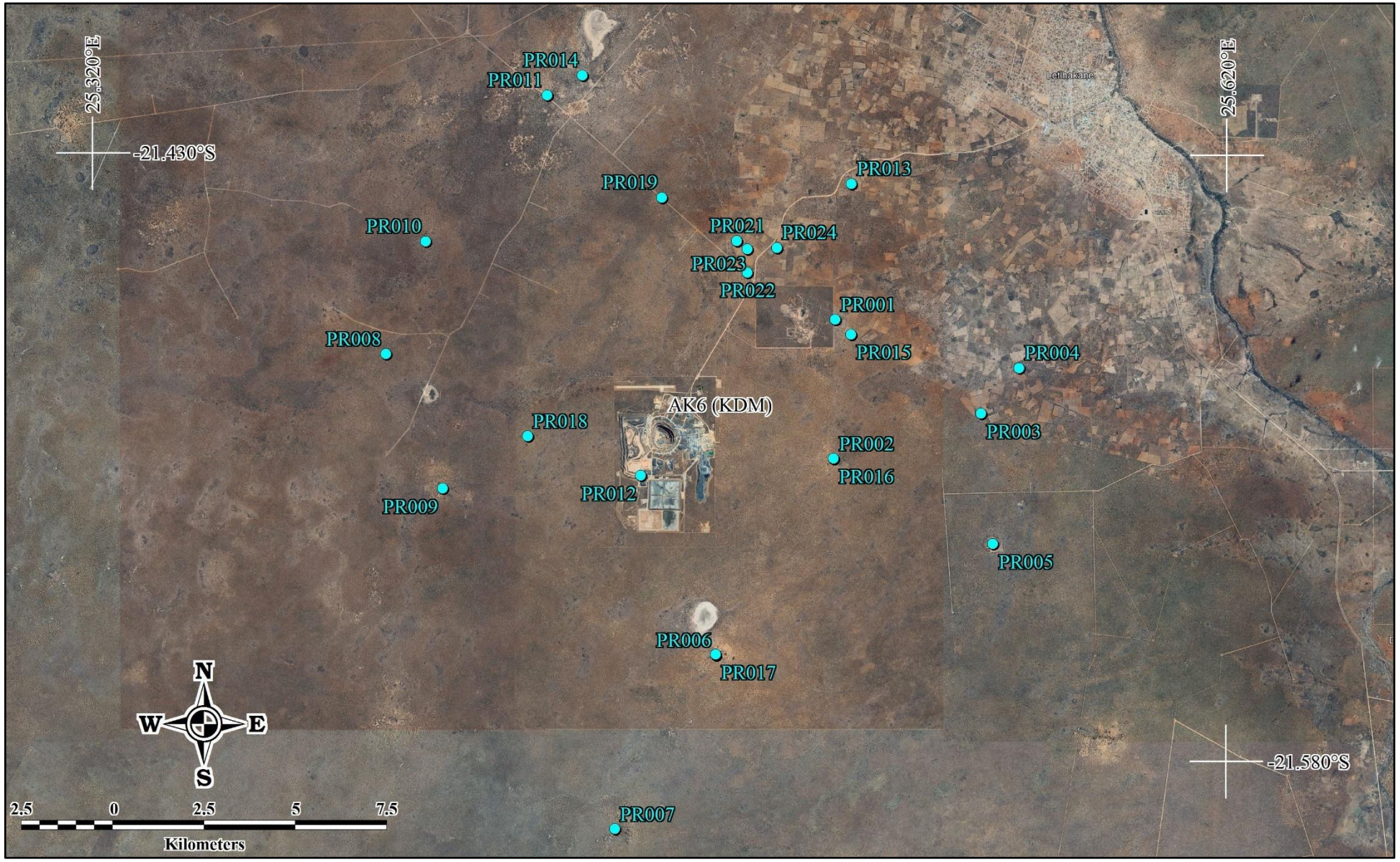

Figure 4.1: Positions of the pre-mining farm boreholes around KDM identified during the 2007 hydrocensus.

Figure 4.2: Positions of the wellfield boreholes at KDM.

4.4.3 Dewatering boreholes

The dewatering borehole network consists of 53 boreholes within and surrounding the pit (Figure 4.4). The depths of the boreholes range from 60 m (in-pit boreholes INPT01, 04 and 08) to 760 m (borehole Z33764). The distribution of the borehole depths is shown in Figure 4.3. Dewatering boreholes with depths between 250 m and 299 m are the best represented in the distribution; these boreholes extend through the Stormberg basalts into the underlying sedimentary rocks.

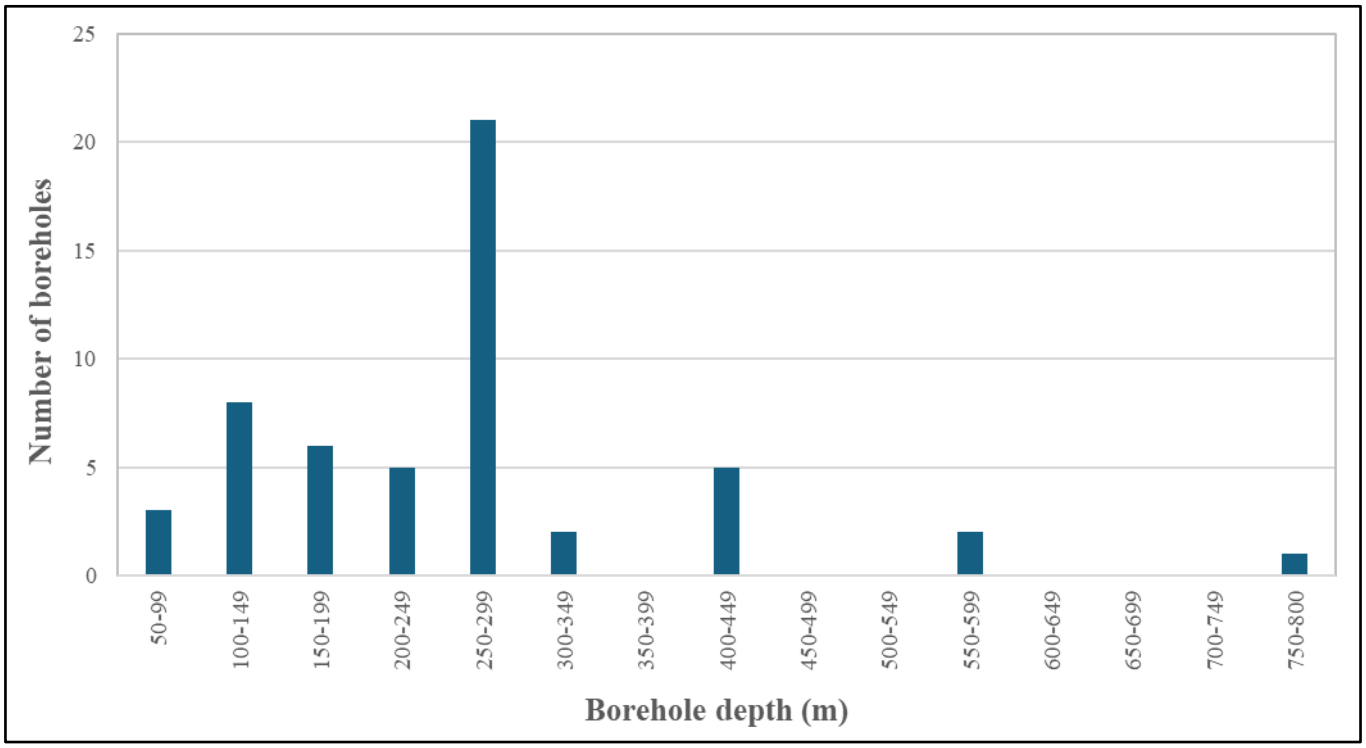

Figure 4.3: Distribution of borehole depths for the dewatering boreholes.

4.4.4 Monitoring boreholes

Although several of the hydrocensus, wellfield and dewatering boreholes form part of the groundwater monitoring network at KDM, there are also dedicated monitoring boreholes across and in the vicinity of the mine site. The positions of these monitoring boreholes are shown in Figure 4.5. Boreholes SMB1 to SMB8 are monitoring boreholes whose purpose is to monitor possible contamination emanating from the slimes dam, while boreholes LMB1 to LMB4 monitor possible impacts on the groundwater environment due to leaching from the waste disposal site (landfill site).

Figure 4.4: Positions of the dewatering boreholes at KDM.

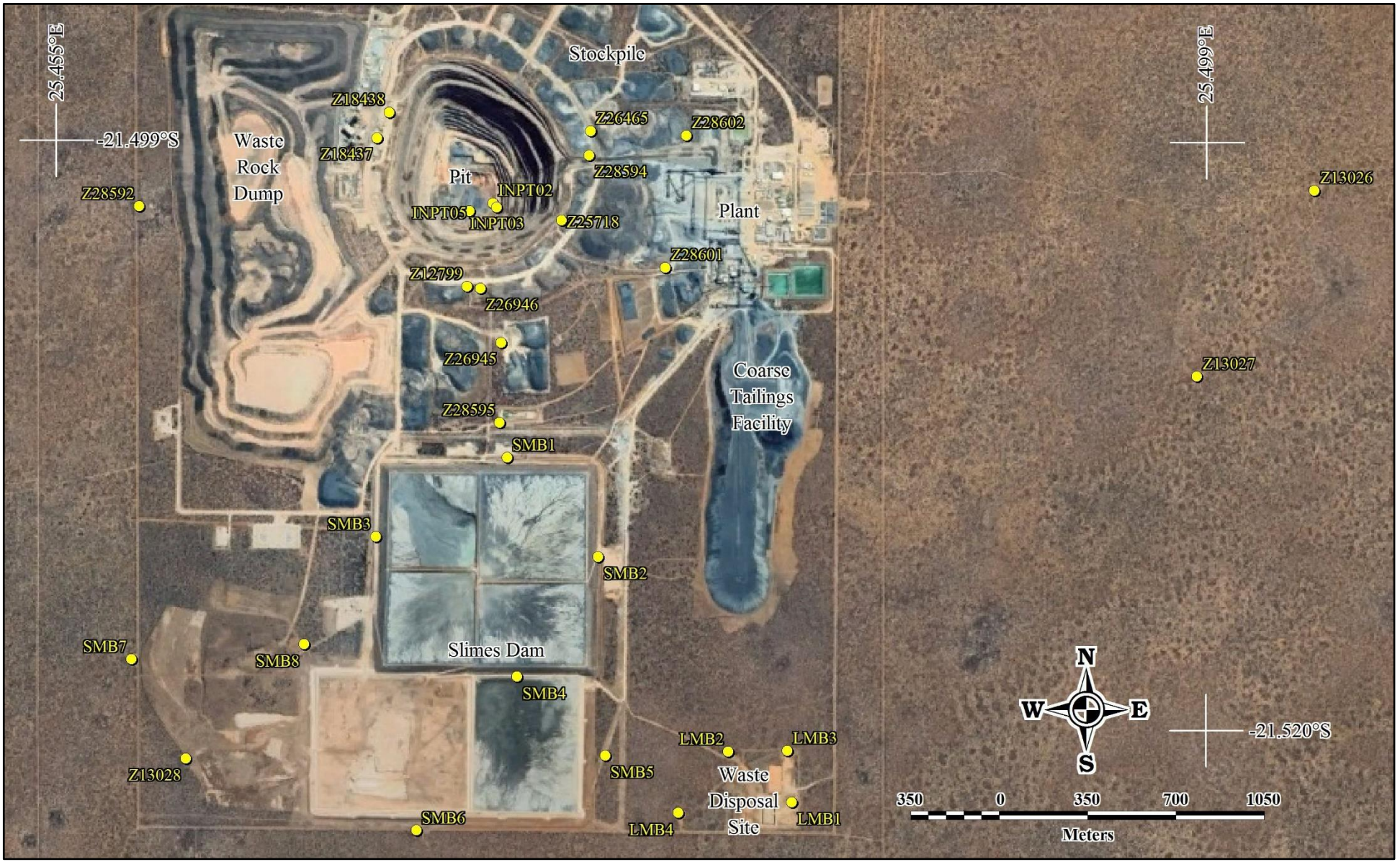

Figure 4.5: Positions of the dedicated monitoring boreholes at KDM.

4.5 BASELINE INVESTIGATIONS

Prior to commencement of mining activities at KDM (formerly known as the AK6 kimberlite pipe) in July 2012, baseline investigations into the groundwater conditions were conducted. The baseline study was based on water quality data collected pre-2009 and obtained from various reports. Baseline data are used as a benchmark against which the impact of mining activities and the effectiveness of interventions can be measured. It should be noted that other diamond mines near KDM (e.g., the Letlhakane Diamond Mine) had been in operation since long before 2009. The baseline investigations therefore reflect the groundwater conditions as they were shortly before mining commenced at KDM and not the groundwater conditions unaffected by mining activities.

4.5.1 Pre-mining groundwater quality

The existing water quality data was collected by WSB (2007) by means of sampling and field measurements. Water samples collected during this investigation were submitted for hydrogeochemical analyses. In the current study, the results of the baseline analyses are compared against the standards specified in the BOS 32:2015 Botswana Drinking Water Guideline as listed in Table 4.4. In this table, the standards of the three water classes are displayed in different colours. Note that not all three water classes are defined for Mn and NO_3. Mn concentrations above 0.5 mg/L and NO_3 concentrations above 45 mg/L are deemed to exceed the maximum allowable concentrations.

The results of the analyses of groundwater samples from the basalt and sandstone aquifers are discussed below.

Table 4.4: BOS32:2015 Drinking Water Standards.

Parameter	Unit	Class I (Ideal)	Class II (Acceptable)	Class III (Maximum Allowable)
pH at 25 ℃	-	6.5 - 8.5	5.5 - 9.5	5.0 - 10.0
EC at 25 ℃	µS/cm	700	1500	3100
TDS	mg/L	450	1500	2000
Ca	mg/L	80	150	200
Mg	mg/L	30	70	100
Na	mg/L	100	200	400
K	mg/L	25	50	100
Fe	mg/L	0.03	0.3	2
Mn	mg/L	0.05	0.5	
Cl	mg/L	100	200	600
SO_4	mg/L	200	250	400
F	mg/L	0.7	1	1.5
NO_3	mg/L	45		

4.5.1.1 Basalt aquifer

The basalt layer hosts both a fractured and weathered aquifer system and has a thickness varying between 20 m and 115 m (WSB, 2007). WSB (2007) sampled four farm boreholes that were pumping from the upper fractured basalt aquifer system. The positions of these boreholes relative to KDM are shown in Figure 4.6.

The results of the hydrochemical analyses performed on the groundwater samples are presented in Table 4.5. The results are colour-coded according to the water quality classes shown in Table 4.4. From Table 4.5, it is seen that the water samples collected by WSB (2007) were dominated by Na-Cl ions. The Cl, Na, Mg and F concentrations exceeded the limits of Class I for most samples. The F concentrations at three boreholes (shown in orange) exceeded the maximum allowable limits as prescribed by the drinking water standards.

The concentrations of other parameters, such as Ca, SO_4, K and NO_3, were below the limits of Class I water (ideal water quality). The TDS concentrations of the groundwater samples ranged between 741 and 1032 mg/L, while pH values varied between 7.1 and 8.1. The values were within the acceptable and ideal limits for drinking water, respectively.

Table 4.5: Hydrochemical analyses of groundwater from boreholes tapping the basalt aquifer

Borehole	pH (-)	TDS (mg/L)	Ca (mg/L)	Mg (mg/L)	Na (mg/L)	K (mg/L)	HCO_3 (mg/L)	CO_3 (mg/L)	SO_4 (mg/L)	Cl (mg/L)	NO_3 (mg/L)	F (mg/L)	Br (mg/L)	SiO_2 (mg/L)
Moremi (PR010)	7.2	1032	74	23	267	4.6	603	12	58	170	23	1.0	4.3	44
Kabakae (PR011)	8.1	741	32	21	225	4.3	486	36	30	102	17	1.9	3.4	35
Binang (PR019)	7.1	880	55	49	198	5.8	161	124	34	234	22	4.1	5.0	38
Moiteelasilo (PR024)	7.5	1018	20	40	327	4.5	676	31	45	129	24	2.2	5.6	41

4.5.1.2 Sandstone aquifer

WSB (2007) sampled 15 boreholes that fully penetrated the deep sandstone aquifer underlying the basalt system. The positions of these boreholes are shown in Figure 4.6, while the results of the chemical analyses are listed in Table 4.6.

Groundwater from the sandstone aquifer is also of the Na-Cl type. The Na and Cl concentrations at almost all the sampled sites exceeded the maximum allowable limits of the BOS32:2015 Drinking Water Standards. The contributions of the high Na and Cl concentrations to the total salt load also caused the TDS concentrations at almost all the boreholes to exceed the maximum allowable limits. Several boreholes intersecting the sandstone aquifer also exhibited elevated SO_4 concentrations.

Figure 4.6: Positions of the boreholes sampling the sandstone and basalt aquifers during the baseline investigations.

Table 4.6: Hydrochemical analyses of groundwater from boreholes tapping the sandstone aquifer.

Borehole	pH (-)	TDS (mg/L)	Ca (mg/L)	Mg (mg/L)	Na (mg/L)	K (mg/L)	HCO_3 (mg/L)	CO_3 (mg/L)	SO_4 (mg/L)	Cl (mg/L)	NO_3 (mg/L)	F (mg/L)	Br (mg/L)	SiO_2 (mg/L)
Z 12239	9.2	2469	5.1	32	773	14	112	125	163	961	23	0.0	0.1	1.0
Z 12299	8.2	2979	32	26	929	13	117	26	678	1025	42	0.0	0.4	2.2
Z 12795	9.7	3326	35	13	998	20	36	67	318	1418	31	0.4	2.7	0.3
Z 12796	8.7	2916	38	14	857	7.7	39	12	494	1085	29	0.0	0.2	1.2
Z 12797	9.0	1436	11	12	435	7.0	98	26	60	592	18	0.5	0.1	0.6
Z 12798	7.9	3376	37	30	1006	13	220	31	332	1317	32	0.0	0.0	2.2
Z 13026	7.1	3074	99	76	842	17	737	19	85	1172	46	0.4	0.6	23
Z 13027	8.2	3836	22	68	1114	20	288	29	292	1555	53	0.0	0.0	1.9
Z 13028	9.3	2053	7.1	22	618	10	39	65	200	764	31	0.0	0.1	0.7
Z 13029	7.5	2457	55	30	675	12	227	29	190	932	34	0.3	0.1	2.5
Z 14846	8.6	2740	7.7	33	861	13	244	24	347	1037	38	0.0	0.1	1.0
Nkalolang (PR009)	7.0	5399	292	68	1448	31	31	0.0	875	2362	49	0.0	2.2	7.6
Kabakae (PR011)	7.9	3395	54	16	1027	12	410	22	258	1245	43	0.0	8.2	8.0
Mokgalo (PR012)	7.2	3609	36	21	696	9.2	473	36	169	696	18	0.1	3.4	8.3
Katholo (PR022)	8.1	1430	33	8.7	399	5.8	136	19	99	484	8.6	0.6	19	19

A single borehole (Nkalalong) had a Ca concentration exceeding the maximum allowable limit, while the Ca concentrations at the remaining boreholes were generally low enough to classify the water quality as ideal. Three boreholes tapping the Mosolotsane sandstone (Z13026, Z13027 and Nkalolang) showed high NO_3 concentrations above the maximum allowable limit of 45 mg/L. Comparison with the water quality data from the basalt aquifer shows that, under natural conditions, the sandstone aquifer carries much higher salt loads.

4.5.2 Pre-mining groundwater levels

The groundwater levels measured in eight boreholes during 2011 can be used to assess the pre-mining conditions. It should be noted that pre-mining conditions refer to the period prior to the commencement of mining at KDM. Other mines in the area had been in operation since long before 2012 when mining activities started at KDM. The groundwater levels measured during 2011 may therefore have been affected by the past activities at the existing mines.

The positions of the boreholes at which the pre-mining groundwater levels were measured are shown in Figure 4.7. These boreholes occur as sets of two to the west, south, east and north-east of KDM. A contour map of the 2011 groundwater levels is presented in Figure 4.9. The groundwater level contours indicate that the pre-mining hydraulic gradient in the vicinity of KDM was to the east and south-east, in the general direction of the Letlhakane River. Although this gradient corresponded to the local topographic gradient, it was likely to have been influenced by groundwater abstraction from Wellfield 6 which occurs east and south-east of KDM (Figure 4.9). The wellfield had been supplying Orapa Diamond Mine since before the start of mining of KDM. Boreholes within Wellfield 6 have shown drawdowns of more than 50 m since abstraction started in the late 1980s (SADC-GMI, 2020).

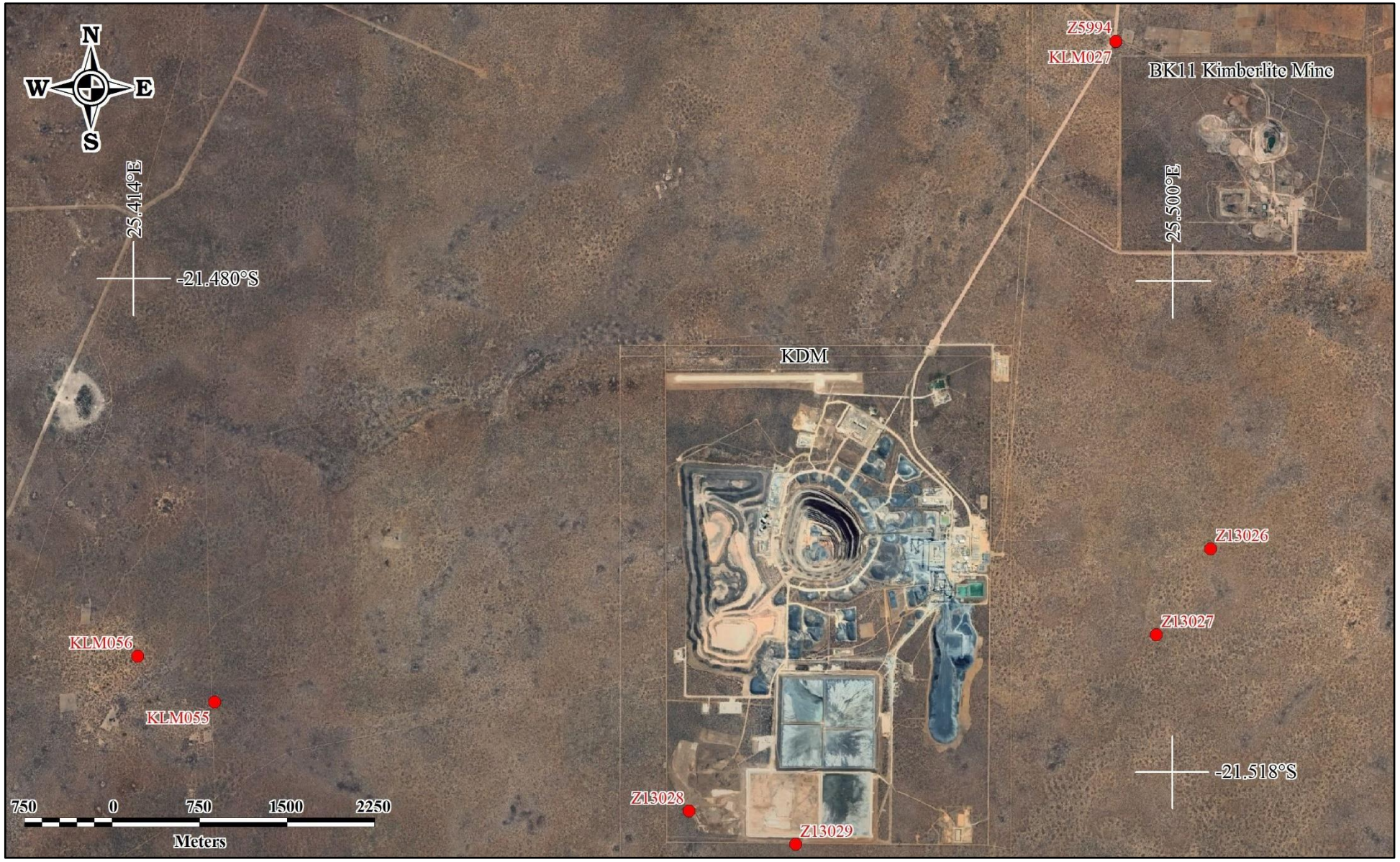

Figure 4.7: Positions of the boreholes in which the pre-mining groundwater levels were measured.

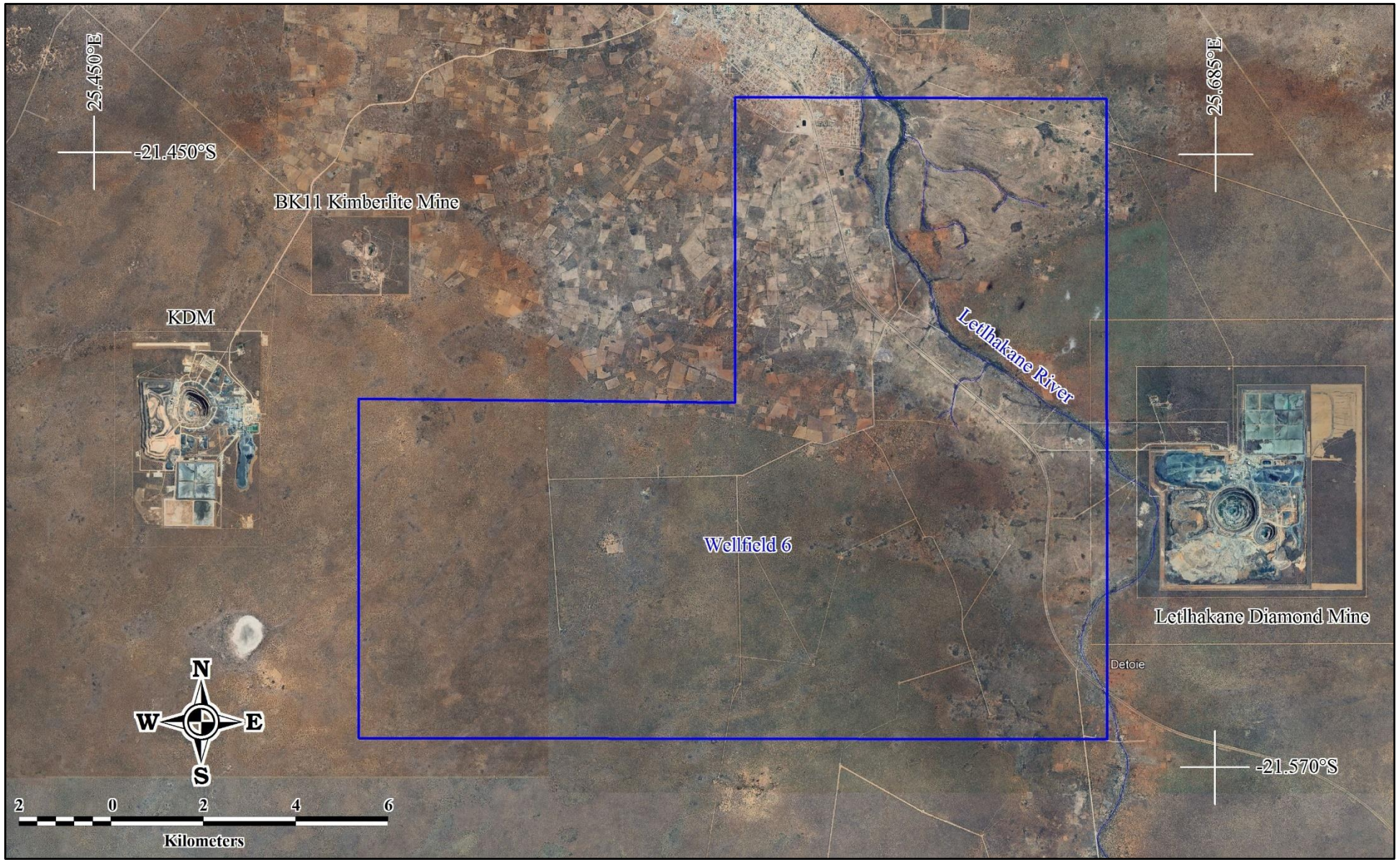

Figure 4.8: Positions of Wellfield 6 relative to KDM and other diamond mines.

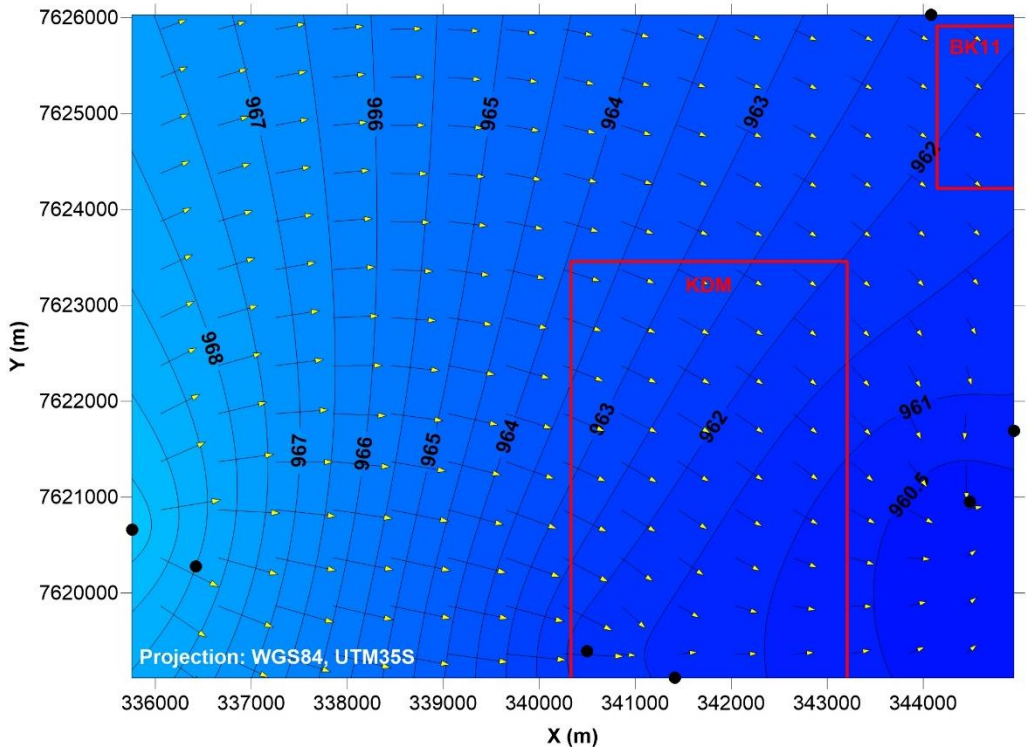

Figure 4.9: The pre-mining (2011) groundwater levels in the vicinity of KDM.

The pre-mining groundwater levels shown in Figure 4.9 reflect the influence of Wellfield 6. Water level data from 2005 (KLMCS, 2018) may be used to determine the regional groundwater levels prior to the development of Wellfield 6 (Figure 4.10).

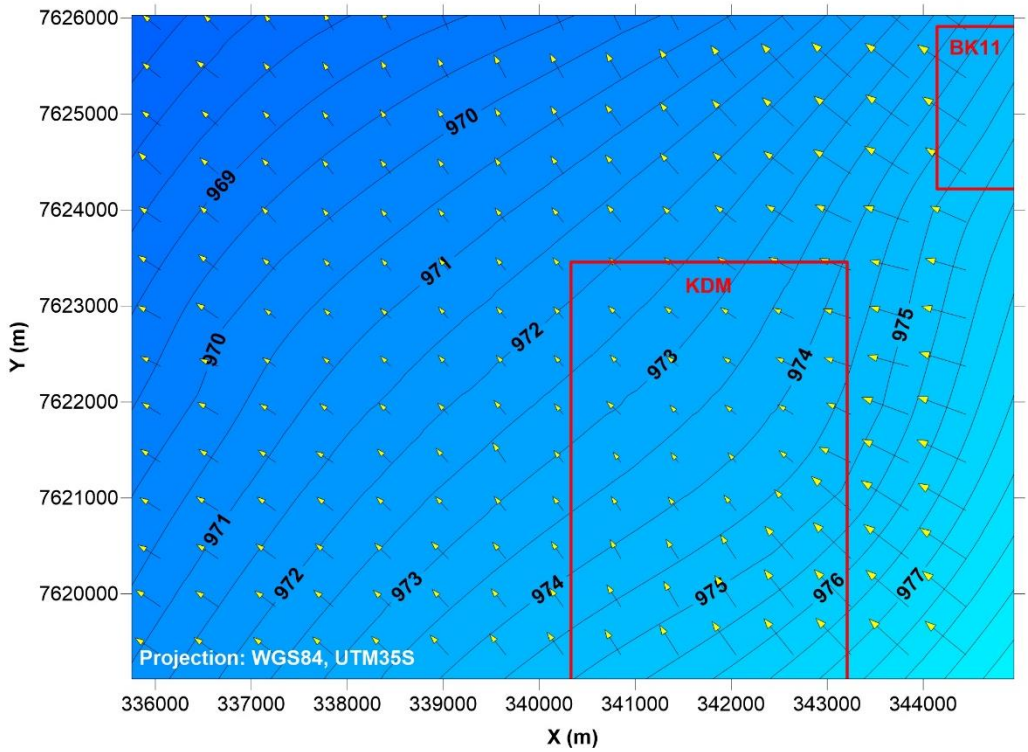

Figure 4.10: The groundwater levels in the vicinity of KDM in 2007, prior to the development of Wellfield 6.

Between 1989 – 2019, wellfield 6 abstracted groundwater in the range 100 000 – 500 000 m^3/yr and that likely influenced the regional water table and shifted the original groundwater flow direction (AquiSim, 2021). However, the data from Wellfield 6 was not available for inclusion in the research study.

Figure 4.10 shows that the regional groundwater flow in the vicinity of KDM was to the north-west prior to the commencement of groundwater abstraction from the boreholes in Wellfield 6. Wellfield 6 is owned and operated by Debswana Mining Company and was initially developed in 1989 (AquiSim, 2021). The regional groundwater flow is SE/SSE to NW/NNW (KLMCS, 2010). The general piezometry was distorted when high gradients developed around Debswana mines of Orapa, Letlhakane and Damtshaa caused by pit dewatering and water supply boreholes (KLMCS, 2010).

4.6 GROUNDWATER MONITORING DURING THE MINING PHASE

This section describes the groundwater monitoring that has taken place during the current mining (production) phase of KDM. The results of a monitoring event that took place during April and May 2023 are discussed and temporal changes in the water quality that have occurred since mining started are described.

4.6.1 Groundwater sampling and analyses

4.6.1.1 Sampling protocol and analysis methods

At each sampling site, TDS, conductivity, pH and temperature were recorded using a portable conductivity meter. Water samples were collected in 500 ml plastic bottles for further analysis in the laboratory. The analysis was done by an independent laboratory. The samples were analysed for physical determinants, and macro and micro parameters. The laboratory used the analysis methods listed in Table 6.1.

Table 4.7: Laboratory methods used for hydrochemical analyses.

Equipment/technique	Parameters/analytes tested
Ion Chromatography (ICS 300)	Mg, F, Br, Cl, NO_2, NO_3, PO_4, SO_4, Ca, Na, K, pH, EC
Auto Titrator	pH, EC, Alkalinity, Cl, TDS
ICP - MS	As, Mn, Fe, K, Si, P

4.6.1.2 Quality control and quality assurance

The purpose of quality control in water sampling is to ensure all processes from pre-sampling to laboratory analysis is scientifically acceptable. Prior to sampling, all field conductivity meters were calibrated. Sample bottles were prepared by the laboratory, one acidified and the other non-acid. The

purpose of the acidified samples was to ensure that the samples were fixed and would not change chemically before analysis. All boreholes were purged by pumping for a minimum of 30 minutes before a sample was taken.

4.6.1.3 Data validation

A series of data checks were performed to identify inconsistencies within the data. The following tests were done:

- Checking the cation – anion balance,
- Checking the correlation between EC and TDS, and,
- Checking if data are reasonable and scientifically sound.

4.6.2 The 2023 monitoring event

4.6.2.1 Sampled sites

The sites sampled during the 2023 monitoring event included 22 KDM boreholes around the pit and north of the Waste Rock Dump, and 10 farm boreholes. All samples were subjected to physicochemical analysis and the results were compared to the BOS 32:2015 drinking water guidelines. The locations of the sampling points are shown in Figure 4.11 (KDM boreholes) and Figure 4.12 (farm boreholes).

Figure 4.11: Positions of the KDM boreholes sampled during the 2023 monitoring event.

Figure 4.12: Positions of the farm boreholes sampled during the 2023 monitoring event.

4.6.2.2 Groundwater quality and type

4.6.2.2.1 Farm boreholes

The results of the hydrochemical analyses performed on the groundwater samples are presented in Table 4.9. The results indicate that the Na, Cl and NO_3 concentrations in the groundwater from the farm boreholes are much higher than the limits of the BOS32:2015 drinking water guidelines. The high concentrations of these ions cause the high TDS concentrations and EC values observed at the farm boreholes. As mentioned in Section 4.5.1, the high Na and Cl concentrations were also observed in the pre-mining analyses of groundwater samples from farm boreholes, particularly from boreholes sampling the sandstone aquifer. The high salt loads therefore appear to have a natural origin, at least partly.

Two farm boreholes (Binang and Moiteelasilo) were sampled during both the pre-mining and 2023 monitoring events. Comparison of the hydrochemical compositions of samples from pre-mining and the 2023 event shows that some changes did occur over this period. While the groundwater quality at Binang (PR019) seems to have improved, higher salt loads (Na, Cl, NO_3) were recorded at Moiteelasilo. The reasons for these changes are uncertain but could include seasonal variations and mining impacts (Table 4.8).

Table 4.8: Comparison of the hydrochemical results from pre-mining and 2023 at two farm boreholes.

Borehole	Date	pH (-)	TDS (mg/L)	Ca (mg/L)	Mg (mg/L)	Na (mg/L)	K (mg/L)	HCO_3 (mg/L)	CO_3 (mg/L)	SO_4 (mg/L)	Cl (mg/L)	NO_3 (mg/L)	F (mg/L)
Binang (PR019)	pre-mining	7.1	880	55	49	198	5.8	161	124	34	234	22	4.1
Binang (PR019)	2023	7.9	627	58	36	76	2.2	449	0	11	43	27	0.1
Moiteelasilo (PR024)	pre-mining	7.5	1018	20	40	327	4.5	676	31	45	129	24	2.2
Moiteelasilo (PR024)	2023	7.6	1476	46	28	502	6.4	854	0	64	280	108	1.0

Of the farm boreholes, four samples had TDS concentrations within the Class I limits of the BOS32:2015 drinking water guidelines, while five samples exhibited Class II TDS concentrations. Five samples had NO_3 concentrations above the maximum allowable for drinking water (Table 4.9). Farm boreholes exhibiting lower TDS concentrations could represent groundwater from the weathered and fractured basalt aquifer system. The two samples with elevated manganese concentrations could reflect either weathering of manganese-bearing rocks or impacts from external source such as landfill leachate and sewage (Lucara Botswana, 2023).

Table 4.9: Results of hydrochemical analyses performed on samples from the farm boreholes.

Sample ID	Date sampled	pH	EC (µS/cm)	TDS (mg/L)	Alkalinity (mg/L $CaCO_3$)	T. Hardness (mg/L $CaCO_3$)	Ca Hardness (mg/L $CaCO_3$)	Ca (mg/L)	Mg (mg/L)	Na (mg/L)	K (mg/L)	Fe (mg/L)	Mn (mg/L)	HCO_3 (mg/L)	CO_3 (mg/L)	SO_4 (mg/L)	Cl (mg/L)	NO_3 (mg/L)	F (mg/L)	Ionic bal. (%)
Leitshokile (PR002)	25/04/23	7.62	2680	1600	428	236	116	46	29	480	8.8	0.01	0.28	522	0	130	420	37	0.2	4.24
Mothelo (PR018)	25/04/23	7.42	3120	1840	508	300	146	58	37	462	11	0.02	0.02	620	0	83	410	57	0.1	3.94
Binang (PR019)	25/04/23	7.92	925	627	368	294	146	58	36	76	2.2	0.05	0.00	449	0	11	43	27	0.1	-0.08
Masego (PR021)	25/04/23	8.00	3140	1830	416	234	140	56	23	551	9.2	0.14	0.34	508	0	100	580	0	0.2	3.80
Katholo (PR022)	25/04/23	7.61	1462	808	266	234	166	66	17	209	4.2	0.12	0.00	325	0	36	180	108	0.2	3.67
Bright (PR023)	25/04/23	7.57	2936	1692	292	350	208	83	35	444	13	0.12	0.00	356	0	121	535	117	0.0	2.54
Moiteelasilo (PR024)	25/04/23	7.58	2513	1476	700	230	114	46	28	502	6.4	0.11	0.00	854	0	64	280	108	1.0	3.08
Israel (PR024)	25/04/23	7.90	1467	1024	550	114	64	26	12	302	2.2	0.14	0.00	671	0	23	70	51	0.9	3.92
Ookeditse (Nkwe Farm)	25/04/23	7.93	3040	1674	290	222	128	51	23	520	9.2	0.15	0.00	354	0	121	560	39	0.3	4.90

Figure 4.13 is a Piper diagram of the groundwater samples from the farm boreholes. Although many of the farm boreholes contain groundwater with high Na and Cl concentrations, the dominant water type at many boreholes is Na-HCO_3. There is also evidence for mixing of groundwater from different sources, as suggested by the large range of Cl and Na concentrations observed at the different boreholes. Much lower Na and Cl concentrations were recorded at the Binang farm. These concentrations were even significantly lower than the pre-mining concentrations. The reason for the low salt loads at Binang as compared to the other farm boreholes during the 2023 monitoring event is currently unknown but may indicate that the groundwater in this borehole predominantly comes from the shallow basalt aquifer with little influence form the deeper more saline sandstone aquifer.

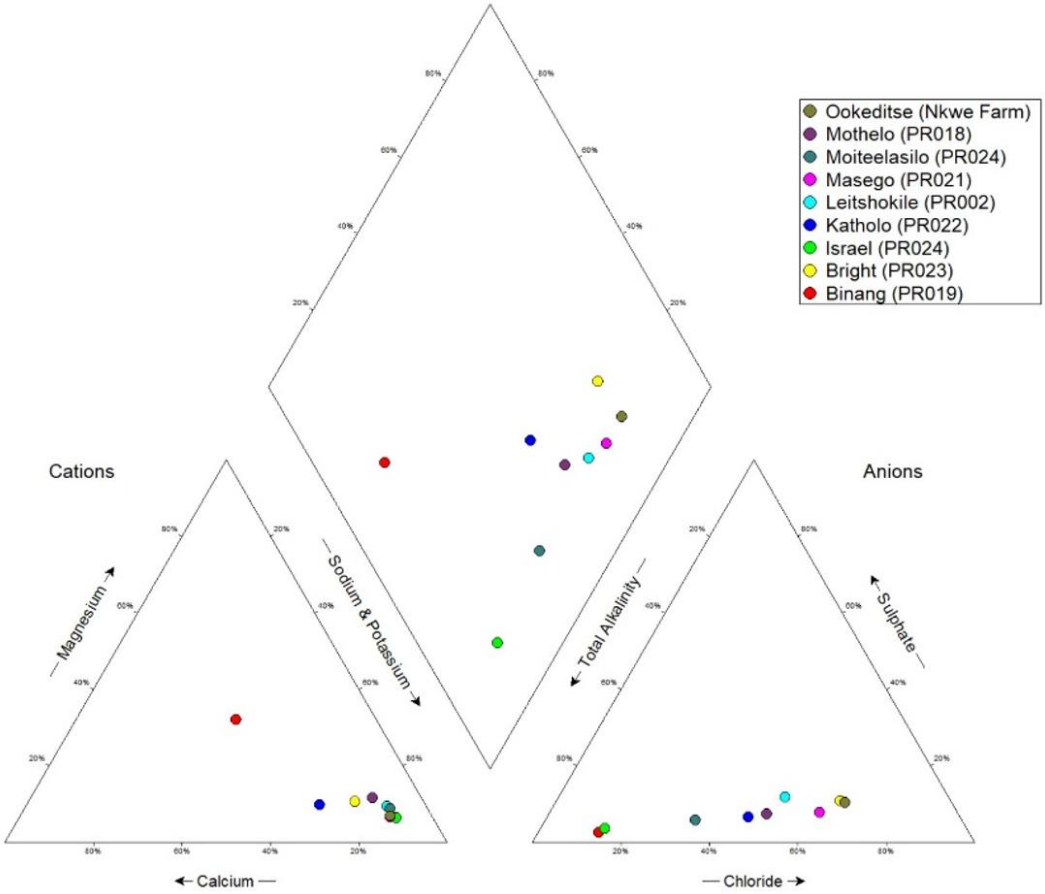

Figure 4.13: Piper diagram of the groundwater samples from the farm boreholes (2023).

An Expanded Durov diagram of the groundwater samples from the farm boreholes is presented in Figure 4.14. The groundwater samples plot in four different fields of the diagram. Binang (PR019) plots in Field 2, representing fresh, clean and relatively young groundwater. Israel (PR024) and Moiteelasilo (PR024) plot in Field 3, representing fresh, clean and relatively young groundwater that has undergone Na ion-exchange or has become contaminated with a Na-rich source. Katholo (PR022) and Mothelo (PR018) fall in Field 6, which indicates that mixing of different water types has occurred and that the water has been enriched with Na. Bright (PR023), Ookeditse, Masego (PR021) and

Leitshokile (PR002) plot in Field 9, which corresponds to very old, stagnant water or water that has undergone significant ion exchange.

The fact that different water types are observed at the different boreholes may be related to the aquifers intersected by the boreholes. Binang, Moiteelasilo and Isreal all sample the shallow basalt aquifer with its lower salt loads. This aquifer is more likely to be recharged with fresh rainwater than the deeper sandstone aquifer. The groundwater characteristics at boreholes Bright, Ookeditse and Masego indicate that these boreholes sample the sandstone aquifer.

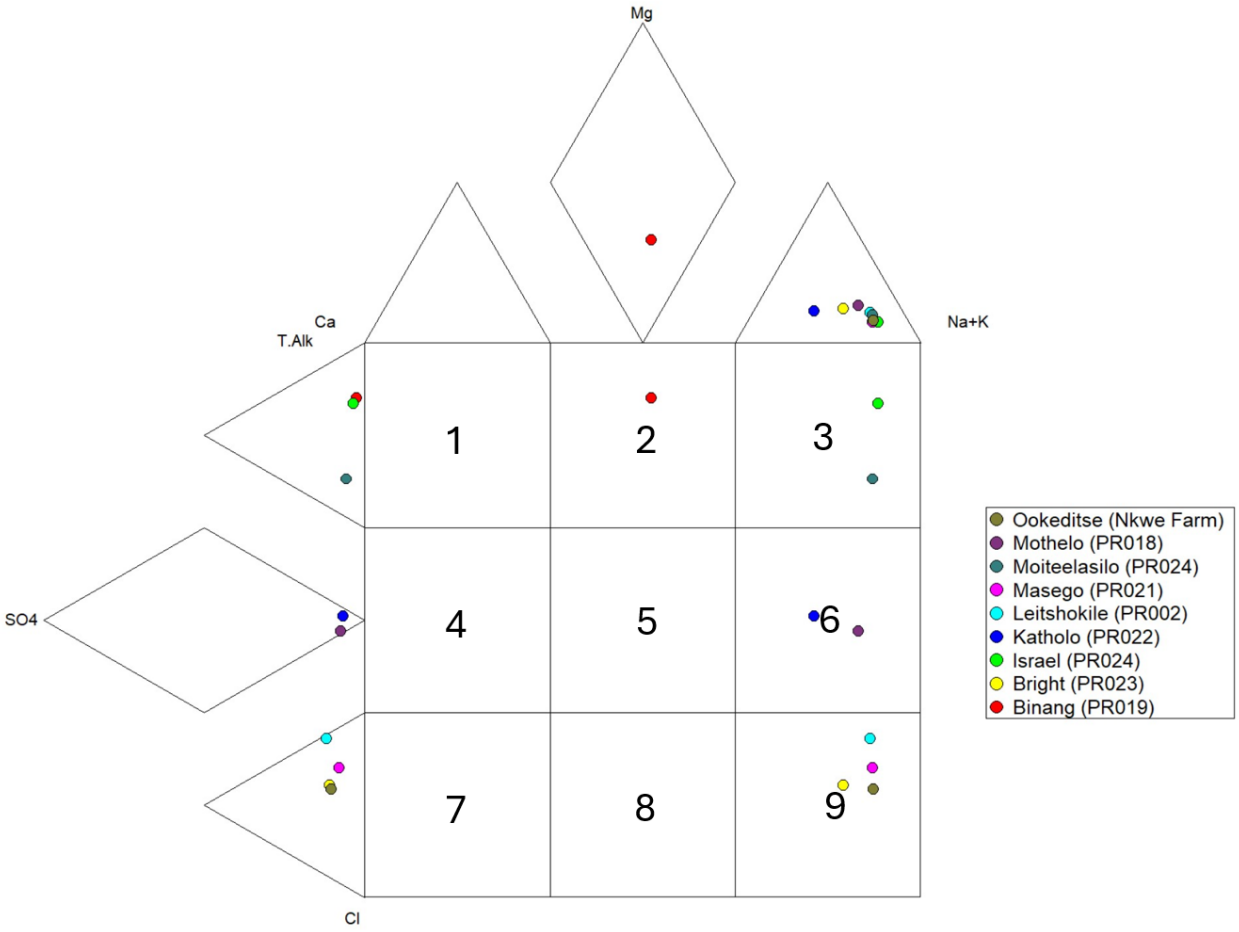

Figure 4.14: Expanded Durov diagram of the groundwater samples from the farm boreholes (2023).

4.6.2.2.2 KDM boreholes

The results of the hydrochemical analyses performed on water samples taken from the KDM boreholes during the 2023 monitoring event are presented in Table 4.10. What is immediately apparent is that all the boreholes exhibit Na and Cl concentrations exceeding the maximum allowable limits of the drinking water standards.

Table 4.10: Results of hydrochemical analyses performed on samples from the KDM boreholes.

Sample ID	Date sampled	pH	EC (µS/cm)	TDS (mg/L)	Alkalinity (mg/L $CaCO_3$)	T. Hardness (mg/L $CaCO_3$)	Ca Hardness (mg/L $CaCO_3$)	Ca (mg/L)	Mg (mg/L)	Na (mg/L)	K (mg/L)	Fe (mg/L)	Mn (mg/L)	HCO_3 (mg/L)	CO_3 (mg/L)	SO_4 (mg/L)	Cl (mg/L)	NO_3 (mg/L)	F (mg/L)	Ionic bal. (%)
Z12299	07/05/23	7.98	3761	2294	408	476	396	158	19	640	11	0.04	0.13	498	0	297	665	70	1.0	4.66
Z12796	07/05/23	7.92	3683	2172	414	392	356	142	8.8	720	11	0.50	0.09	505	0	285	797	72	0.3	2.02
Z12797	07/05/23	7.91	3958	2494	386	424	364	146	15	780	12	0.03	0.20	471	0	353	815	39	1.0	4.88
Z12798	07/05/23	8.02	4333	2526	430	336	280	112	14	960	11	0.03	0.18	525	0	689	795	29	1.0	3.03
Z15562	07/05/23	8.10	5003	3036	476	432	396	158	8.8	1000	11	0.03	0.18	581	0	645	980	39	2.0	1.07
Z15563	07/05/23	7.91	3940	2442	448	368	316	126	13	880	11	0.17	0.09	547	0	507	755	47	1.0	4.92
Z15564	07/05/23	8.00	4029	2440	454	356	320	128	8.8	880	11	0.02	0.13	554	0	604	825	31	1.0	0.22
Z15565	07/05/23	7.86	3957	2276	428	388	348	139	9.7	800	12	0.02	0.18	522	0	381	827	71	1.0	2.19
Z15567	07/05/23	8.20	3981	2352	372	320	284	114	8.8	880	10	0.03	0.16	454	0	521	762	67	0.2	4.73
Z15568	07/05/23	7.99	3875	2370	400	364	320	128	11	800	12	0.04	0.13	488	0	359	842	67	2.0	2.35
Z15570	07/05/23	7.93	3804	2256	412	388	356	142	7.8	780	12	0.11	0.20	503	0	319	800	65	0.3	4.35
Z15572	07/05/23	7.85	4130	2468	412	424	396	158	6.8	750	12	0.02	0.07	503	0	389	725	45	2.0	4.81
Z15575	07/05/23	7.99	4084	2562	430	384	336	134	12	880	11	0.02	0.11	525	0	598	755	35	2.0	3.61
Z18434	07/05/23	8.22	3443	2058	390	308	256	102	13	720	9.4	0.02	0.20	476	0	398	660	64	0.2	2.68
Z18435	07/05/23	8.18	3712	2140	388	296	244	98	13	720	12	0.03	0.16	473	0	292	690	52	0.3	4.72
Z26457	07/05/23	7.87	3670	2239	394	352	312	125	9.7	680	11	0.02	0.20	481	0	299	652	65	0.6	4.71
Z26458	07/05/23	7.61	3705	2246	478	384	332	133	13	720	11	0.08	0.05	583	0	365	757	45	1.0	-0.01
Z28597	07/05/23	7.51	9643	6144	312	1460	1380	552	19	1500	15	0.02	0.20	381	0	472	2524	45	1.0	2.89
Z28598	07/05/23	7.66	4444	2614	368	424	388	155	8.8	1500	11	0.07	0.22	449	0	582	2524	62	1.0	3.10
Z28600	07/05/23	7.58	18930	13786	238	3390	3310	1324	19	3040	18	0.03	0.18	290	0	1579	6039	23	2.0	-1.98
Z28605	07/05/23	8.01	3605	2068	390	340	300	120	9.7	720	11	0.08	0.18	476	0	286	707	60	2.0	4.95
Z33763	07/05/23	7.70	4344	2596	548	484	400	160	20	800	13	0.01	0.17	669	0	493	708	40	2.0	3.30

The NO_3 and SO_4 concentrations at most boreholes are also much higher than at the farm boreholes. The contribution of these salts to the TDS concentration causes the KDM borehole with the lowest TDS value (Z18434, 2058 mg/L) to have a higher concentration than the farm borehole with the highest TDS value (Mothelo, 1840 mg/L). The above observations show the impact that mining has had on the groundwater quality. The parameters most affected by mining impacts are Na, Cl, NO_3 and SO_4 (along with TDS and EC). These parameters can therefore be used to assess mining impacts on the groundwater environment.

All the groundwater samples from the KDM boreholes were taken from the deep aquifer system below the basalt, at depths exceeding 130 mbgl. Sample Z28600 recorded the highest TDS concentration because the sample was a blend of sandstone water and water originating from depths greater than 400 mbgl. All groundwater samples indicate alkaline conditions with a pH ranging between 7.51 to 8.22.

A Piper diagram of the groundwater samples from the KDM boreholes is presented in Figure 4.15. All the KDM boreholes are seen to contain groundwater of similar characteristics, belonging to the Na-Cl type.

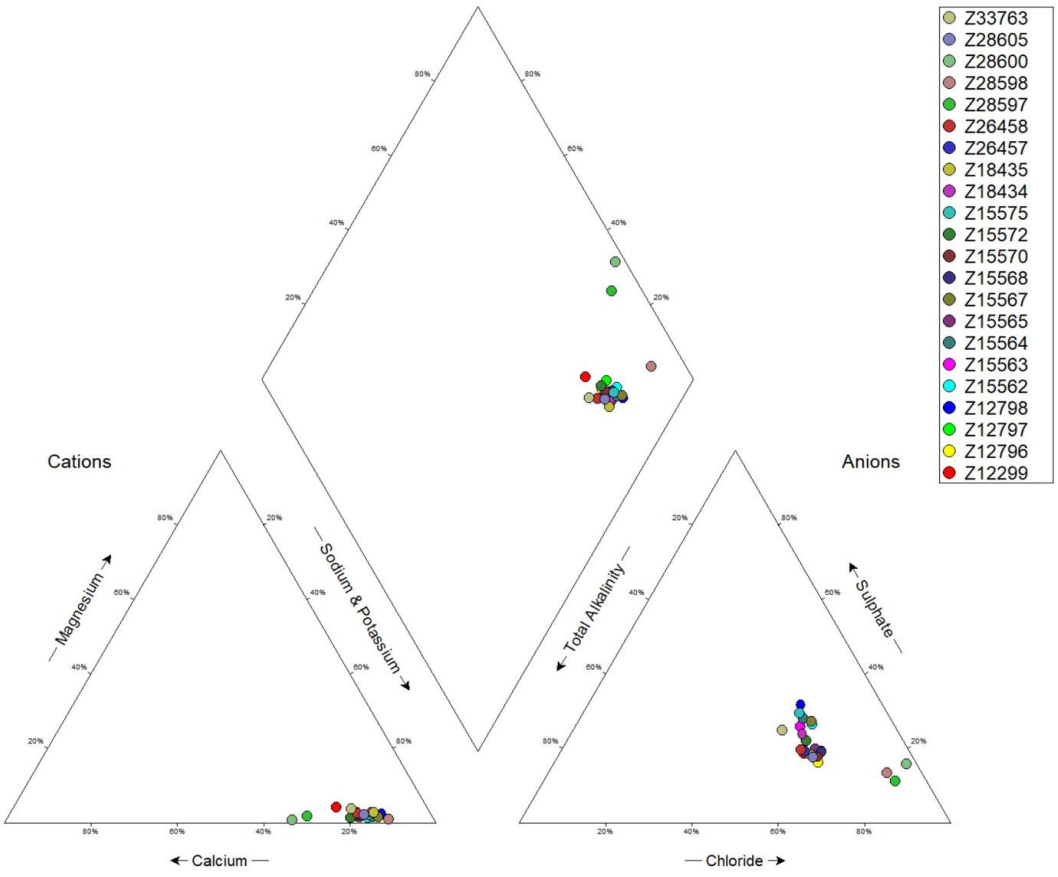

Figure 4.15: Piper diagram of the groundwater samples from the KDM boreholes (2023).

Figure 4.16 is an Expanded Durov diagram of the groundwater samples from the KDM boreholes. All the borehole samples plot in Fields 6 and 9, typical of old or stagnant water, or water that has been enriched with Na from either natural sources or contamination.

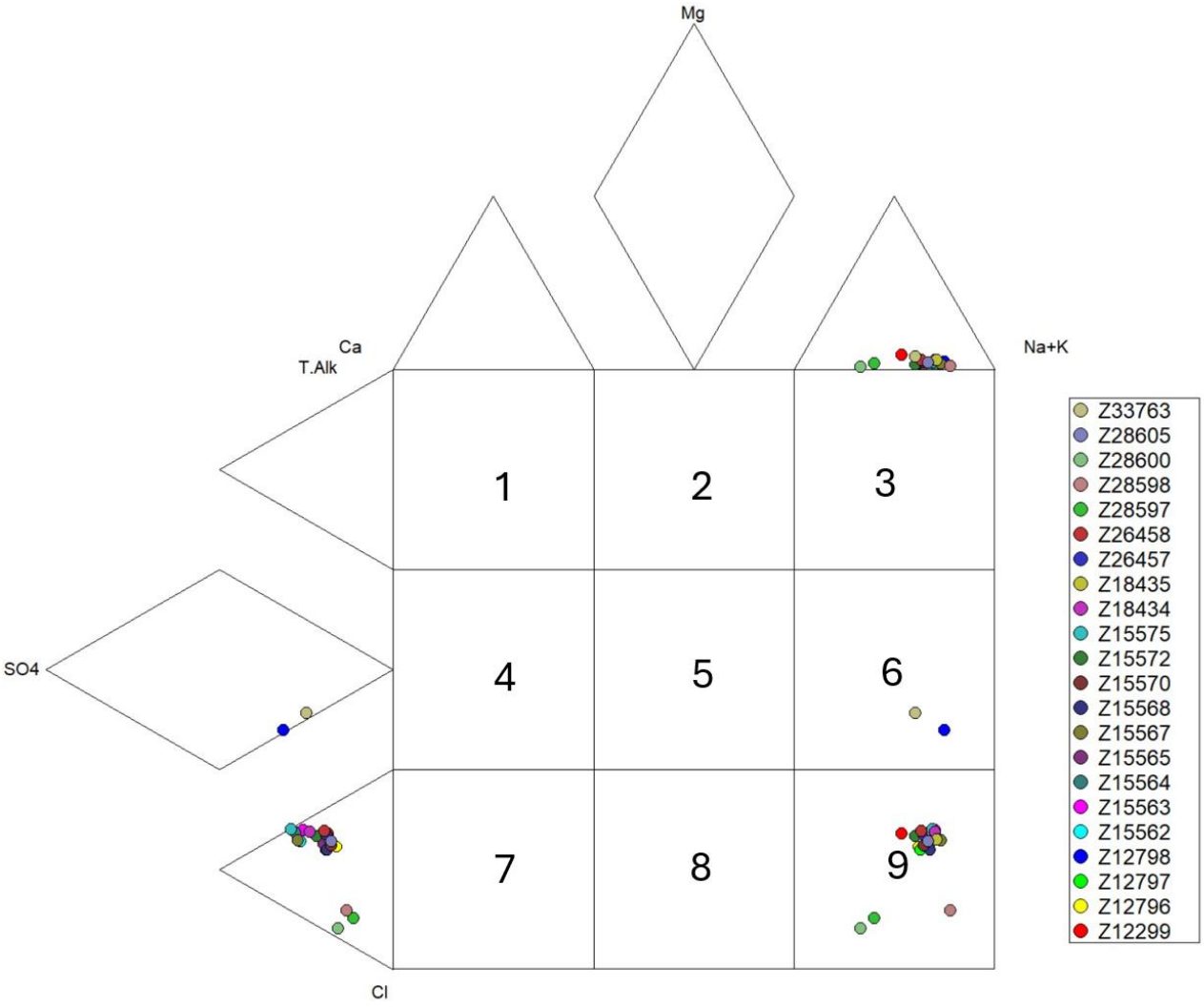

Figure 4.16: Expanded Durov diagram of the groundwater samples from the KDM boreholes (2023).

4.6.3 Water quality of the Mea-arkose and weathered granite

Between 2018 and 2021, six dewatering boreholes around the pit were drilled through the Mea-arkose into the underlying basement granites (Lucara Botswana, 2023) (Figure 4.17). The depths of these boreholes range between 519 m and 760 m. Two to four water strikes occurred in each of the boreholes, with the deepest water strikes occurring at depths of 540 mbgl and 565 mbgl, within the granite basement. Groundwater from the granites is predominantly of the Na-Cl type. Two of the six boreholes drilled within the granite recorded TDS concentrations exceeding 15 000 mg/L (Lucara Botswana, 2023). The HCO_3 concentrations at both boreholes were less than 100 mg/L, indicating the absence of freshwater recharge into the granite system (KLMCS, 2007a).

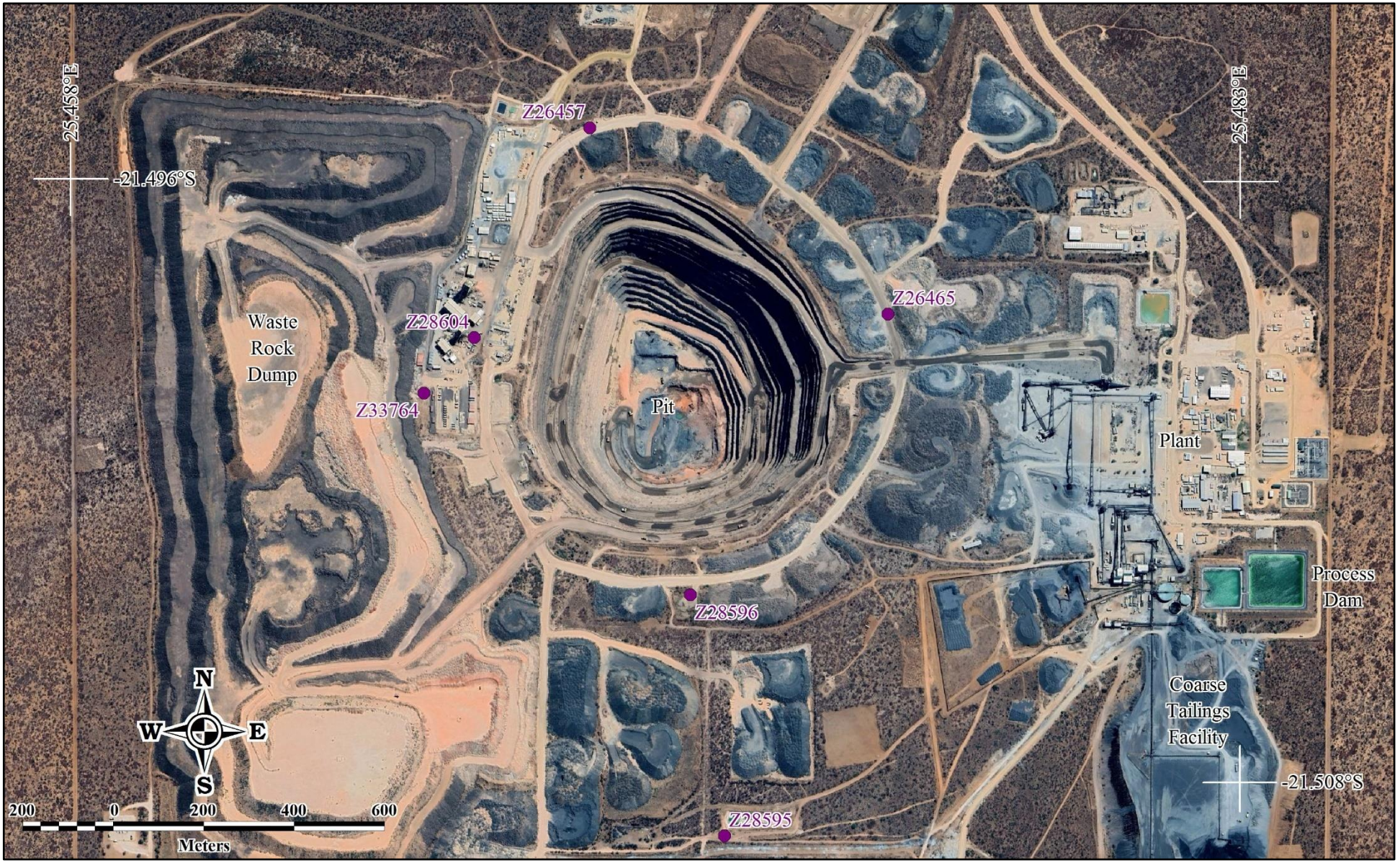

Figure 4.17: Positions of the six boreholes drilled into the Mea-arkose and the weathered granite.

4.6.4 Temporal changes in the groundwater quality

In this section, the variations in the groundwater quality as observed in the KDM and farm boreholes are discussed. Time graphs of the Na, Cl, SO_4 and NO_3 concentrations as well as the pH values recorded at the different boreholes are presented in **Appendix A**.

4.6.4.1 Water quality at the KDM boreholes

Although some variations in the water quality of the KDM boreholes are apparent, in general no increasing trends in the parameter concentrations are observed. The TDS concentrations at the KDM boreholes are shown in Figure 4.18. Some variability in the TDS concentrations is seen at boreholes Z28597, Z28598 and Z15569. These boreholes all occur on the northern perimeter of the pit. Most of the other boreholes display high, but stable, TDS concentrations. The only borehole at which a clear increasing trend in the TDS concentration is observed is borehole Z28600 on the western perimeter of the pit. It is currently unknown why this borehole displays an increasing trend, inconsistent with the other boreholes.

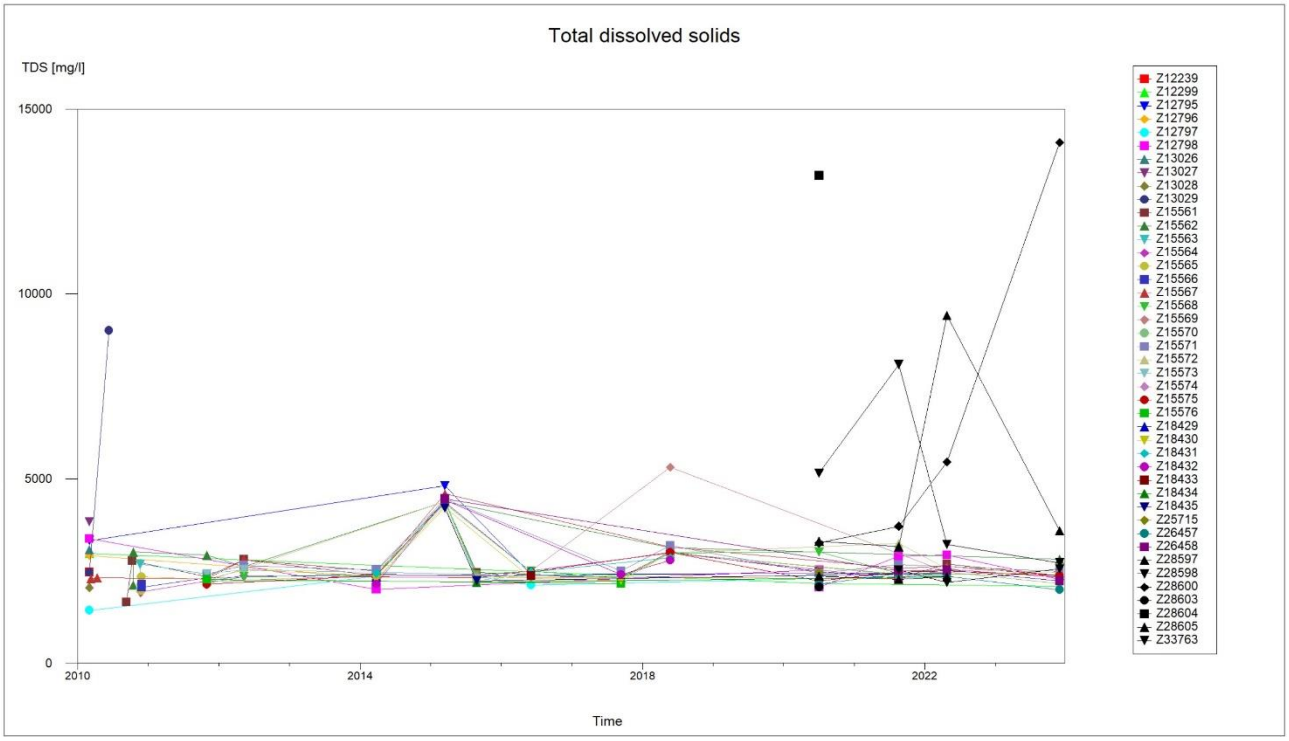

Figure 4.18: Temporal changes in the TDS concentrations of the groundwater from the KDM boreholes.

4.6.4.2 Water quality at the farm boreholes.

Only a few measurements of the water quality at the farm boreholes are available from which to investigate the temporal trends in the parameter concentrations. The TDS concentrations recorded at the farm boreholes are shown in Figure 4.19. From the limited available data, it appears that the salt

loads at the farm boreholes have remained over the period spanned by the monitoring events. Only borehole Nkwane (PR021) displays a sharp increase in its TDS concentration. However, only two data points are available for this borehole and no trend can therefore be identified with certainty.

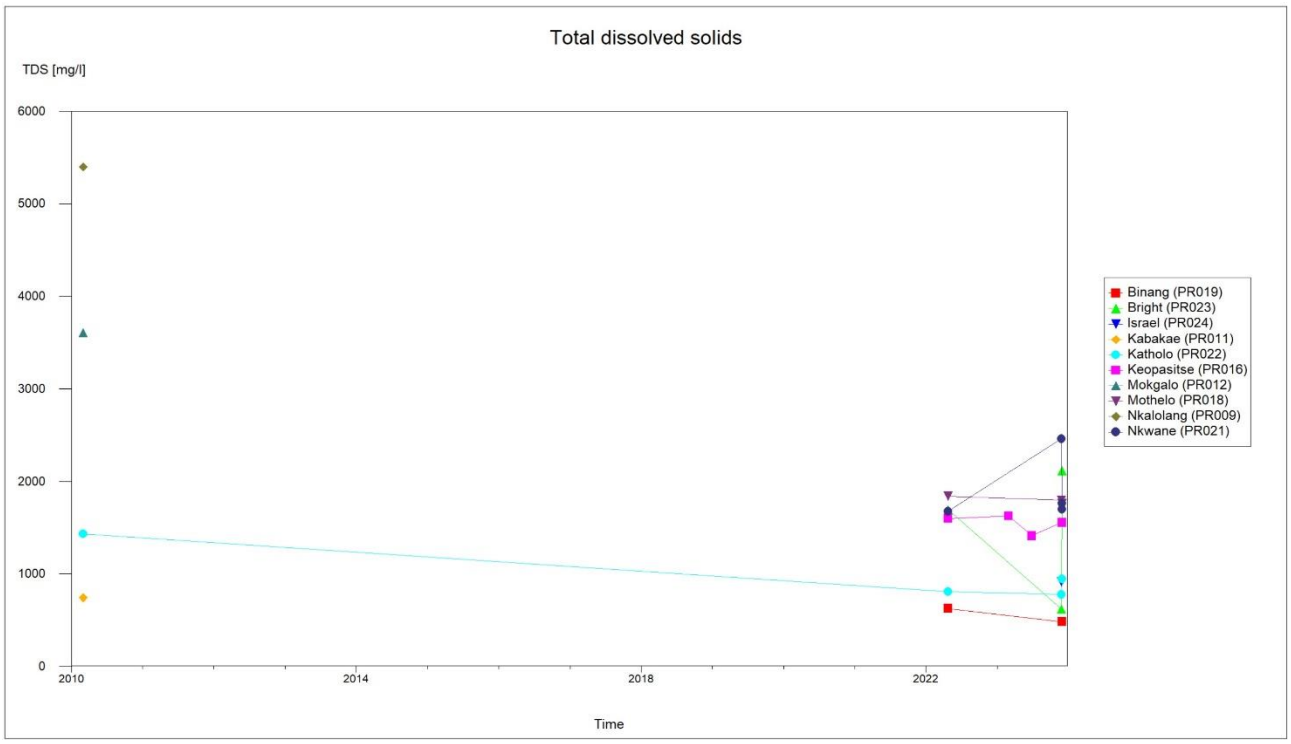

Figure 4.19: Temporal changes in the TDS concentrations of the groundwater from the farm boreholes.

4.6.4.3 Water quality around the slimes dam

Four water quality monitoring boreholes (SMB1 to SMB4) were drilled in 2014 around the slimes dam. When the dams were expanded in 2023, four additional boreholes (SMB5 to SMB8) were drilled and incorporated into the monitoring program. The positions of these boreholes relative to the slimes dam are shown in Figure 4.21.

The temporal variations in the TDS concentrations at the monitoring boreholes around the slimes dam are shown in Figure 4.20. All four of the initial monitoring boreholes (SMB1 to SMB4) initially had TDS concentrations exceeding 10 000 mg/L, but over time these concentrations have decreased and stabilised at below 5000 mg/L. Some variability in the TDS concentrations is also apparent. These variations may be partly due to seasonal effects (e.g., dilution after rainfall events), but may also be due to the residence time of slurry in the slimes dam. Increases in the TDS concentrations may occur when slurry is pumped to the dams and water is not immediately pumped back to the plant, giving it enough residence time to seep into the subsurface and recharge the shallow water table. Similar trends are observed in the Na and Cl concentrations (refer to **Appendix A**).

The SO_4 and NO_3 concentrations at the slimes dam boreholes displayed somewhat different trends. Large variability in the NO_3 concentration at borehole SMB1 was observed between 2016 and 2022, while the SO4 concentration was also variable at boreholes SMB1, SMB2 and SMB4 (**Appendix A**). These variations could again be attributed to seasonal variations and the residence time of slurry in the slimes dams.

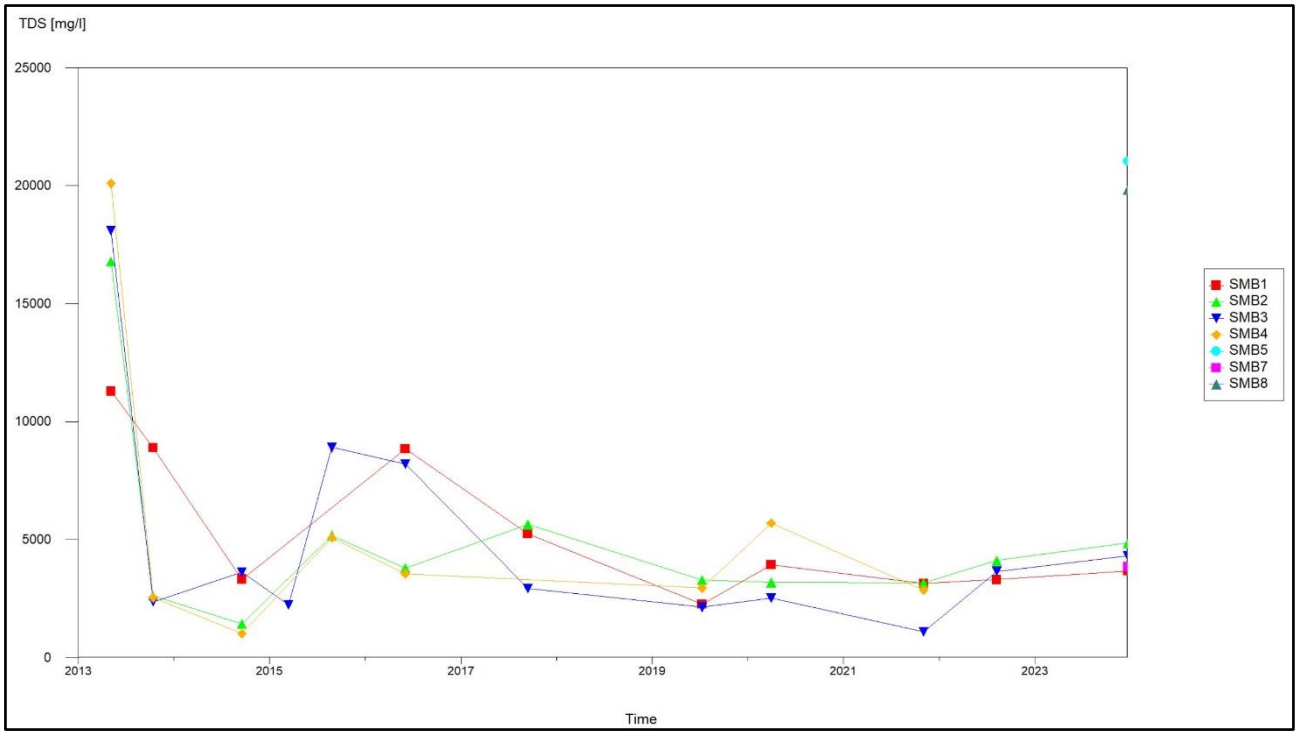

Figure 4.20 Temporal variations in the TDS concentrations in boreholes around the slimes dam.

4.6.4.4 Water quality around the landfill site

In 2014, KDM drilled two boreholes (LMB1 and LMB2) outside the waste disposal (landfill) site to monitor water levels and quality. KDM commissioned a new waste disposal site in 2023 and as a result two additional monitoring boreholes added to the monitoring network, LMB3 and LMB4 (Figure 4.22).

The TDS concentrations recorded at the boreholes of the landfill site are shown in Figure 4.23. The TDS concentrations at boreholes LMB1 and LMB2 were initially below 2000 mg/L in March 2014, but increased to more than 17 000 mg/L (LMB1) and 8600 mg/L (LMB2) by March 2015, suggesting that impacts of seepage from the landfill site had caused deterioration of the groundwater quality. The average TDS values for uncontaminated groundwater from the shallow basalt aquifer is less than 1000 mg/L.

Figure 4.21: Monitoring boreholes for the slimes dam.

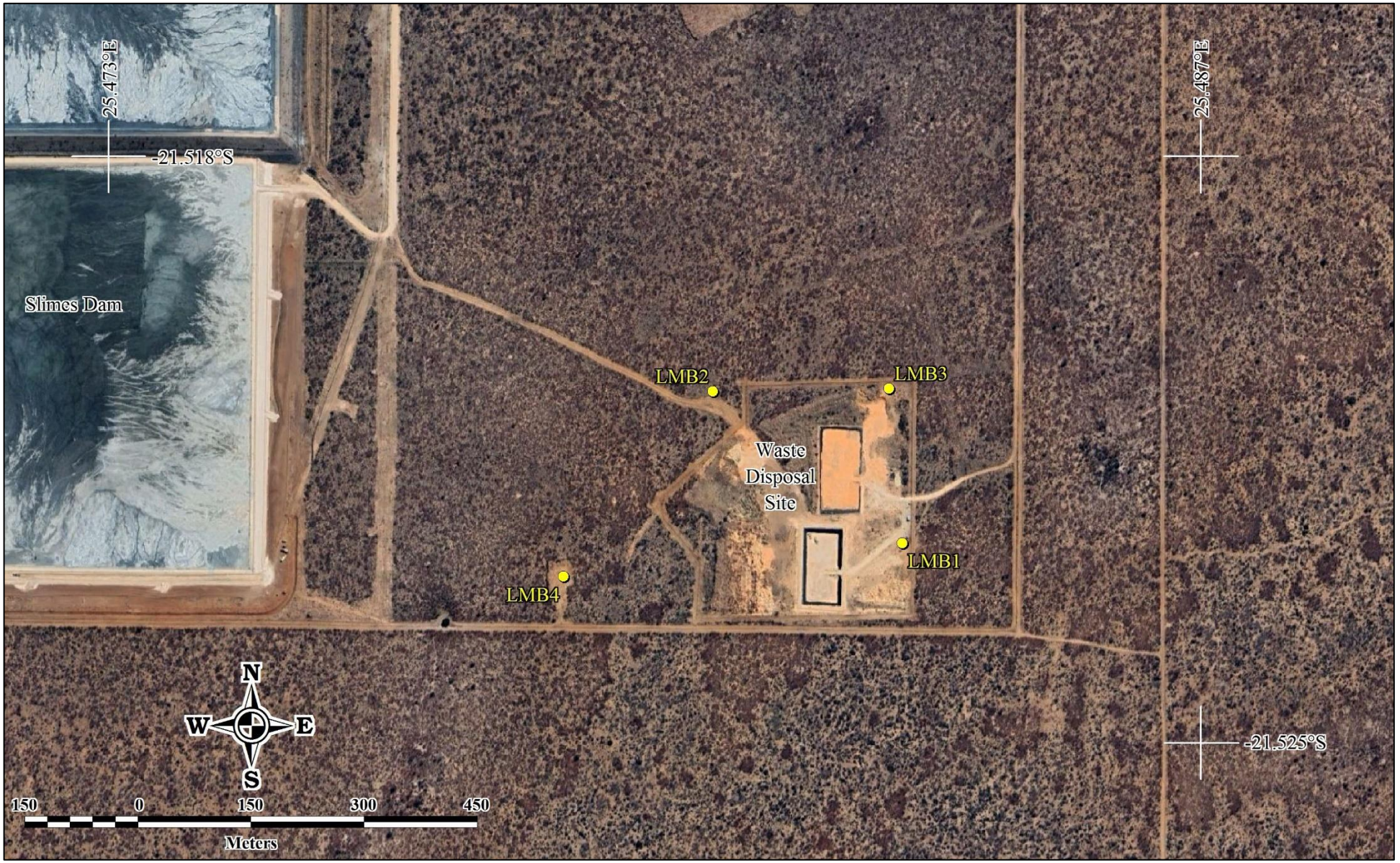

Figure 4.22: Monitoring boreholes for the landfill site (waste disposal site).

After March 2015, decreases in the TDS concentrations were observed, so that by December 2016 much lower TDS concentrations occurred at boreholes LMB1 and LMB2. Some variability in the TDS concentrations have been seen at these boreholes since 2016.

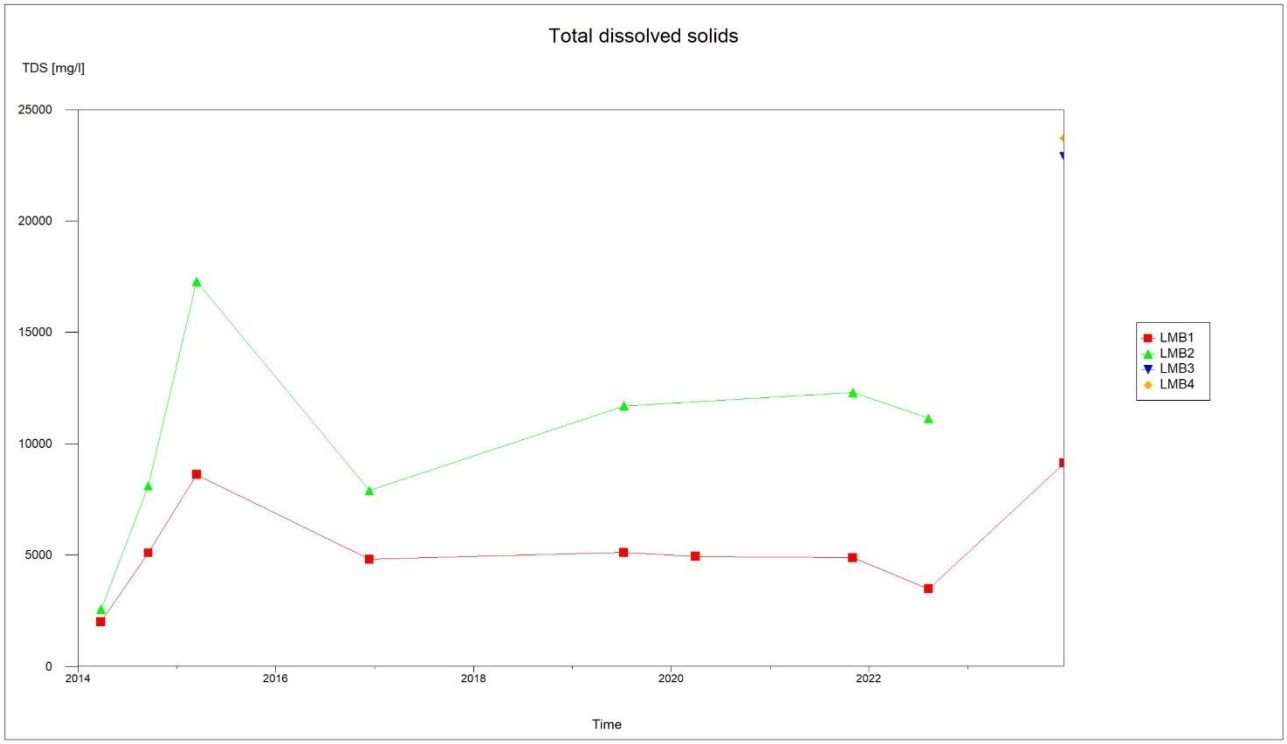

Figure 4.23: TDS concentrations recorded at boreholes surrounding the landfill site.

The TDS concentrations at the two new boreholes (LMB3 and LMB4) were much higher (~23 000 mg/L) than at the older boreholes during the December 2023 monitoring event. It is unknown why these boreholes displayed such high TDS concentrations, but further monitoring will be done to investigate.

4.6.4.5 Groundwater chemistry evolution

From the hydrochemical analyses performed on groundwater samples from different sampling events, evolution of the groundwater in terms of its dominant ions is apparent at some boreholes. Table 4.11 lists the dominant ions observed at five dewatering boreholes during different phases of the installation and testing of these boreholes. The positions of these boreholes relative to the pit at KDM are shown in Figure 4.4. The groundwater samples collected in 2010 during the drilling of these boreholes do not exhibit HCO_3, an indication that the basalt aquifer had been dewatered of its fresh water. The presence of HCO_3 in the water samples from the test pumping (2011) and dewatering phases (2012) suggests hydraulic connectivity between the sandstone and basalt aquifers.

Table 4.11: Dominant ions in the groundwater during different sampling events (WSB, 2007).

Borehole	Drilling (2010)	Test pumping (2011)	Dewatering (2012)
Z15563	Na-Cl	Na-Cl-CO_3	Na-Cl-HCO_3-CO_3
Z15564	Na-Cl	Na-Cl-CO_3-HCO_3	Na-Cl-HCO_3-CO_3
Z15567	Na-Cl	Na-Cl	Na-Cl-CO_3
Z15568	Na-Cl	Na-Cl	Na-Cl-HCO_3
Z15569	Na-Cl	Na-Cl-CO_3-HCO_3	

4.6.5 Groundwater quality statistics (2010-2023)

Descriptive statistics of chemical constituents of collected groundwater samples are presented in Table 4.12. The results were assessed against published BOS32:2015 drinking water guidelines. Note that the data in this table are for all groundwater samples analysed from 2010 to 2023 and make no distinction between farm boreholes and KDM boreholes, or between boreholes extracting from the basalts and boreholes extracting from the sandstones. The statistics therefore only give a general overview of the groundwater quality in the vicinity of KDM.

Water in the research area contains different dissolved inorganic minerals. The major cations are Ca^{2+}, Mg^{2+}, Na^{+} and K^{+} with mean values of 108, 57.6, 1297, 19.27 mg/L respectively. The anions in the research area are dominated by Cl^{-}, SO_4^{2-}, CO_3^{2-}, SO_4^{2-}, NO_3^{-} and HCO_3^{-} with mean values of 1669, 322, 151, 322, 59 mg/L, respectively. The dominance of Na^{+} and Cl^{-} ions in groundwater is related to leaching process of soluble minerals in the host rocks. Fe and Mn averages 1.9 mg/L and 0.44 mg/L, respectively. Fluoride exists in small quantities with a mean of 1.1 mg/L. The leaching of minerals in groundwater is an indication of their presence in the source rock (Mills, 2019). The major ions dominant in Kalahari, Stomberg, Mosolotsane and Kimberlite lithologies are sodium and sulphate while calcium is highly leached from carbonaceous mudstones (Mills, 2019).

The pH ranged between 7.02 and 11.9 with a mean value of 7.8. The high pH indicates that the waters in the research area is of alkaline nature, which is probably caused by high concentrations of sodium, calcium, magnesium, carbonate, and bicarbonate ions in the area. These ions are known to increase pH when present in water (Rao *et al*., 1982).

Electrical conductivity values range between 864 µS/cm and 40500 µS/cm. The lower EC values represent water from basalts that receives recharges from rainfall while high EC values are due to water coming from the deeper sandstones and fractured granites. Mineral dissolution and lack of recharge contributes to high EC conditions for water in the sandstones and granites.

Table 4.12: Groundwater quality statistics.

Parameter	pH	EC (µS/cm)	TDS (mg/L)	Alkalinity (mg/L $CaCO_3$)	T. Hardness (mg/L $CaCO_3$)	Ca (mg/L)	Mg (mg/L)	Na (mg/L)	K (mg/L)	Fe (mg/L)	Mn (mg/L)	HCO_3 (mg/L)	CO_3 (mg/L)	SO_4 (mg/L)	Cl (mg/L)	NO_3 (mg/L)	F (mg/L)
Mean	7.8	6006	3582	422	733	108	58	1297	19	1.97	0.44	490	152	323	1669	59	1.1
Median	7.7	4557	2460	382	354	50	43	823	14	0.13	0.03	450	160	202	1022	54	1.0
SD	0.5	6005	3530	238	977	218	66	1437	17	16	1.60	306	193	276	2136	37	1.0
Range	5.3	39636	23246	2135	5180	2200	689	11599	110	217	18	2600	1300	2097	15707	260	7.7
Min	6.6	864	484	15	20	0.0	1.4	50	1.2	0.00	0.00	0.10	0	6.8	43	0.5	0.0
Max	11.9	40500	23730	2150	5200	2200	690	11649	112	217	18	2600	1300	2104	15750	260	7.7
1st Quartile	7.5	3891	2240	340	236	34	30	701	12	0.03	0.01	370	0	165	869	34	0.5
3rd Quartile	8.0	5130	3314	428	680	87	64	1091	18	0.44	0.10	510	230	398	1350	84	1.2
BOS 32:2015																	
Class I	**6.5-8.5**	**700**	**450**			**80**	**30**	**100**	**25**	**0.03**	**0.05**			**200**	**100**	**45**	**0.7**
Class II	**5.5-9.5**	**1500**	**1500**			**150**	**70**	**200**	**50**	**0.30**	**0.50**			**250**	**200**		**1.0**
Class III	**5.0-10.0**	**3100**	**2000**			**200**	**100**	**400**	**100**	**2.00**				**400**	**600**		**1.5**

The TDS concentration in the study area ranges between 484 mg/L and 23 730 mg/L. The low TDS water represents water from shallow fractured basalt system while TDS of >1000 mg/L may be attributed to leaching of salts at depth greater than 125 mbgl. Total hardness ranges between 20 mg/L and 5200 mg/L and this is caused by Mg and Ca detected in water.

Salinity in the research area is known to increase with depth (WSB, 2007). All KDM boreholes sampled during the 2023 monitoring event displayed TDS concentrations exceeding 2000 mg/L (Table 4.10). Water analyses from private boreholes indicate TDS ranging between 627 mg/L and 1840 mg/L (Table 4.9). Groundwater from the upper Ntane sandstone has been depleted around the pit and the more recent water quality is representative of the lower Mosolotsane aquifer.

4.6.6 Temporal changes in groundwater levels

4.6.6.1 Water levels in the pit dewatering boreholes

Eleven monitoring boreholes are placed strategical around the pit to monitor the impact of mining activities immediately around the pit perimeter (Figure 4.24). Of these 11 boreholes, three form part of the pit dewatering borehole network shown in Figure 4.4 (Z15563, Z15566 and Z15576), while the remaining eight are new dewatering boreholes drilled in 2018. Boreholes Z15563, Z15566 and Z15576 were initially used for dewatering purposes and when their yields decayed to <2 m^3/hr, they were converted to monitoring boreholes.

Graphs of the water levels measured in the 11 monitoring boreholes between April 2019 and April 2023 are presented in Figure 4.25. The water levels in all boreholes decreased significantly during this four-year period. Maximum drawdowns of 41.16 m, 30.82 m and 22.22 m were recorded at boreholes Z15563, Z26465 and Z15566, respectively. These boreholes occur on the eastern perimeter of the pit.

The pit dewatering and water supply boreholes at KDM are equipped with automated loggers for continuous data capturing. The boreholes are also equipped with variable speed drives which allow the water levels to be controlled as per the dewatering requirements. The water levels at the different dewatering boreholes have been set to depths ranging between 140 mbgl and 255 mbgl.

Figure 4.24: Positions of the pit water level monitoring boreholes.

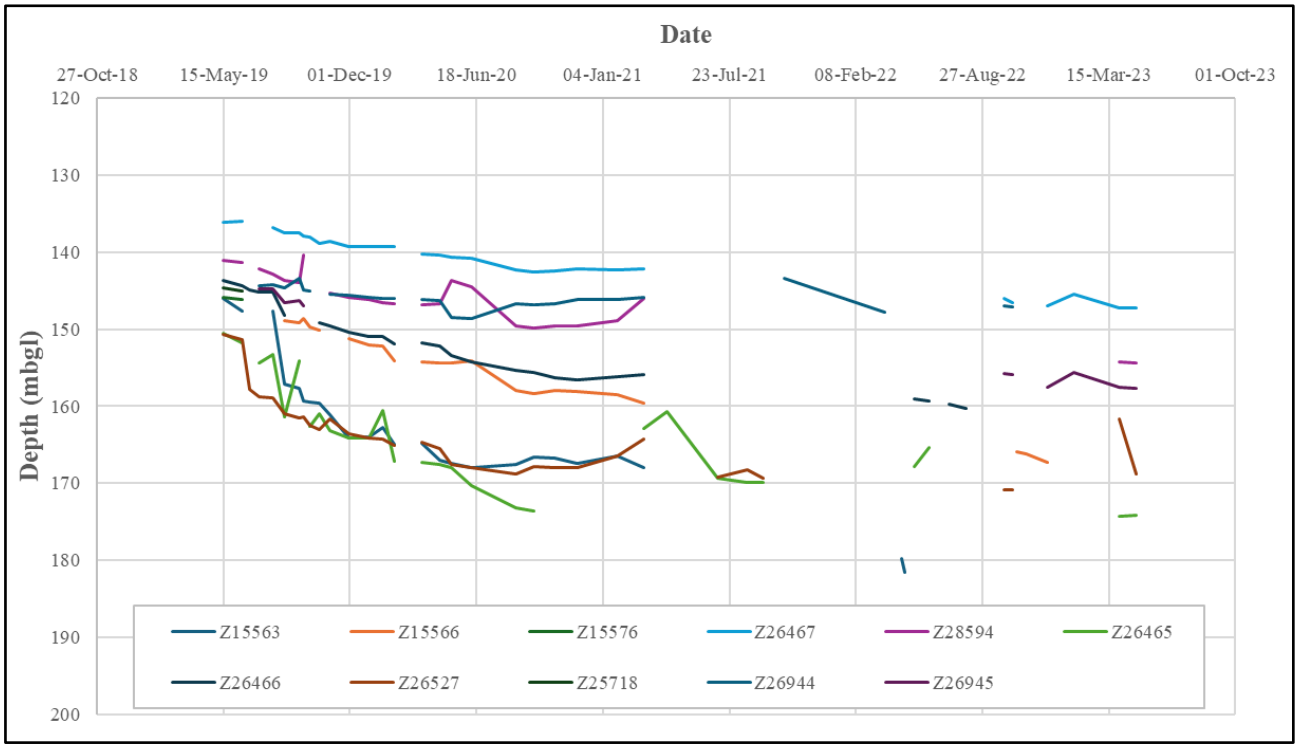

Figure 4.25: Water levels measured in the pit monitoring boreholes between April 2019 and April 2023.

4.6.6.2 Changes in the groundwater levels due to pit dewatering

The pumping system at KDM uses variable speed drives to control water levels and pumping rates. The dynamic water levels for the pit dewatering boreholes are controlled and set at certain levels to reduce water levels within the vicinity of the pit.

To evaluate the impact of pit dewatering on the groundwater levels, the both the pre-mining groundwater levels (shown as a contour map in Figure 4.9) and the groundwater levels as they were during a 2019 monitoring event are shown in Figure 4.26. The impact of pit dewatering over the seven years from the commencement of mining (2012) to the 2019 monitoring event is evidenced by the large decreases in the groundwater levels at and around the pit. Drawdowns exceeding 140 m were observed at the pit boreholes.

The changes in the water levels between 2012 and 2023 in monitoring boreholes Z13026 to Z13029 are shown in Figure 4.27. The water levels in boreholes Z13026, Z13027 and Z13028 declined steadily over this period. By contrast, the water level in Z13029 appears to have not been affected by pit dewatering. This borehole occurs immediately south of the slimes dam and its water level is probably influenced by seepage from the slimes dam. It is also possible that this borehole is shielded from the effects of dewatering by one of the dolerite dykes that occur in the vicinity of the pit (see Figure 3.3). Such dykes could act as barriers to groundwater flow.

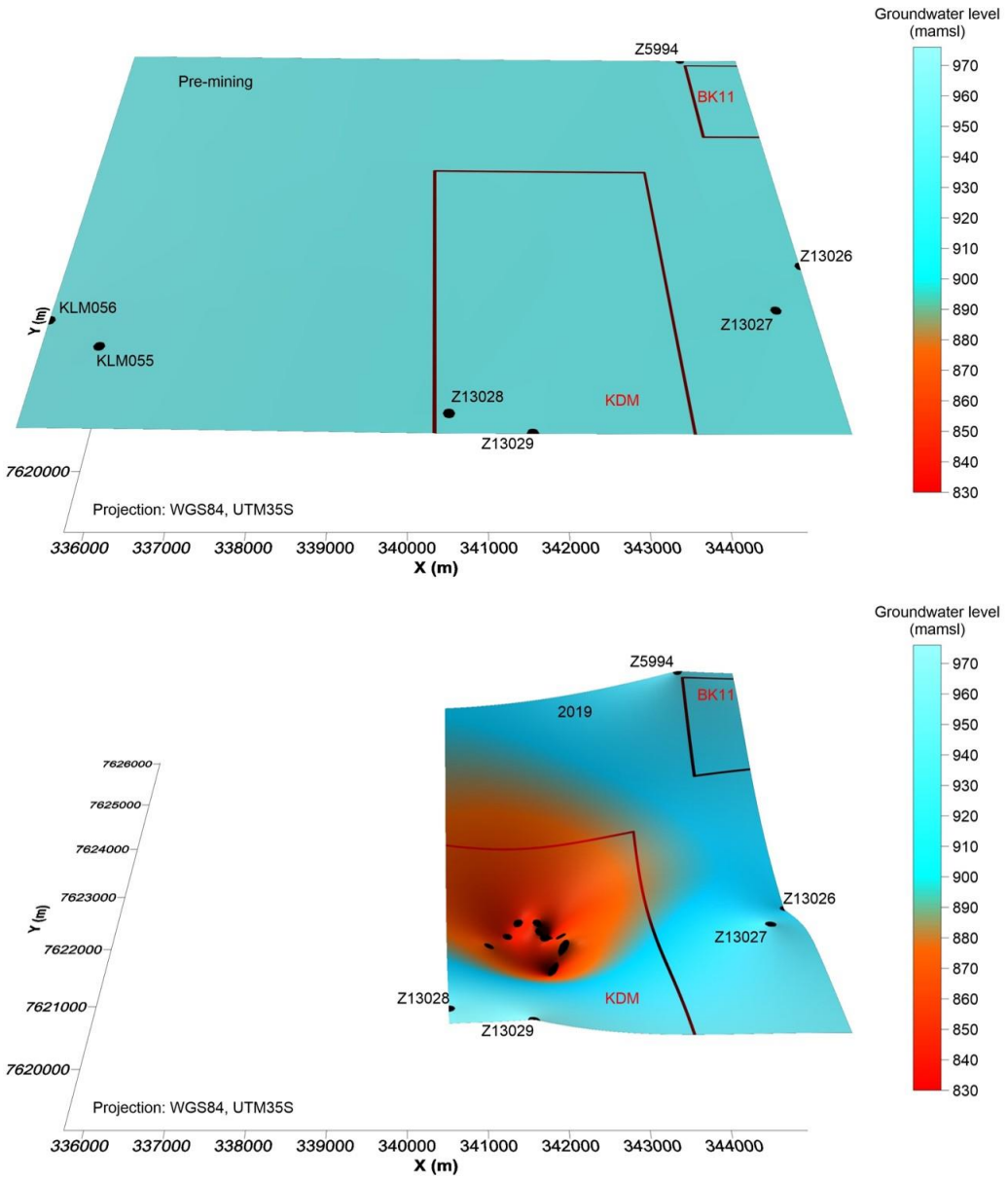

Figure 4.26: The pre-mining groundwater levels (top) and groundwater levels in the vicinity of KDM in 2019 (bottom).

The cone of depression caused by pit dewatering appears to extend well beyond the boundaries of the mine. In 2019, drawdowns of 54.6 m, 16.5 m, and 13.9 m were recorded at boreholes Z13026, Z13027 and Z5994, respectively. These three boreholes occur to the east and north-east of the mine and their water levels may also have been influenced by groundwater abstraction from boreholes in Wellfield 6 which occurs east of KDM (Figure 4.8). Pit dewatering activities are, however, expected to have little impact on existing wellfields due to the pit location in an area of thick Ntane sandstones with a relatively high hydraulic conductivity, and its isolation from wellfields to the north by a low permeability lineament, and from Letlhakane by a fractured and weathered dyke (KP, 2019).

Figure 4.27: Water levels in monitoring boreholes around KDM (2012-2023).

4.6.6.3 Water levels at the slimes dam

Between 2012 and 2024, groundwater levels in the eight monitoring boreholes near the slimes dam increased from approximately 30 mbgl to <5 mbgl (Figure 4.28). This indicates that leakage from the slimes dam contributed to anthropogenic recharge of the groundwater system. The water level graph (Figure 4.28) shows an almost immediate response following commissioning of the slimes dam, recording significant recharge within the first two years. Thereafter, the groundwater water levels stabilised at depths of around 5 mbgl.

Boreholes SMB05 to SMB08 were drilled early in 2023. Since then, the groundwater level in SMB05 has increased from approximately 11.9 mbgl to 7.4 mbgl, while small increases in the water level at SMB08 have also been recorded. This observation again suggests that leakage from the slimes dam is recharging the groundwater system.

KDM continues to monitor groundwater quality and potential seepage from the slimes dam (JDS, 2019). Where anomalies are noticed during monitoring, actions are taken, and plans are developed and implemented over time.

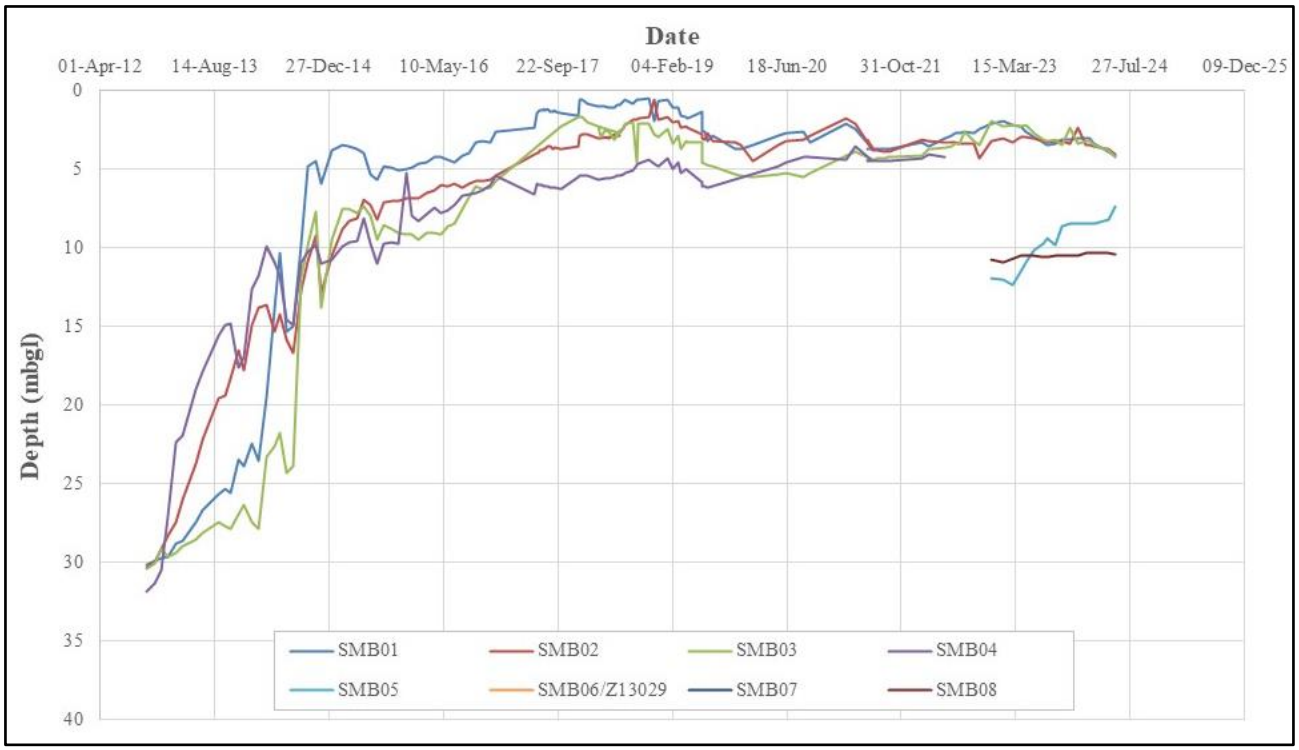

Figure 4.28: Water levels in monitoring boreholes around the at slimes dam (2012-2023) (KDM, 2023).

4.6.7 Temporal changes in borehole yields

The blow yields of boreholes around the KDM pit are displayed in Figure 4.29 for both 2013 and 2023. The high borehole yields (>20 m^3/hr) observed at some boreholes during 2013 correspond to the positions of well-developed fractures.

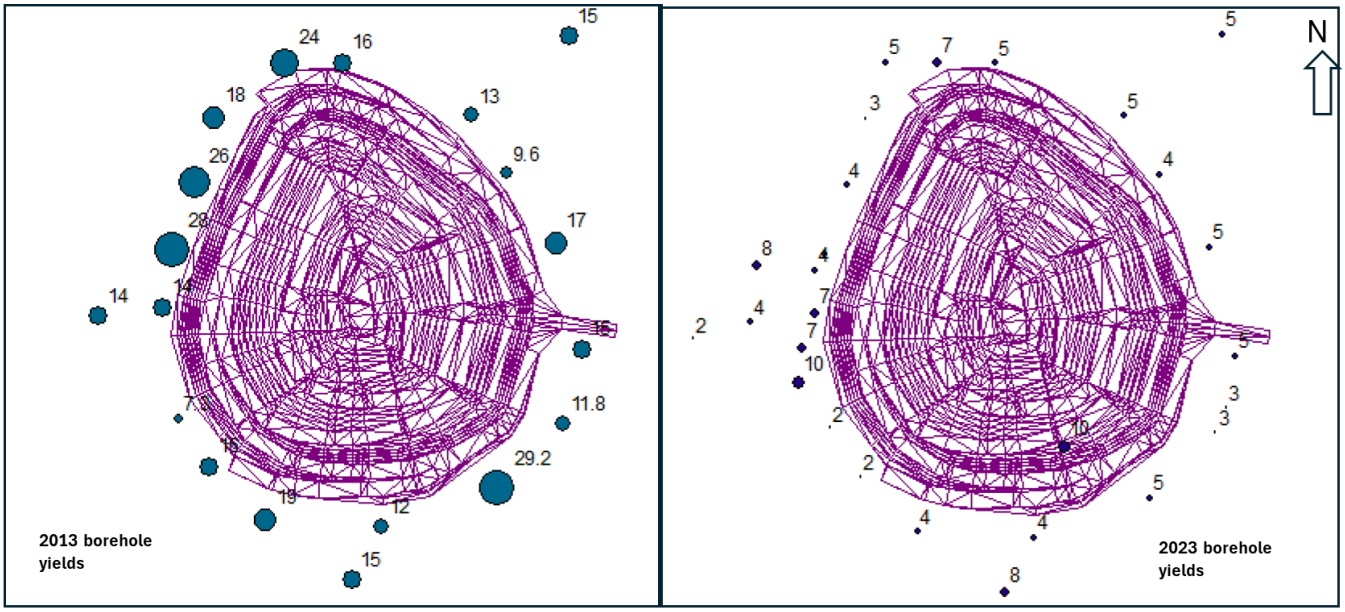

Figure 4.29: Final blow yields of boreholes around the KDM pit (2013 and 2023).

Borehole yields have significantly decreased over the period from 2013 to 2023 because of the intensive dewatering programme at the mine. However, some 1000 m from the pit, high yields can still be realised because the aquifer system farther away is still saturated (KDM, 2023).

4.7 GROUNDWATER ABSTRACTION

KLMCS (2007b) developed a local groundwater flow model for the AK6 pipe. The objective of the model was to provide predictive simulations for dewatering of AK6 open pit. The model estimated that a dewatering volume of 5.6 Mm^3/year was needed to depressurise the pit to 300 mbgl.

In 2012 when mining commenced, KDM drilled 16 pit dewatering boreholes. This number has increased over the years to 32. The license to abstract water for both pit dewatering and water supply was granted to KDM by the Water Apportionment Board (WAB). WAB approved a water right of 8 Mm^3/year based on the anticipated volumes of water needed to be pumped for pit depressurisation (KDM, 2014).

KDM is required by law to report all abstraction made annually. The annual volumes of groundwater abstracted at KDM between 2012 and 2022 are presented in Table 4.13.

Table 4.13: Annual pit dewatering and wellfield volumes abstracted at KDM.

Year	Groundwater abstracted (m^3)
2012	1 498 683
2013	2 107 764
2014	2 221 175
2015	1 749 977
2016	2 576 974
2017	2 048 290
2018	2 284 861
2019	2 541 499
2020	2 450 774
2021	1 942 618
2022	2 023 715

The pumping volumes from the pit averaged 5840 m^3/d for the period from 2012 to 2022. In 2016, the highest volume of 2 576 974 m^3/annum was abstracted. The variation in water use was influenced by the tonnage of ore milled, borehole breakdowns and decay in the borehole yields. A decrease in abstraction also occurred when six wellfield boreholes were rested, and all water demand was met from pit dewatering boreholes. In 2019, new boreholes were drilled and incorporated into the dewatering programme and the abstraction rate increased again to 2 541 861 m^3/annum.

Groundwater abstraction at KDM is mainly by means of boreholes. Other abstractions include sump pumping. More sump abstraction is expected after 2025 when inflows into the underground working are anticipated. Volumes as high as 300 m^3/hr are anticipated to come from the underground mine.

Wellfields 6 and 7 of Debswana borders the project area on the east and west, respectively, and abstract a combined volume of 11 988 m^3/d. It is estimated that groundwater uses for agricultural activities accounts for 5% of the total abstraction (Statistics Botswana, 2022).

CHAPTER 5:
CONCEPTUAL HYDROGEOLOGICAL MODEL

5.1 INTRODUCTION

The underlying principle of any numerical simulation is the conceptual model, incorporating relevant aquifer domains (AquiSim, 2020). The conceptual model is developed with the sole purpose of simplifying the complex hydrogeological problems being investigated to allow for an effective analysis of the groundwater system. The model is a simplified representation of the groundwater system and its flow patterns. Development of a model is a continuous process, and the model should get updated with new data when such data become available. The validity of any model is achieved by implementing its recommendations and comparing actual data with simulated information (Betancur *et al*., 2012).

5.2 GEOLOGICAL UNITS

Groundwater systems and behaviours are often complicated, and much detail is needed to describe such environments. Between 2005 and 2022, over 40 boreholes were drilled in the research area. From the information on the subsurface conditions gained from these boreholes, the conceptual model shown in Figure 5.1 was developed.

The Kalahari beds are made up of sands, calcrete and silcrete and range in thickness from 10-20 m around KDM pit (Itasca, 2015). This system has not intersected water in the research area and was not considered in the groundwater flow model.

The Stomberg basalt overlies the Ntane sandstone and has a thickness ranging between 80 m and 140 m (KLMCS, 2010). The basalts have limited aquifer potential and are not important on a regional scale other than that the permeability of the contact zone between the Ntane sandstone and the basalt is sometimes increased due to fracturing. Basalt produces water where it is weathered and fractured, and fracturing may aid in localised recharge.

The Ntane sandstone is the main source of water in Boteti Region with a thickness between 20 m and 80 m. The Ntane sandstone aquifer has a transmissivity of approximately 22 m^2/day and a horizontal hydraulic conductivity ranging between 0.05 m/d and 0.15 m/d (KLMCS, 2010).

The Mosolotsane sandstone is made up of two units separated by a lens of red mudstone. The upper layer sandstone is fine to medium grained and approximately 30 m thick and the lower coarser layer is 20 m thick (KLMCS, 2010). The red mudstone lenses act as aquitards and impede flow in the

vertical direction. The horizontal hydraulic conductivity of the Mosolotsane sandstone ranges between 0.05 m/d and 0.1 m/d (KLMCS, 2010).

The Tlhabala Formation underlies the Mosolotsane sandstone and is made up of non-carbonaceous mudstones and shales with a thickness ranging between 80 m and 155 m (Itasca, 2015). The horizontal hydraulic conductivity was estimated at 0.0005 m/d (KLMCS, 2010). The Tlapana Formation is a carbonaceous sequence of mudstones and shales and sandstones. It is 40 m thick with a hydraulic conductivity of approximately 0.0004 m/day (KLMCS, 2010). The Tlhabala and Tlapana mudstones act as aquicludes separating the Ntane and Mosolotsane formations form the fractured granitic aquifer.

The Mea Arkosic sandstone underlies the Tlapana mudstones and has a thickness of 9 m (SRK, 2019) and a horizontal hydraulic conductivity of 0.02 m/d. The basement is made up of granitic gneiss and ultramafic schists. The basement only forms an aquifer where there are open fractures and has an estimated horizontal conductivity of 0.0005 m/d to 0.05 m/d.

The kimberlite is made up of three lobes and the contact zone with the country rock is a highly permeable zone caused by weathering and fracturing. The contact zone is a conduit for groundwater flow around the kimberlite and has a horizontal hydraulic conductivity 0.001 m/d.

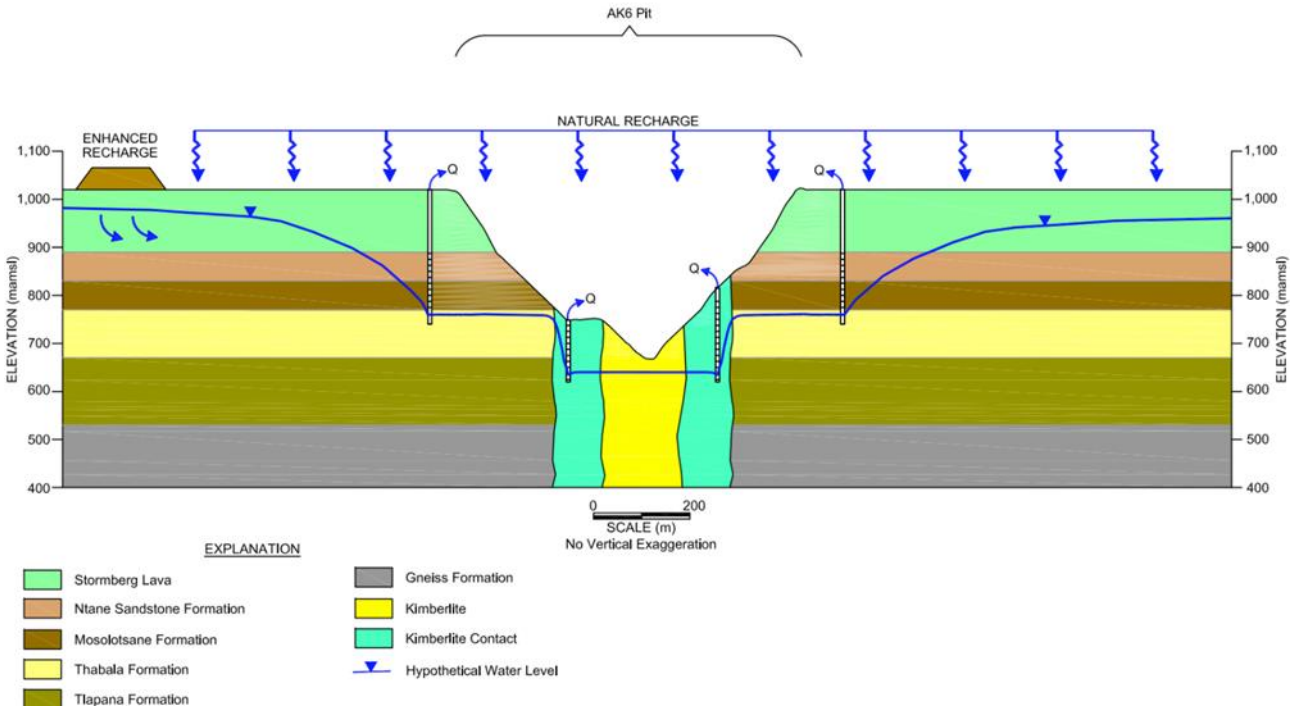

Figure 5.1: Conceptual hydrogeological model for KDM (Itasca, 2015).

5.3 GEOLOGICAL STRUCTURES

The geological structures used in the model were derived from the country rock model (SRK, 2019b) and the structural model (Barnnet, 2006). The research area is characterised by the presence of dolerite dykes and faults (GMS, 2019). The faults were assumed to extend through the entire bedrock units simulated in the model as well as to the model boundaries. Regional dykes were assumed to be semi-permeable and were assigned a horizontal and vertical hydraulic conductivity of 0.001 m/d. A regional fracture zone traverses the model domain in a SE–NW direction. This zone is considered a major structure that transports water into the pit (GMS, 2019). The model domain is also crosscut by faults and fractures that were previously mapped by Barnnet (2006) and these are orientated in the SE–NW direction.

There is a correlation between the general structural orientation, which is SE-NW and the regional groundwater flow direction, indicating that the SE-NW structures are regional groundwater conduits and barriers (KLMCS, 2010).

5.4 HYDROCHEMICAL CONCEPTUAL MODEL

Two dominant water types have been observed in the aquifers at KDM. The two types of water encountered are:

- Na-Cl water
- Na-HCO_3-Cl/Na (Mg/Ca)-HCO_3-Cl water

The evolution sequence of the groundwater is depicted in Figure 5.2. Calcium and magnesium are water soluble minerals that dissolve in water. When the concentration of calcium ions increases, it displaces the weakly bounded sodium. Then, the sodium ion becomes available and forms a bond with chloride giving groundwater is signature Na-Cl nature.

The presence of Ca and HCO_3 in groundwater samples is an indication of fresh water only intersected in the basalt aquifer system. Ca- and Mg-enriched water is also present in the sandstone system as the two ions can replace the Na ion. However, water encountered in the sandstone system is predominantly of the Na-Cl type.

Na and Cl are the major ions in the groundwater from the research area. Groundwater quality deteriorates with depth with the Kalahari/basalt contact providing a freshwater system with a TDS concentration of less than 1000 mg/L, while the sandstone exhibits a brackish water quality with TDS concentrations in the range of 2000 mg/L to 4500 mg/L. The TDS concentration within the granites can be as high as 30 000 mg/L. Water quality changes have been observed at monitoring boreholes

around the slimes dam. Shallow ground geophysics showed that there is seepage from the slimes dams and conductivity measurements indicate that seepage water has a pathway towards the pit (GMS, 2019). Seepage water from the slimes and stormwater dams was mapped on the pit highwalls; however, this cannot be explicitly modelled using MINEDW.

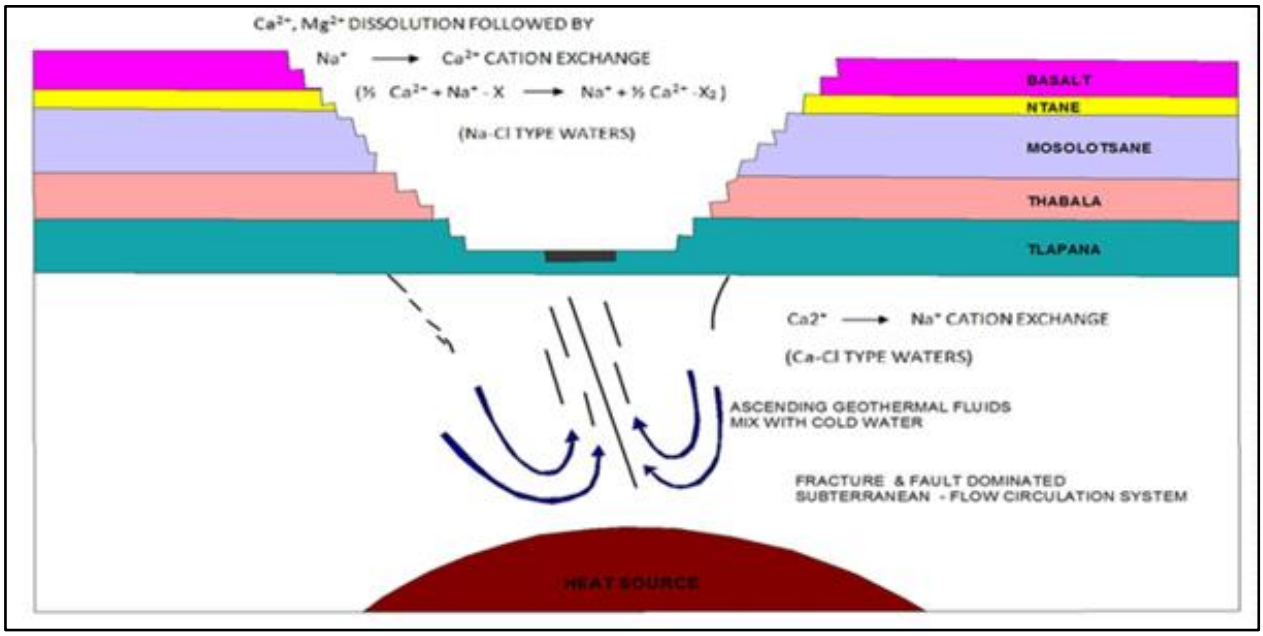

Figure 5.2: Conceptual hydrochemical model for KDM (KDM, 2023).

CHAPTER 6:
NUMERICAL MODELLING

6.1 INTRODUCTION

This chapter describes the development and predictions of a three-dimensional groundwater flow model that has been constructed to help assess local and regional impacts of mining activities on groundwater resources. The three-dimensional groundwater flow model will address the impact of mining activities have on water levels. MINEDW has limited application in transport modelling and as such mass transport will not be addressed by this research study.

Numerical models are not just simulation tools, they also simplify complex hydrogeological processes by providing answers to questions about the behaviour of the subsurface (Terisita *et al*., 2012). The constructed model will address the impacts of mining activities on water levels within a radius of 10 km from the centre of the KDM open pit.

Models have limitations and cannot represent the complexity that comes with geological setup. The model used will simulate simplified geological environment in the project area. The model will not simulate all the geological structures in the project area. The layers used in the model have not been studied explicitly and limited information on the aquifer parameters is available. Therefore, a simplified version of the individual layers will be used.

6.2 MEASURING FIELD DATA

Different types of data sets were prepared for the research project. Field visits were conducted monthly to measure water levels and abstraction data from both private and KDM boreholes.

Water levels at observation and pumping wells were monitored using a tape measure and data loggers, respectively. Abstraction data were obtained from automated flow meters for KDM boreholes, and a bucket system was used to measure pumping rates from private wells.

6.3 DESCRIPTION OF THE SIMULATION TOOL

A fully three-dimensional numerical, finite element, ground water flow model of KDM was constructed using the MINEDW code. The MINEDW code has several specific attributes that were developed to address dewatering requirements for mining operations (Azrag *et al*., 1998). The specific features include:

- The ability to collapse grids to simulate open pit excavations,

- Pinch-out capability to simulate underground mines, and,
- The use of drain nodes to represent excavations, both open pit and underground programs.

6.4 THE GOVERNING EQUATION

The general mathematical governing equation that describes groundwater flow form the basis for models developed to simplify and understand groundwater flow and its transport of dissolved solutes. The equation further describes how hydraulic heads within the model domain are distributed under a set of specified conditions. The equations are combined with hydraulic heads, aquifer parameters, boundary conditions and hydrogeological terms to generate head distributions and water balances for the aquifer system being investigated.

In this research, groundwater flow conditions are considered semi-confined, three-dimensional, steady state, anisotropic, and heterogenous. The flow equation for these conditions is:

$$0 = \frac{\partial}{\partial x}\left(K_x \frac{\partial h}{\partial x}\right) + \frac{\partial}{\partial y}\left(K_y \frac{\partial h}{\partial y}\right) + \frac{\partial}{\partial z}\left(K_z \frac{\partial h}{\partial z}\right) \quad 1$$

where K_x, K_y, K_z are hydraulic conductivity [L/T], and h is the hydraulic head [L]. On the other hand, confined, three-dimensional, transient, anisotropic, heterogeneous conditions of groundwater flow are represented by Equation 2:

$$S_s \frac{\partial h}{\partial t} = \frac{\partial}{\partial x}\left(K_x \frac{\partial h}{\partial x}\right) + \frac{\partial}{\partial y}\left(K_y \frac{\partial h}{\partial x}\right) + \frac{\partial}{\partial z}\left(K_z \frac{\partial h}{\partial x}\right) \quad 2$$

where S_s is the specific storage [1/L], K_x, K_y, K_z are hydraulic conductivities in the horizontal and vertical directions [L/T], and h is the hydraulic head [L].

6.5 MODEL DOMAIN

The boundary of the model domain was placed 10 km from the pit perimeter to ensure that hydraulic stress due to KDM dewatering activities and water supply boreholes do not propagate to the model boundary, thereby limiting the boundary effects. The boundary was also set to include all private boreholes within the KDM groundwater monitoring program. The eastern boundary of the model domain is formed by the Letlhakane River. The bottom of the model, which is also the planned bottom of the underground mine, occurs at 760 mbgl.

6.6 MODEL GRID

The finite-element grid of the modelling domain is shown in plan view in Figure 6.1, while the vertical discretisation of the model is shown in cross-sectional view in Figure 6.2. The mesh is finely discretised around the pit and future underground mine development, as well as around the linear geological features intersecting the mine. The finer discretisation allows better numerical resolution where the hydraulic gradients are greatest in the vicinity of the open pit and underground mine. The elements within the mesh depict the top or bottom of triangular prisms and the corners of the prisms are the nodes.

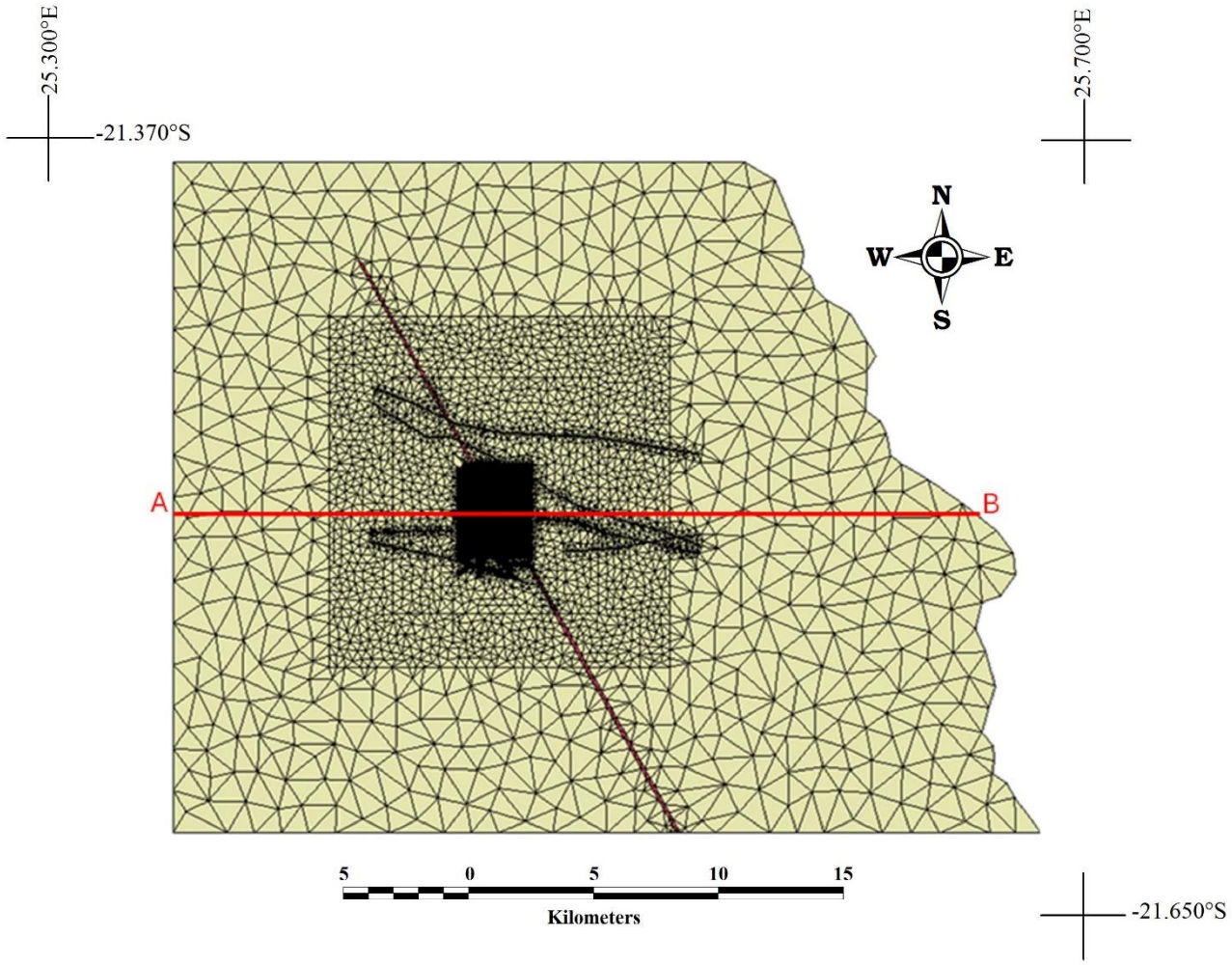

Figure 6.1: Model domain and grid (plan view) showing the position of transect AB through the centre of the pit.

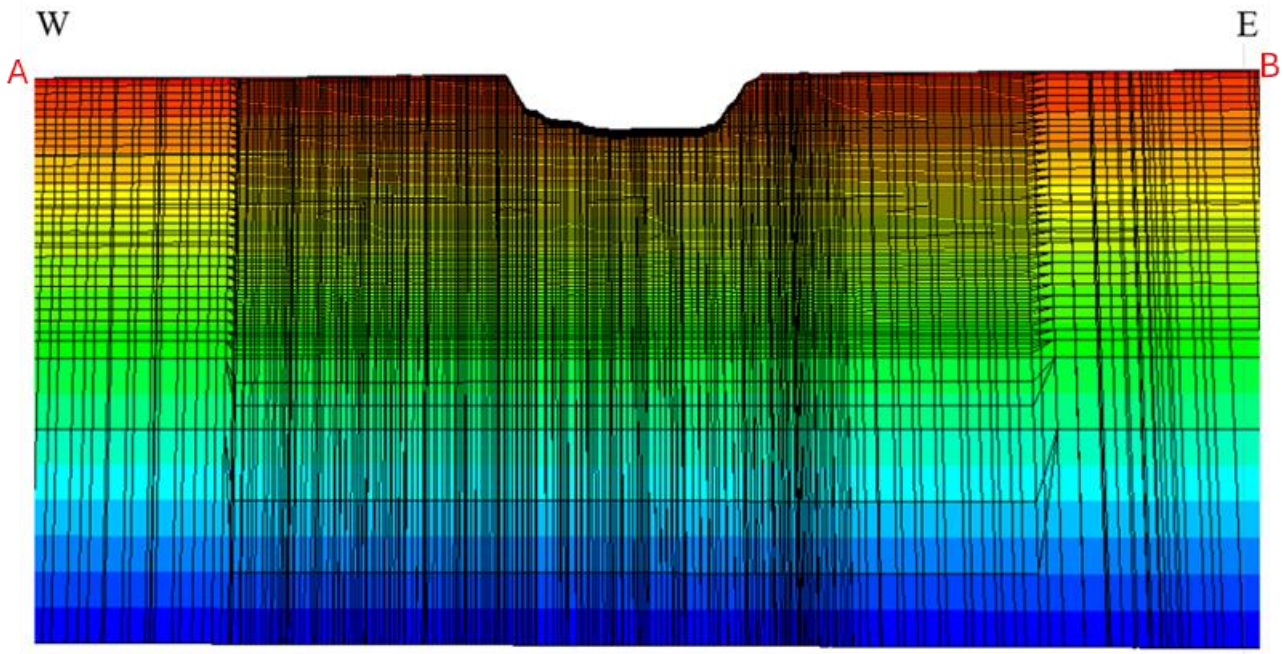

Figure 6.2: Vertical discretisation of the model domain along transect AB.

The model grid has 15 layers in and near the excavations. The detailed layering is then reduced to 10 layers representing major regional hydrogeologic units away from mining excavations and within a 10 km radius from the pit. The three-dimensional finite element grid has 2 827 321 elements and 1 426 836 nodes.

6.7 HYDRAULIC PROPERTIES

The primary hydraulic properties are assigned to the elements of the various layers representing the geological units in the model (Table 6.1). These assigned hydraulic parameters were based on the values described in Chapter 5.

Table 6.1: Physical and hydraulic properties assigned to the different layers of the numerical model.

Layer #	Unit	Thickness (m)	Horizontal hydraulic conductivity (m/day)	Vertical hydraulic conductivity (m/day)	Specific storage (m^{-1})	Specific yield (-)
1	Basalt	130	0.05	0.01	3.00E-06	0.001
2	Ntane Sandstone	68 - 72	0.15	0.15	3.00E-05	0.050
3	Upper Mosolotsane Sandstone	40	0.024	0.024	2.00E-06	0.010
4	Lower Mosolotsane Sandstone	12	0.035	0.035	2.00E-06	0.001
5	Tlhabala Mudstone	90 - 100	0.0005	0.0005	3.00E-05	0.001
6	Tlapana Mudstone	45	0.0005	0.0005	3.00E-05	0.001
7	Mea Arkosic Sandstone	9	0.02	0.02	5.00E-06	0.010
8	Upper Granite	100	0.05	0.05	2.00E-06	0.001
9	Lower Granite	>300	0.005	0.005	2.00E-06	0.001
10	Kimberlite	>700	0.005	0.005	5.00E-06	0.001
11	Dyke		0.001	0.0001	1.00E-06	0.001

6.8 BOUNDARY CONDITIONS

The following boundary conditions were assigned to the model:

- For steady-state simulation, a specified head was assigned to the southeastern and northwestern model boundary. The hydraulic head was set equal to the topographical elevation and based on the regional groundwater levels. A specified head boundary is one in which a hydraulic head is assigned to the node and groundwater can be discharged by or withdrawn from the node depending on hydraulic heads at neighbouring nodes. The remaining boundaries were set at an arbitrary from the pit centre so that the boundary would not influence the predictive simulations of the model. These were assigned as no flow boundaries during steady state calibration.
- Internal partial barrier boundaries are represented by SE/SSE–NW/NNW faults and dykes.
- For transient simulations, the no-flow boundaries were changed to reflect pumping conditions in the model. A variable flux boundary condition was assigned to the south, west and north of the model. The fluxes across the boundary are determined using the computed head along the boundary. The variable flux boundary extends the aquifer indefinitely. The top and bottom boundary conditions were assigned as phreatic surface and no-flow respectively. No flow boundary conditions are used at the base of the model in the transient and predictive simulations as it is assumed that at depth there is no significant flow across the boundary.

6.9 RECHARGE

WSB (2008) concluded that recharge to Ntane sandstone aquifer is negligible. Recharge estimates of 0.1% to 0.2% of the mean annual precipitation (MAP) were used by HCI (2007). Regional groundwater recharge was assumed to be 1% to 3 % of the annual rainfall (KLMCS, 2010). Natural recharge in the area around KDM is limited given the nature of the semi-arid environment and was estimated to be 0.1% of the MAP (Itasca, 2015). Enhanced recharge from slimes and storm water dams was recorded from monitoring boreholes (KDM, 2019). Recharge estimated from these facilities stand at 35 mm/year (Itasca, 2015). Recharge estimates for the research area range between 0.3% and 1.5 % of the annual rainfall (AquiSim, 2020). Recharge was assumed to be constant through the entire transient and predictive model simulations. For the research study, a recharge value of 0.05% of the MAP was applied to the model based on rainfall records within the research area.

6.10 SIMULATION OF OPEN PIT

The excavation of the pit was simulated in the model with nodes within the pit being assigned time-variable elevations using the collapsing grid capability of MINEDW. The elevation of the pit bottom was assumed to change every month during the period of simulation for the planned life of mine to 2025. A node represents the pit sides or bottom. A special type of drain node produces water if the model calculated groundwater level at the node is higher than the specified elevation of the node. If the calculated groundwater level is lower, the drain node remains dry. MINEDW enables a very realistic simulation of the pit configuration and inflow conditions. In each time step of numerical simulation, the elevations of all the drains nodes are specified and changed as necessary to replicate the mine plan.

6.11 SIMULATION OF PUMPING

Pumping at KDM started in 2010 with four boreholes developed for water supply during the early stages of mine development. The number of boreholes has increased over the years as part of the dewatering requirements of KDM. For transient simulations, the boreholes were simulated in the model using pumping rates with LPE (low pumping elevation). LPE represents the minimum water level required to maintain proper operational conditions for pumps. If the minimum water level elevation is not met, dewatering rates will decline to maintain the minimum water level. The pumps are on a variable speed drive (VSD) that is used to set and maintain water level above the pump. The pumps in all the boreholes were placed at 230 mbgl. The LPE was set at 10 m above the pump in all pumping boreholes.

The dewatering rates were obtained from the SCADA system used by KDM for gathering real-time monitoring data. The data were used during simulation to better represent variations in pumping over time.

6.12 MODEL CALIBRATION

A groundwater model is a mathematical representation of a groundwater system and therefore, the model and its parameters should reasonably represent actual conditions on site. To effectively achieve this, a process called model calibration is undertaken. This process involves varying some hydraulic parameters until the simulated groundwater levels match the field values. The flow model was calibrated for the period from 2005 to 2025 using transient conditions because extensive water level data from this period are available. The calibration process involves both steady-state and transient conditions.

6.12.1 Steady-state calibration

Steady-state simulations do not involve changes in hydraulic head over time. For steady-state calibration, hydraulic conductivity and recharge were varied within reasonable limits until the simulated heads were comparable to water levels from the pre-mining data. For calibration, the water level data from 2007 (Figure 4.10) were used to reflect the groundwater conditions prior to the establishment of Wellfield 6; these data were obtained from KLMCS (2018). The boreholes used for calibration were terminated in the Tlhabala Formation, with the sandstones contributing a major share of the water abstracted.

The pre-mining groundwater levels as found from the calibrated steady-state model for KDM are shown in Figure 6.3.

For flow models, the accuracy of the simulated results may be assessed by evaluating the differences between the simulated and actual groundwater levels (referred to as the errors). The mean error (ME) is calculated by summing all the errors and dividing the result by the number of sample points. The ME is used as an indication of how close the simulated values are to the actual data. The mean absolute error (MAE) is calculated as the arithmetic average of the absolute errors. The lower the MAE, the better the model predictions. The MAE is commonly used in model setup because it is interpretable, resistant to outliers and provides information about error size. The value of the MAE depends on the quality of data. The root mean square error (RMSE) is defined as the square root of the average squared errors.

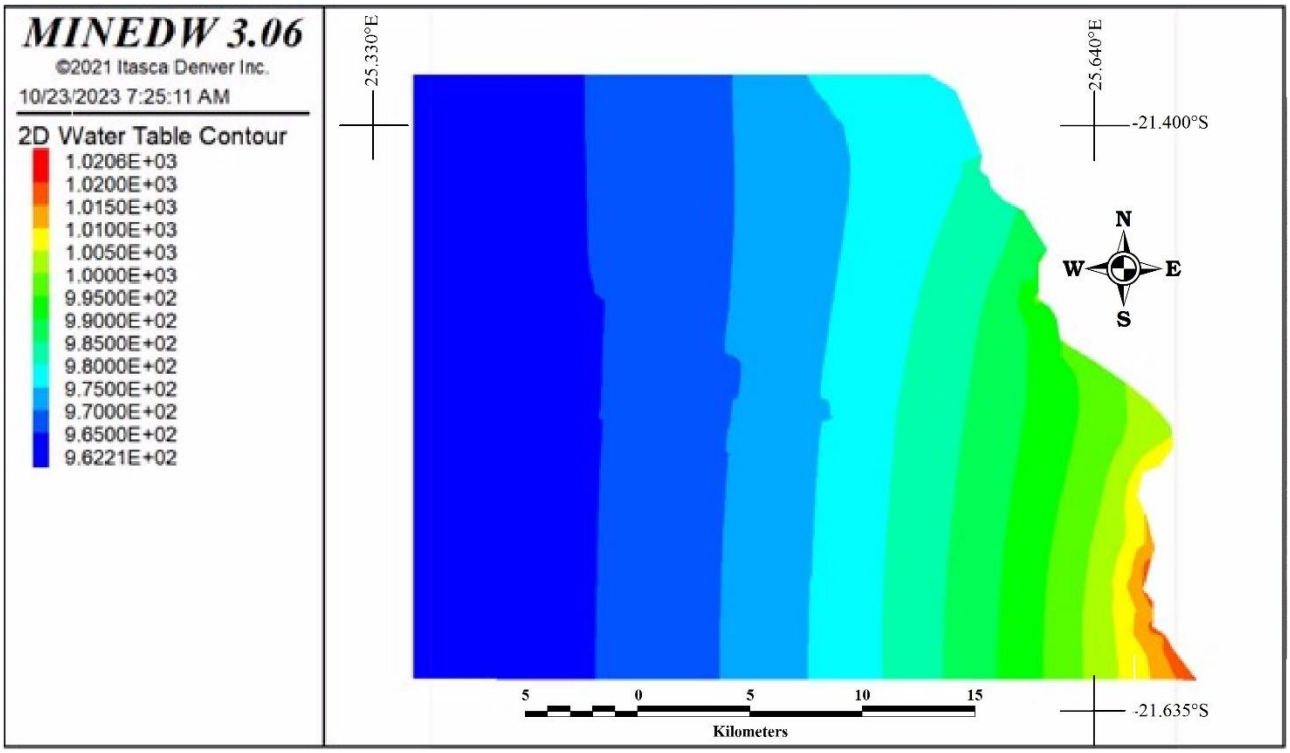

Figure 6.3: Simulated steady-state (pre-mining) water levels.

Statistical analysis of the simulations of the calibrated model is presented in Table 6.2. The maximum difference between the measured and simulated water levels is 1.65 m at borehole Z15562. The errors in the model calibration were estimated using the RMSE and MAE. The metrics give an indication of the accuracy of model predictions (Rastogi, 2023). For the simulated groundwater levels, an MAE of 0.73 and an RMS of 0.86 were estimated from the 25 groundwater level pairs (measured and modelled).

In Figure 6.4, the simulated water levels are plotted against the observed values. A correlation coefficient of 0.82 was estimated, indicating a strong linear relationship between the model calculated values and the actual data. The groundwater levels obtained from steady-state calibration were used as the initial heads in the transient model.

Table 6.2: Analysis of the results of steady-state calibration.

Site #	Borehole ID	X (m)	Y (m)	Z (mamsl)	Water level (mbgl)	Actual head (mamsl)	Simulated head (mamsl)	Difference (m)	Absolute difference (m)	Squared difference (m^2)
1	H002	341 757	7 621 983	1012.90	48.10	964.80	964.97	-0.17	0.17	0.03
2	Z12795	341 972	7 622 224	1012.19	47.59	964.60	965.97	-1.37	1.37	1.87
3	Z12796	341 466	7 622 438	1012.64	47.74	964.90	965.47	-0.57	0.57	0.33
4	Z12797	341 150	7 621 733	1014.13	48.93	965.20	966.38	-1.18	1.18	1.39
5	Z12798	341 592	7 621 272	1014.87	50.57	964.30	964.61	-0.31	0.31	0.10
6	Z13026	344 944	7 621 691	1012.66	47.07	965.59	965.57	0.02	0.02	0.00
7	Z13027	344 486	7 620 951	1014.87	49.17	965.70	965.75	-0.05	0.05	0.00
8	Z13028	340 497	7 619 392	1017.73	51.73	966.00	965.67	0.33	0.33	0.11
9	Z13029	341 415	7 619 119	1018.00	51.20	966.80	966.34	0.46	0.46	0.21
10	Z15561	341 645	7 621 366	1014.45	43.75	970.70	970.17	0.53	0.53	0.29
11	Z15562	341 846	7 621 434	1014.27	46.27	968.00	969.65	-1.65	1.65	2.73
12	Z15563	341 962	7 621 546	1013.71	47.41	966.30	966.59	-0.29	0.29	0.09
13	Z15564	341 994	7 621 676	1013.47	47.47	966.00	967.44	-1.44	1.44	2.09
14	Z15565	341 950	7 621 861	1012.83	44.73	968.10	966.88	1.22	1.22	1.49
15	Z15566	341 864	7 621 985	1012.65	46.94	965.70	966.57	-0.87	0.87	0.75
16	Z15567	341 575	7 622 174	1012.65	49.15	963.50	964.41	-0.91	0.91	0.82
17	Z15568	341 475	7 622 176	1012.78	48.48	964.30	965.16	-0.86	0.86	0.74
18	Z15569	341 352	7 622 081	1013.11	48.91	964.20	965.16	-0.96	0.96	0.92
19	Z15570	341 316	7 621 966	1013.42	50.22	963.20	964.16	-0.96	0.96	0.92
20	Z15573	341 290	7 621 553	1013.75	46.95	966.80	968.07	-1.27	1.27	1.60
21	Z15575	341 440	7 621 376	1014.32	45.92	968.40	967.86	0.54	0.54	0.30
22	Z15576	341 802	7 622 084	1012.64	45.24	967.40	967.77	-0.37	0.37	0.14
24	EB12	344 118	7 626 121	1001.47	35.75	965.72	966.70	-0.98	0.98	0.97
25	OB23	336 454	7 620 371	1016.97	51.09	965.88	966.68	-0.80	0.80	0.64
								-0.48 ME	**0.73 MAE**	**0.86 RMSE**

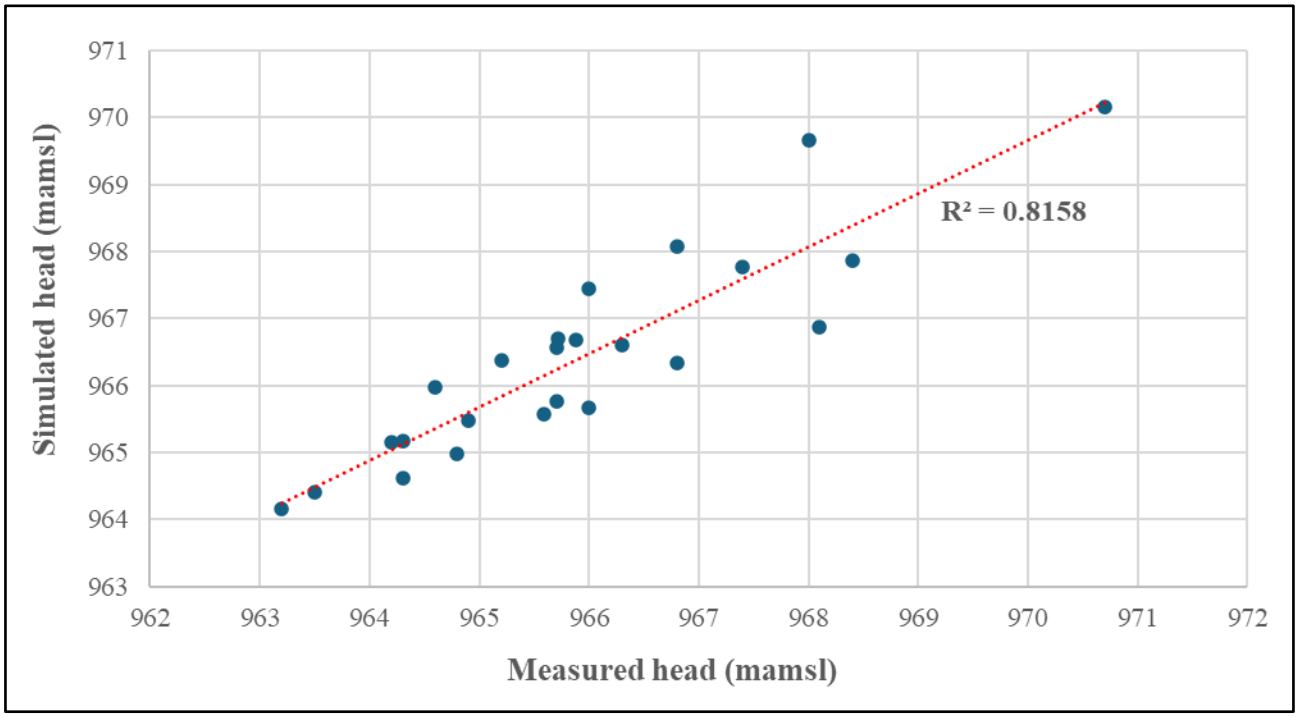

Figure 6.4: Simulated vs measured groundwater levels as obtained with steady-state calibration.

6.12.2 Transient-state calibration

Groundwater systems are by nature not in steady state, hence the need for a transient-state calibration. Transient conditions occur when inflows and outflows are not equal. For transient conditions, the hydraulic head changes with time. The calibration of the numerical model for transient conditions was conducted to further test the how well the model represented the actual field conditions.

At KDM, dewatering activities caused hydraulic stress to be exerted on the groundwater system, resulting in changes in the measured hydraulic head over time. Pumping at KDM started in 2009 with four boreholes commissioned for water supply during the initial stages of construction. Between 2007 and 2013, 16 boreholes were drilled and equipped for pit dewatering. The number of dewatering boreholes was increased to 31 by 2020 and as a result, drawdowns increased by 2 m to 40 m Drawdowns increased by ~2 m for boreholes Z18434, Z18435, Z26944, Z26945, Z28594, Z25718 and Z26467. These boreholes are located between 100 m and 200 m from the pit perimeter. Boreholes Z26527, Z26465, Z15566 recorded drawdowns of approximately 40 m drawdown because of their proximity to the pumping boreholes. The total pit abstraction rate increased from 180 m^3/hr to 250 m^3/hr between 2017 and 2020 (KDM, 2023).

In 2014, six wellfield boreholes were drilled and installed for pumping. The wellfield boreholes were used intermittently. These are located more than 2 km from the pit perimeter. The wellfield boreholes were more active between 2014 and 2018. After the increase in the number of pit dewatering boreholes, the six wellfield boreholes were put on standby for future use. The boreholes have not been active since 2020.

Calibration of the transient state was conducted for the period 2009 to 2023. The transient model calibration was conducted using the data from pit dewatering, wellfield, piezometers and monitoring boreholes. The transient calibration of the model was achieved by altering hydraulic parameters and recharge until reasonable best fit water levels were achieved. When recharge values were adjusted to more than 0.05% of the MAP, the simulated heads became much higher than the observed heads. The recharge of 0.05% of the MAP was used to obtain an acceptable fit between simulated and observed monitoring values. The hydraulic parameters obtained from both steady-state and transient calibrations are listed in Table 6.3.

The basalt aquifer system exhibits a high vertical hydraulic conductivity of 0.025 m/d where fracturing is more enhanced. The Ntane sandstone is less cemented and therefore has high conductivity compared to the other layers. The upper Mosolotsane sandstone shows specific yield of 0.01 compared to 0.001 of the lower Mosolotsane sandstone. This difference is caused by the lens of red mudstone in the lower Mosolotsane sandstone which reduces the permeability of the formation. The Tlhabala and Tlapana mudstones have very low hydraulic conductivity because these units have

low permeabilities. The MEA arkosic sandstone has a conductivity and specific yield of 0.02 m/d and 0.01, respectively. This unit is highly permeable. The upper granite is weathered and fractured and returned a hydraulic conductivity of 0.05 m/d. The properties of the kimberlite, lower granite and dyke remained unchanged during calibration. These zones do not produce any water apart from where fracturing is present.

Table 6.3: Model parameters as obtained from transient calibration.

Layer #	Unit	Thickness (m)	Horizontal hydraulic conductivity (m/day)	Vertical hydraulic conductivity (m/day)	Specific storage (m^{-1})	Specific yield (-)
1	Basalt	130	0.075	0.025	2.00E-06	0.002
2	Ntane Sandstone	68 - 72	0.05	0.05	1.00E-05	0.010
3	Upper Mosolotsane Sandstone	40	0.05	0.05	5.00E-06	0.010
4	Lower Mosolotsane Sandstone	12	0.5	0.5	1.00E-06	0.001
5	Tlhabala Mudstone	90 - 100	0.00045	0.00045	1.00E-05	0.001
6	Tlapana Mudstone	45	0.00045	0.00045	1.00E-05	0.001
7	Mea Arkosic Sandstone	9	0.04	0.04	5.00E-06	0.010
8	Upper Granite	100	0.005	0.005	5.00E-06	0.001
9	Lower Granite	>300	0.0001	0.0001	1.00E-06	0.001
10	Kimberlite	>700	0.01	0.01	1.00E-06	0.001
11	Dyke		0.002	0.002	1.00E-06	0.001

A total of 80 monitoring points were used for transient calibration. Figure 6.5 shows selected comparisons between the simulated and observed values (also see **Appendix B**). Drawdown in all the monitoring points is caused by groundwater abstraction or partial recharge in the case of boreholes monitoring the slimes dams. Generally, the observed and simulated values display similar trends. However, some boreholes display erratic water level trends. This erratic behaviour was caused by among others erroneous data, unplanned pump stoppages and breakdowns.

The simulations display a lower drawdown than the actual drawdown at the piezometers REP3, especially sensors REP3_T2 and REP3_T3. This might be caused by inconsistency in borehole abstraction data because the time at which some of the boreholes were commissioned was uncertain. REP3_T1 shows lower actual drawdown than simulated values.

Piezometer GT2_T2 and GT3_T2 display a similar pattern to the boreholes: the actual and calculated water levels match in the period 2017 to 2020. The drawdown observed in the two piezometers is caused by active pumping from the in-pit boreholes. The erratic behaviour observed in GT2 is attributed to recharge coming as seepage from the storm water dam. In the period from 2016 to 2021, GT3_T1 displays lower actual drawdown than simulated values. The simulated and observed values then match better between 2021 and 2022.

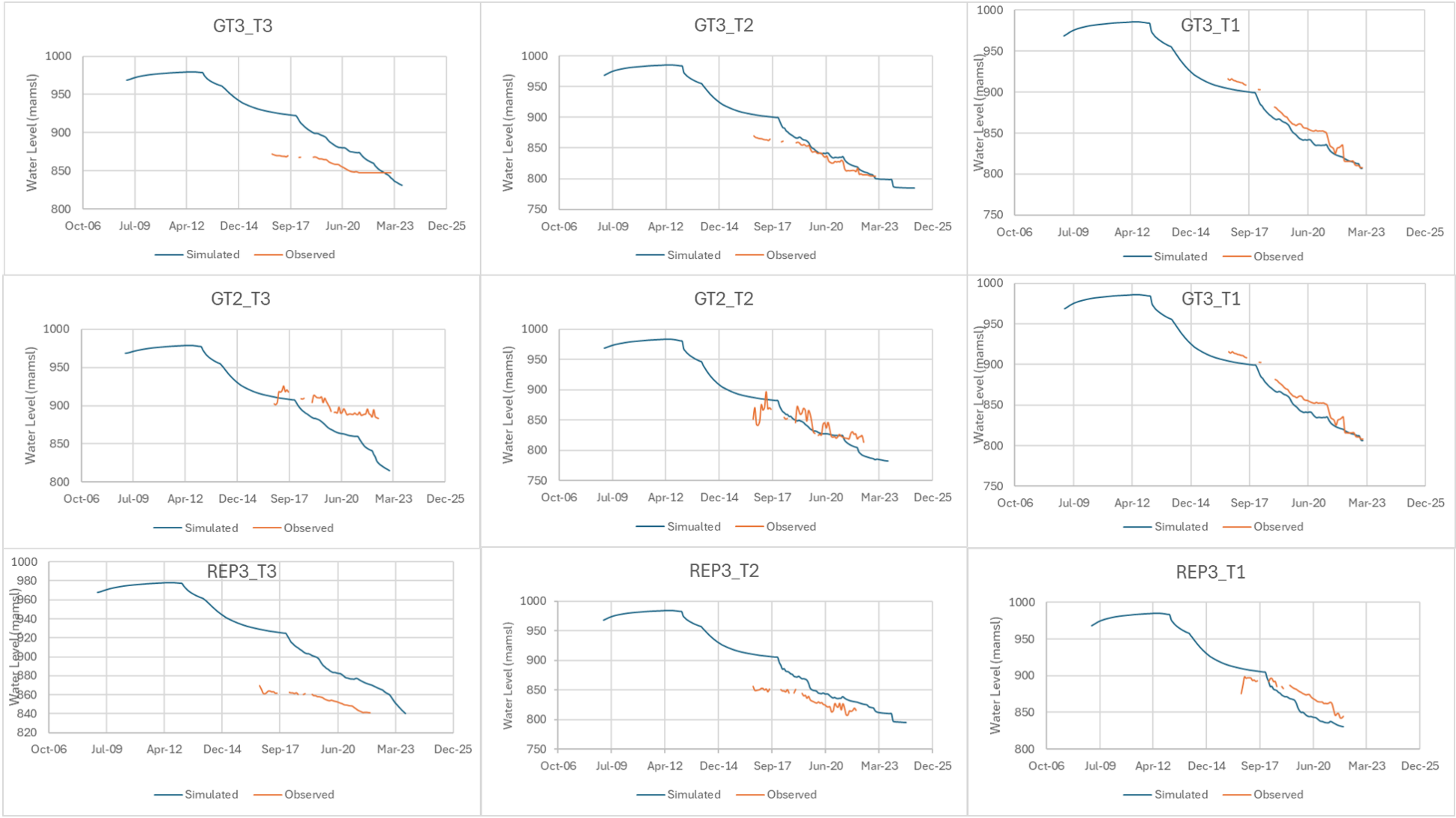

Figure 6.5: Measured and simulated water levels in selected boreholes during transient-state calibration.

SMB01 and SMB02 show recovering water levels because of induced recharge from the slimes dam. Boreholes Z15563 shows matching water levels between 2018 and 2023. Borehole Z15563 is located closer to a pumping borehole, Z25718. When Z25718 is switched off, water levels at Z15563 will immediately increase. Borehole Z26527 displays matching fit between 2019 and 2022. Boreholes Z26466, Z26465, 26467, and Z26944 show smaller true drawdown than the simulated values, even though they display a matching cause-effect response. Boreholes Z15569 and Z18437 display higher drawdowns than the simulated values. Borehole Z13026 and Z13028 are located more than 2 km from pit perimeter. High water level at Z13026 is an indication that the cone of depression caused by dewatering is localised around the pit.

Uncertainties in the model calibrated hydraulic parameters were caused by:

- The lack of long-term water level monitoring from WF6. The wellfield is located approximately 15 km east of Karowe Diamond,
- The impact of geological structures on groundwater flow. The model could not explicitly represent the geological lineaments traversing the research area, and,
- The recharge is not well studied in the research area and previous studies have used recharge rates ranging from 1% to 5% of the MAP.

6.13 MODELLING RESULTS

6.13.1 Introduction

Water Surveys (2008) developed a groundwater flow model to inform water supply requirements during the initial stages of operational development. The open pit model was also used to determine the impacts of mining activities on water resources with emphasis on water levels. The model indicated that mining operations, including the underground excavations, would cause a localised water level decline of 10 m by 2050. AquiSim (2020) noted that groundwater abstraction by mining operations in the Boteti region has lowered the regional water table by between 5 m and 10 m.

This chapter presents the results of the numerical model developed during the current investigation. The model was run from 2009 when mining started to 2025 when open pit mining is planned to cease. Water level and abstraction data from farm boreholes were not available because farmers do not keep records of their pumping activities. The impact caused by pumping from farm boreholes on the aquifer system could therefore not be quantified.

6.13.2 Results and discussion

The deepest and largest areas of water level drawdown are the pit, and the area defined by the SE–NW fracture zone. The SE–NW fracture zone is the main conduit that brings water into the pit.

The results from transient simulation show variations between the observed and simulated values. The performance of each borehole should be looked at individually because some mining activities influence groundwater flow direction. The boreholes are interconnected by a network of fractures, with the SE–NW as the main fracture zone that supplies all other minor structures. Some of the boreholes that were drilled between 2010 and 2019 were grouted with cement as part of an underground project to reduce inflows into the underground workings. The grout alters the hydraulic properties of the formations and hence affect groundwater flow. This was not simulated in the model because it was not easy to determine how the grout could have affected the fracture system.

The model did not simulate pumping from the sump. The sump collects not only storm water but seepage water coming from the geological units. The sump is dynamic and changes positions within the pit as mining advances deeper and the model could not simulate this. The sump also acts as a large diameter borehole and therefore contributes to water level fluctuations within the aquifer units.

The large variations are observed in boreholes Z26466, Z13026, Z13027, Z13029, Z15561, LMB1 and LMB2. The variation observed from these boreholes range between 14 m and 40 m. Smaller variation of less than 1 m were observed on boreholes SMB1, SMB2, SMB3, SMB4, Z15563 and Z26945. The data are still acceptable and have been used to successfully inform future water management plans for KDM.

The impact of pumping on water levels in 2010 is shown in Figure 6.6. The figure shows water level conditions after pumping had started. The cone of depression is not well established because there were only four active boreholes at the time. The water level around the pit averaged 977 mamsl. Farther away from the pit, conditions changed slightly. Water levels around the slimes dams increased from 968 mamsl to 1006 mamsl. The increase was caused by seepage water coming from slurry deposition at the slimes dams.

In 2013, the number of active pit dewatering boreholes was increased to 16, resulting in the expansion of the cone of depression. In 2015, the water level 5 km from the pit perimeter was 960 mamsl compared to 964 mamsl in 2009. Water levels changed by <1 m some 10 km from the pit perimeter. The piezometric levels in 2015 are depicted in Figure 6.7.

The period from 2018 to 2022 experienced the implementation of an accelerated dewatering program. KDM increased the number of pit dewatering by nine. The impact of dewatering is seen in the water levels as modelled for 2025 (Figure 6.8). The maximum simulated drawdown in the pit is to an

elevation of 777 mamsl by end of open pit mining in 2025. Water levels are drawn down to within the Tlhabala mudstone. Within a radius of 1 km from the pit, water levels will be drawn down by 40 m at the end of 2025. In the area 10 km from the pit perimeter, water levels will experience a drawdown of >10 m by 2025.

The simulated drawdowns at neighbouring farm boreholes are displayed in Table 6.4 with drawdowns ranging from 3.23 m to 99.04 m by 2025. The most impacted farm borehole belongs to Mokgalo at a drawdown of 99.04 m. Mokgalo is located within the KDM lease area and is situated very close to the pit, hence the large drawdown. The farmer was relocated at the beginning of mining and placed more than 50 km northeast of KDM. Boreholes along the NW–SW fracture zone appear to be the most impacted with a drawdown >10 m by 2025.

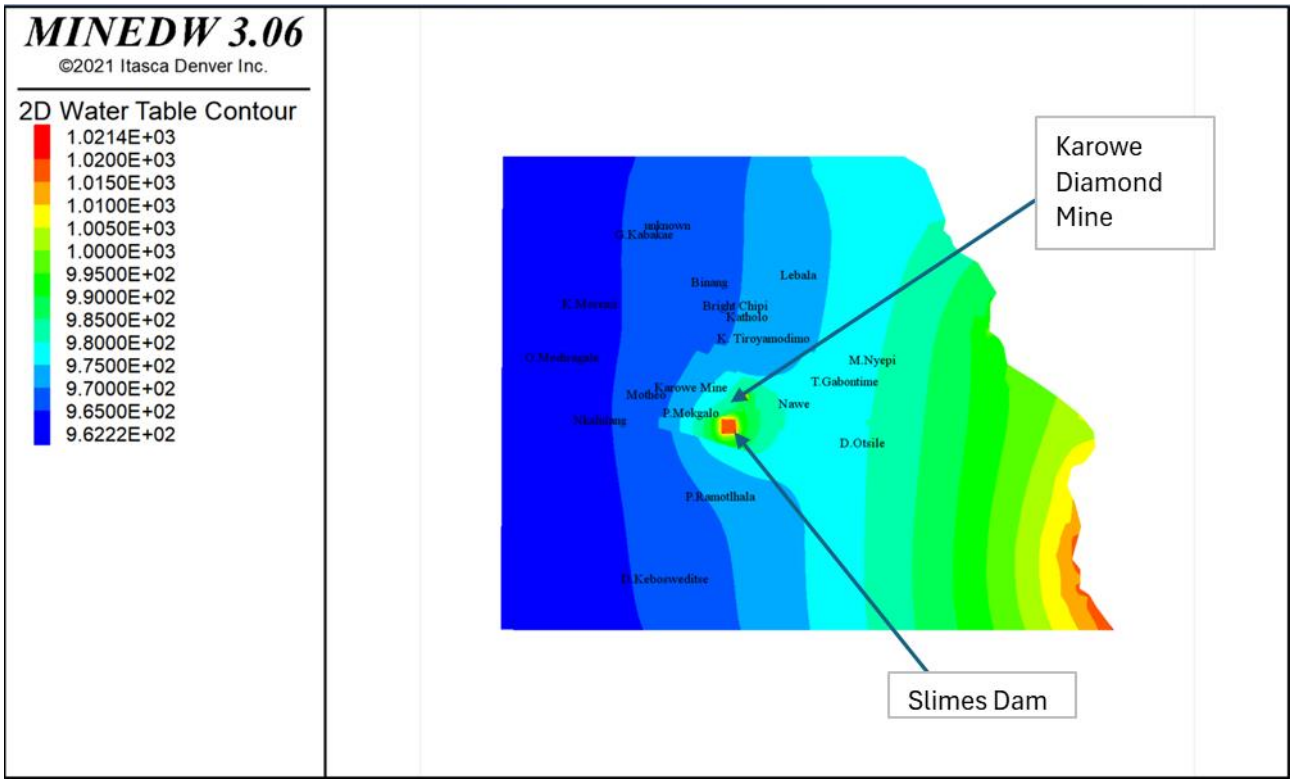

Figure 6.6: Simulated water level impact – 2010.

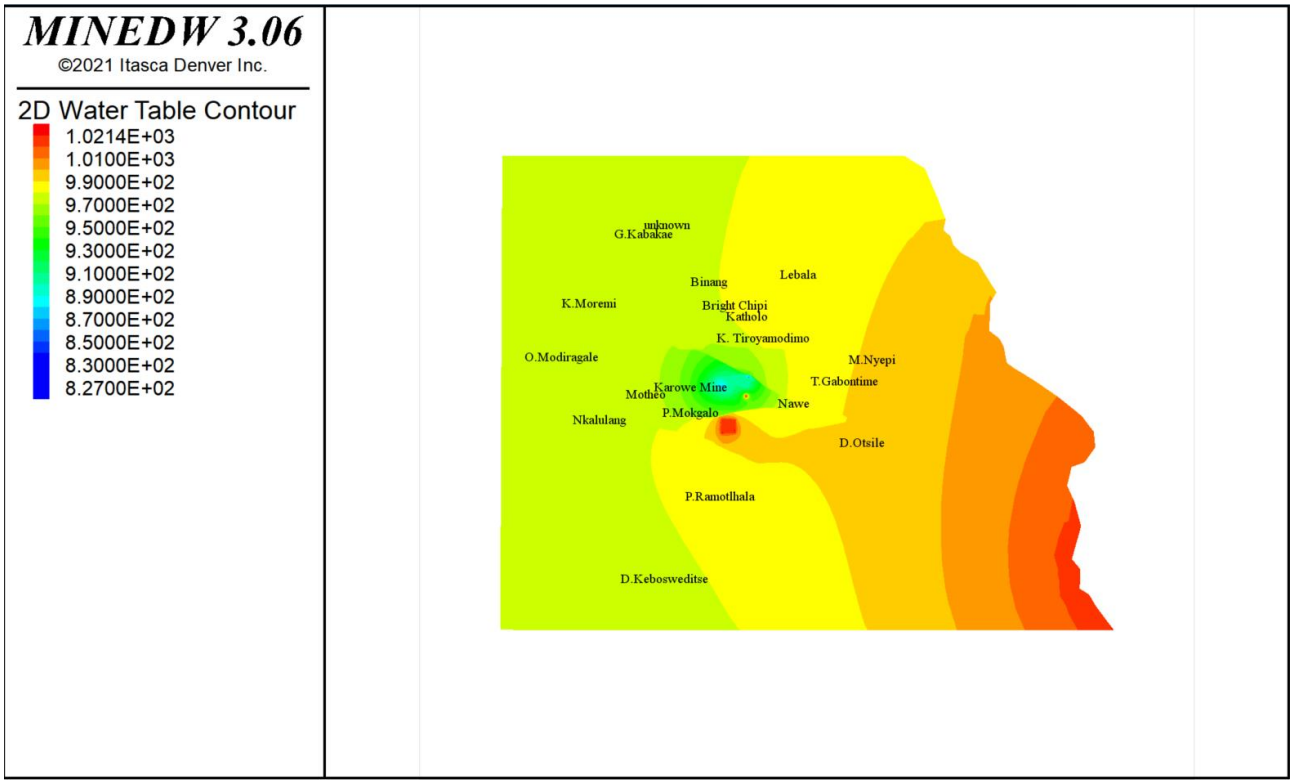

Figure 6.7: Simulated water level impact – 2015.

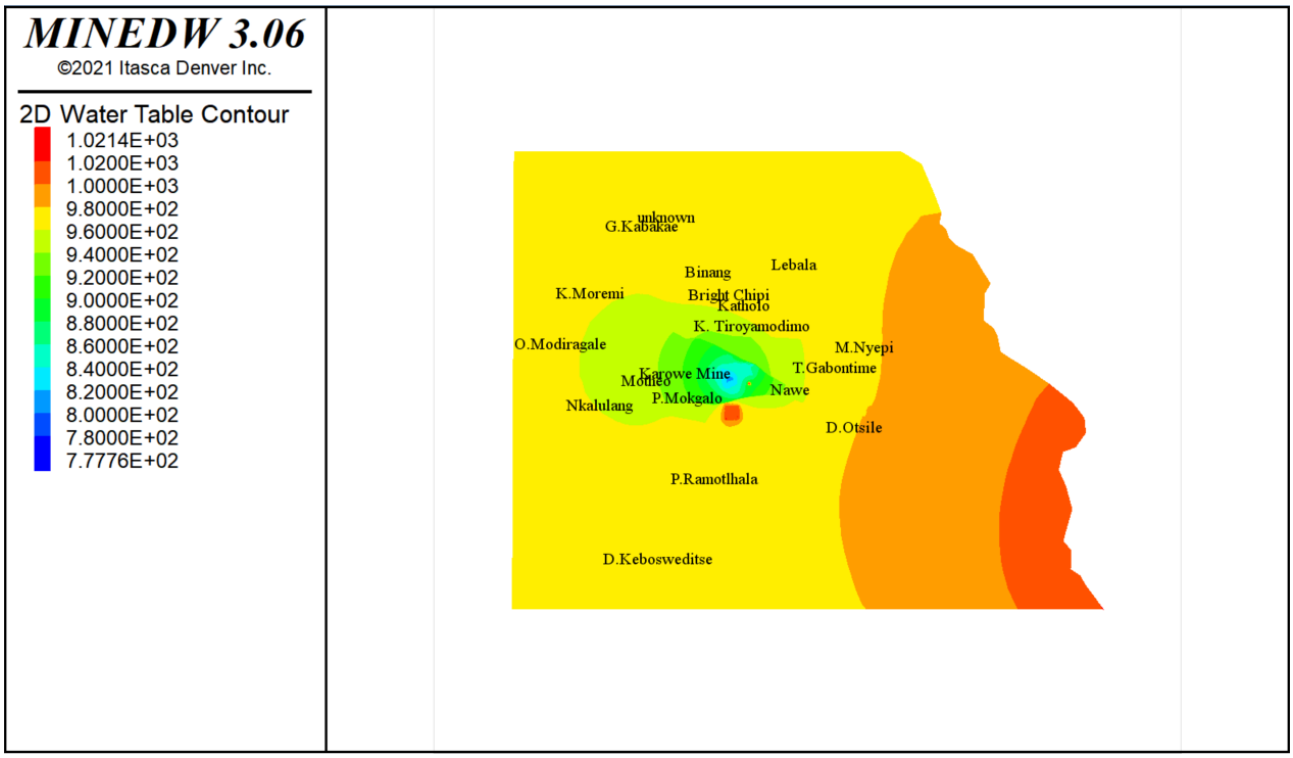

Figure 6.8: Simulated water level impact – 2025.

The measured and simulated total discharge rates are listed in Table 6.5 and shown as graphs in Figure 6.9. The simulated discharges do not show a large variation from the actual abstracted volumes. In 2012, eight dewatering boreholes produced 4105 m^3/day. The amount abstracted from boreholes was determined by the need to dewater the open pit and mine wide water requirements. Boreholes

increased from 16 in 2013 to 31 by 2021. The volumes abstracted from pit dewatering increased to 5775 m^3/day in 2013 to 7060 m^3/day in 2016. The volume abstracted had decreased to 5381 m^3/day by 2023. The decrease was caused by decaying borehole yields and low borehole efficiency. The average total simulated, and actual discharge were 5861 m^3/day and 5801 m^3/day, respectively, for the period 2009 – 2025.

Table 6.4: Simulated water levels and drawdowns at farm boreholes.

Farm borehole	Simulated water level (mamsl)				Total drawdown (m)
	2009	2015	2020	2025	
M. Nyepi	975.70	974.98	974.47	964.58	11.12
T.Gabontime	971.98	965.45	964.01	958.50	13.48
Nawe	970.28	967.85	961.30	955.91	14.37
Nkalolang	966.24	963.73	961.15	954.77	11.47
Mokgalo	968.64	917.00	876.00	869.60	99.04
Tiroyamodimo	967.76	965.87	957.97	952.84	14.92
Moremi	965.33	963.37	962.37	953.97	11.36
Katlholo	968.62	965.53	962.65	954.64	13.98
Motheo	966.74	961.00	955.10	947.66	19.08
Binang	968.90	967.36	967.80	955.29	13.61
Bright	968.69	968.33	965.13	954.23	14.46
Lebala	970.95	968.70	967.77	957.36	13.59
Kabakae	964.39	964.30	963.58	961.16	3.23
Oitsile	973.82	971.96	970.69	968.10	5.72

Table 6.5: Simulated vs actual total discharge.

Year	Number of boreholes	Simulated total borehole discharge (m^3/day)	Total borehole discharge (m^3/day)
2012	8	5282	4105
2013	16	5714	5775
2014	16	5948	6085
2015	16	4635	4794
2016	16	6935	7060
2017	16	5987	5612
2018	16	6179	6260
2019	16	6912	6963
2020	24	6745	6714
2021	31	5293	5322
2022	24	5416	5544
2023	25	5297	5381

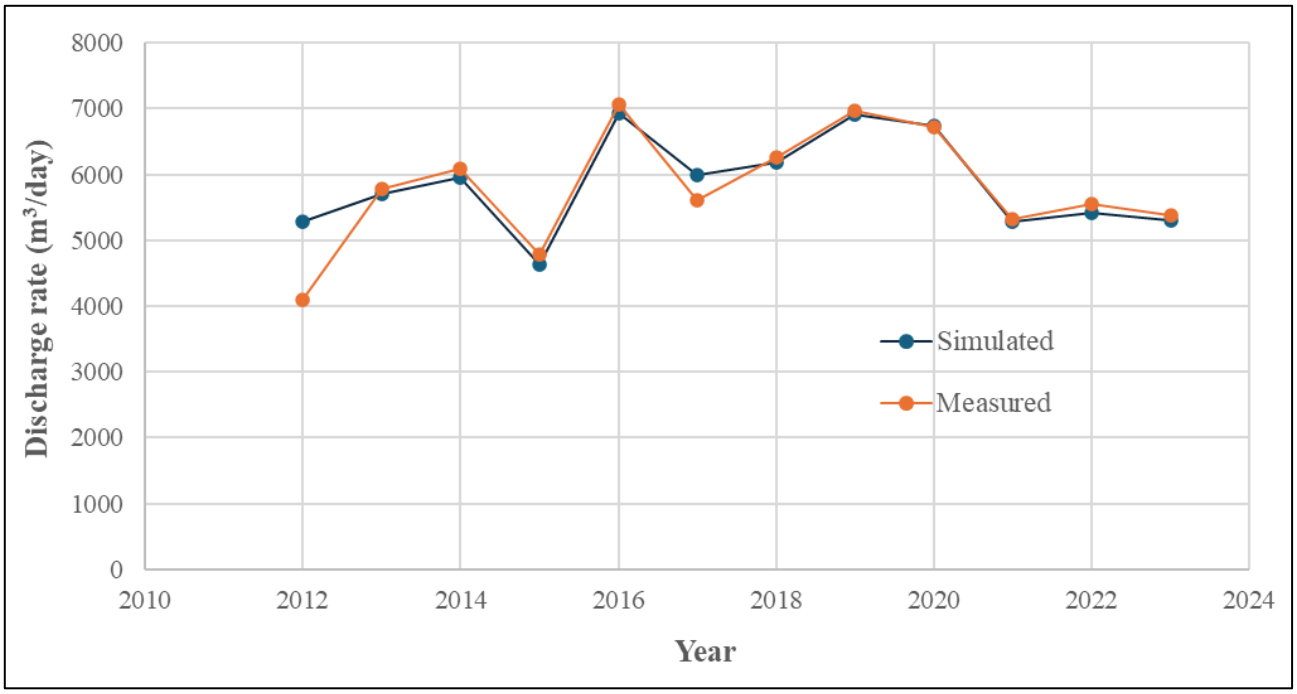

Figure 6.9: Measured and simulated discharge rates (2012- 2023).

CHAPTER 7: CONCLUSIONS AND RECOMMENDATIONS

The research area is located on the eastern fringes of the Kalahari Desert in central Botswana. Groundwater is the main source of water, and it is supplied from three different aquifer systems. The basalt aquifer is characterised by TDS <1000 mg/L, sandstone aquifer at TDS between 1500 mg/L and 4500 mg/L, and the granite system at TDS >10 000 mg/L. A numerical groundwater flow model was developed to assess the impact of mine dewatering on groundwater resources in the vicinity of KDM. The conceptual and numerical models were built using hydrogeological data available for the research area. Model calibration was done to obtain estimates of the hydraulic parameters of the different layers in the numerical model that produce a better correlation between the actual data and simulated results.

To address the aims of the study, different actions were taken to understand the groundwater conditions and the impact of mine dewatering on the groundwater resource. These actions, the information gathered, and the results obtained, are described below:

1. A hydrocensus was conducted to collect data from all existing boreholes within the research area. Boreholes owned by KDM had water levels, abstraction rates, and water quality data. However, records from KDM indicate gaps in water levels, abstraction rates and water quality between 2007 and 2023. The gaps in data are periods where there was no data collected. Farm boreholes had no records on either water levels, abstraction rates and water quality data. Data from WF6 to the east of the research area was not available for the study. WF6 is owned and operated by Debswana Mine. WF6 started operating in 2005. Pre-mining water levels used in the research study were influenced by pumping of WF6. The eastern boundary of the numerical model was set at an arbitrary so that it would not influence predictive simulations of the model. All the available data was compiled into a database, errors and suspicious values were removed from the database. The database was considered adequate to develop a reasonable conceptual and a numerical groundwater flow model.

2. A hydrogeological conceptual model was developed and was used to construct a groundwater numerical flow model. The zones included in the model represent a simplified hydrogeology of the research area and does not include details associated with the heterogeneity of a complex systems. Groundwater movement is controlled by fractures and geological discontinuities and therefore the model could not explicitly represent these features. The variations observed between actual and simulated values may be caused by the inability of the model to accurately represent the actual hydrogeological system.

3. The pre-mining phreatic surface in the research area ranged between 964 mamsl and 970 mamsl. Regional groundwater flow is from SE-NW draining into the Makgadikgadi salts pans to the north of the research area. In 2010, the hydraulic gradient caused by dewatering activities caused flow to move in the direction of open pit. At the end of 2010, the deepest and largest areas of water level drawdown are the pit, and the area defined by the SE–NW fracture zone. The SE–NW fracture zone is the main conduit that brings water into the pit. This zone brings water into the pit and supplies other smaller fractures around the research area. Boreholes that intersected this zone have produced yields >20 m^3/hr.

4. A database for water quality was compiled. The data was collected from reports and sampling exercise conducted during the research. There were limited records of baseline data from farm boreholes. The impact of mining activities on water quality at individual farms could not be assessed adequately. The main sources of water of groundwater pollution were identified as seepage coming from slimes dams and waste disposal site. Over time, deposition of slurry at the slimes dam causes increase in concentration of major cations and anions resulting in increase in TDS and EC.

5. The research area is characterised by two types of water, and Na-Cl and Na-HCO_3-Cl/Na (Mg/Ca)-HCO_3-Cl. Sampling results and analysis revealed the dominant ions to be Na^- and Cl^-.

6. The TDS concentration and EC increase with depth. This is caused by limited recharge from either rainfall or fresh water sources. A recharge rate of 0.05% MAP was used for the research study.

7. The Katholo borehole record elevated nitrate levels, and this was caused by poor borehole construction that allows cattle dung and other farm chemicals easy access to the water table. Farm boreholes with a TDS of <1000 mg/L are abstracting water from the fractured basalt and those with a TDS of >1000 mg/L are pumping from the sandstone aquifer.

8. Pumping at KDM started in 2010 with four boreholes supplying water for initial development of the operation. The volumes abstracted from pit dewatering increased from 5775 m^3/day in 2013 to 7060 m^3/day in 2016. The volume abstracted had decreased to 5381 m^3/day by 2023. The decrease was caused by decaying borehole yields and low borehole efficiency.

9. Water levels around the pit averaged 977 mamsl by end of 2010. Within a 5 km radius, conditions remained unchanged. Water levels at the slimes dams increased from 968 to 1006 mamsl. The change was caused by seepage water forming a perched aquifer system

around the slimes dams. The number of dewatering boreholes were increased to 16 and 31 in 2013 and 2020 respectively. The intensified pumping resulted in the expansion of the cone of depression such that by 2020 water levels were drawn down to within Mosolotsane sandstone. At the end of open pit mining in 2025, model predictions indicate that the deepest area of water level drawdown will be at the sump within Tlhabala mudstone. Within a radius of 10 km from the pit perimeter, water levels will experience a drawdown of >10 m by 2025.

10. The simulated drawdowns at neighbouring farms range from 3.23 m to 99.04 m by 2025. The most impacted farm borehole belongs to Mokgalo at a drawdown of 99.04 m. Mokgalo is located within the KDM lease area and is situated very close to the pit, hence the large drawdown. The predicted drawdown (2025) at the Kabakae and Oitsile boreholes are 3.23 m and 5.72 m, respectively. These two farm boreholes are not severely affected by pit dewatering. The dolerite dykes act as barriers to groundwater flow, limiting the extent of the cone of depression in the directions of these farms. Eleven borehole farms are simulated to attain a drawdown of between 11 m and 19 m; these are located along the SE-NW fracture zone.

    At the start of mining in 2010, borehole yields averaged >20 m^3/hr and in 2023 the yields have decayed with an average <7 m^3/hr. Boreholes drilled after 2018, within 150 m radius from the pit perimeter, produce lower pumping rates averaging <7 m^3/hr. This decrease in yield is localised around the pit perimeter boreholes and was caused by dewatering a program that was started in early 2010. Boreholes drilled a further 2 km from the pit perimeter still produce higher yields of 20 m^3/hr. The main sandstone aquifer within the pit perimeter has been depressurised and is now producing less water.

7.1 RECOMMENDATIONS

7.1.1 Monitoring network

The existing groundwater monitoring network is deemed inadequate because farm boreholes do not keep records of their pumping and water usage. The monitoring network should be expanded to include four standpipe piezometers around the pit perimeter. Four other standpipe piezometers should be added >3 km from the pit perimeter. All the standpipe piezometers should target the basalt, Ntane and Mosolotsane sandstone aquifers.

The standpipe piezometers will provide adequate data further away from the pit for use in updating the groundwater model. The piezometers will also provide early warning of changes in water level and quality further away from the pit.

Two boreholes should be drilled around the sewage facilities and fuel depot located within the lease area. The boreholes will provide information on groundwater conditions around the facilities.

7.1.2 Groundwater quality

Waste disposal site and slimes dam are the main sources of groundwater pollution in the research area. Future expansion of these facilities should be carefully planned with a detailed hydrogeological assessment. Water deposited together with slurry at the slimes dam should be immediately returned after settling to reduce the amount of time water takes at the dam. This will reduce the amount of water available for infiltration into the subsurface. Deposition of and concentration of salts at the dams will be reduced.

The current monitoring program collects water samples from KDM and farm boreholes for laboratory analysis. The analysis focuses on major cations and anions, the sampling and analysis should be expanded to include grease, oils, and trace elements. Chemicals used during blasting contribute to elevated levels of nitrate in groundwater and alternative chemical should be used.

7.1.3 Groundwater levels

Water level data used for the research project was collected from KDM boreholes. Water level data from farm boreholes was not available because the owners do not keep records of their pumping. It is recommended that automated monitoring systems be installed at farm boreholes for continuous data collection. The water level database should be updated monthly as new data is collected.

7.1.4 Groundwater seepage

Water deposited with slurry at the slimes dam infiltrate into the subsurface and forms a perched aquifer system immediately around the dams and recharges the perched aquifer system in the immediate vicinity of the dams. The leachate also travels and comes out as seepage in the pit highwalls. The leachate is highly concentrated in salts and once at the pit, the seepage finds its way back into the basalt and sandstone system, altering the groundwater quality in the two systems.

Scavenger boreholes should be drilled between the pit and the slimes dams to intercept seepage. The boreholes will be used to pump seepage back to the plant for reuse. Otherwise, the current management plan of guiding seepage to the bottom of the pit and pumping it out back to the plant should continue.

7.1.5 Management of existing groundwater users

A management plan should be prepared to include all stakeholders. The management plan should include mitigation and management measures for all farm boreholes that fall within the zone of influence of pit depressurisation. All boreholes likely to be impacted by mining activities should be closely monitored for flow, water levels and quality. The farmers should be encouraged to keep records such as water levels and abstraction rates for future model updates.

7.1.6 Modelling of post-closure impacts

The groundwater flow model developed in this study simulated only the impact of mine dewatering on the groundwater resources in terms of groundwater quantity. During the mining phase, the hydraulic gradient created by mine dewatering is towards the pit. However, in the post-closure phase of the mine, the natural groundwater gradient will be reestablished. Any remaining mine waste could then potentially act as sources of contamination, leading to contaminant impacts at positions downgradient from the mine. To investigate the possible off-site migration of contaminants and the related impacts on groundwater quality, it is recommended that a mass transport model be developed for the post-closure phase of the mine. This model could incorporate much of the information gathered during the current study.

7.1.7 Water licensing

It is recommended that all boreholes should be registered with the government for proper accounting of water use.

REFERENCES

Amines and Cecide. 2021. *Grassroots research on local diamond mining impact.* Kimberly Process Civil Society Coalition. Available at: https://www.kpcivilsociety.org/wp-content/uploads/2022/02/KPCSC_Grassroots_Research_Guinee_Summary.pdf.

AquiSim. 2020. *Karowe/Orapa - 2020 groundwater flow model update.* AquiSim Consulting Services, Technical Report G14/50 – Revision 0.

Azrag, E.A., Ugorets, V.I., and Atkinson, L.C. 1998. *Use of a finite element code to model complex mine water problems*: Proceedings of symposium on mine water and environmental impacts, Vol. 1, International Mine Water Association, Johannesburg, September, p. 31-42.

Barnett, W. 2006. *AK6 Structural geology interpretation.* De Beers. Technical Memorandum - August 2006.

Barnett, W. 2007. *AK6 Country Rock Model.* De Beers. March 2007.

Betancur, T., Palacio, T.C.A and Escobar M.J.F. 2012. *Conceptual models in hydrogeology, methodology and results, Hydrogeology - a global perspective,* Dr. Gholam A. Kazemi (Ed.), ISBN: 978-953-51-0048-5, InTech. Available at: http://www.intechopen.com/books/hydrogeology-a-globalperspective/conceptual-models-in-hydrogeology-methodologies-and-results.

Borden, R.K., Brown P.L., and Sturgess S. 2022. *Geochemical and hydrological evolution of mine impacted waters at Argyle Diamond Mine, Western Australia.* Applied Geochemistry, Volume 139, April 2022, 105253. Available at: https://www.sciencedirect.com/science/article/abs/pii/S0883292722000579.

Boteti Mining. 2012. *Groundwater monitoring report – Number 1*. Karowe Diamond Mine.

Brook M.C. 2011. *Water resources management at Debswana Diamond Company: Water use in the mining sector*. Water Pitso. Selebi Phikwe, 9 June 2011.

Brook M.C. 2012. *The journey of Botswana's diamonds – Location of Botswana's diamond mines*. DTC Botswana. ISBN978-99912-941-8-6.

Carney J.N, Aldiss D.T, Lock N.P. 1994. *The geology of Botswana*. Director of Geological Survey, Bulletin 37. Lobatse, Botswana.

Chenjerai E. 2017. *Zimbabweans clash with diamond mining interest over pollution and other plights.* Global Press Journal, February 6, 2017. Available at: https://globalpressjournal.com/africa/zimbabwe/zimbabweans-clash-diamond-mining-interests-pollution-blight/.

CCRAG. 2021. *Effects of artisanal diamond mining on the living conditions of local communities in the Central African Republic. Executive summary: Grassroots research on local diamond mining impacts.* Kimberley Process Civil Society Coalition. Available at: https://www.kpcivilsociety.org/wpcontent/uploads/2022/02/KPCSC_Grassroots_research_CAR_Summary.pdf [Accessed 26 September 2023].

Concor. 2023. *Concor to build key pollution control dam for Venetia*. Available at: https://www.concor.co.za/concor-to-build-key-pollution-control-dam-for-venetia/.

Connelly, R.J. and Gibson, J. 1985. *Dewatering of the open pits at Letlhakane and Orapa Mines, Botswana*. International Journal of Mine Water 4(3): 25–41. Available at: http://www.mwen.info/bibliographie/04_3_025-041.pdf.

Couch W.J. 2002. *Strategic resolution of policy, environmental and socio-economic impacts in Canadian Arctic diamond mining: BHP's NWT diamond project.* Impact Assessment and Project Appraisal 20(4): 265–278. DOI: https://doi.org/10.3152/147154602781766564.

DAA. 2017. *Understanding environmental impacts – when less is more*. Data Analysis Australia. Available at: https://www.daa.com.au/articles/case-studies/understanding-environmental-impacts/.

De Beers. undated. *A general overview: Venetia Mine*. Fund Managers Delegation. Available at: https://www.angloamerican.com/~/media/Files/A/AngloAmericanGroup/PLC/media/presentations/2003pres/gen_over03.pdf [Accessed 27 September 2023].

Deton' Cho Stantec. 2015. *An analysis of 'cumulative effects' in Lac de Gras Water Chemistry over the period of record*. Final Report. Government of Northwest Territories. Project Number 144901977 – SC440008. Available at: https://www.emab.ca/sites/default/files/cimp_-_report_lacdegras_20150430_fin_-_2015-16_-_stantec.pdf.

Diamant-Gems. undated. *Alluvial deposits of China*. KOH Diamonds, Bourse du Diamond Centre, Schupstraat 9-11, 2018 Antwerpen, Belgium. Available at: https://www.diamant-gems.com/en/diamond-china [Accessed 20 June 2024].

Dold. 2014. *Evolution of acid mine drainage formation in sulphidic mine tailings*. Minerals 4(3): 621–641. DOI: https://doi.org/10.3390/min4030621.

Domininion Diamonds. 2019. *Ekati Diamond Mine – environmental agreement and water licence* Annaul Report Summary 2019. Available at: https://www.naturaldiamonds.com/wp-content/uploads/2021/07/Ekati-2019-WL-and-EA-Annual-Report-Plain-Language-Summary-Jul-2_20.pdf.

DWA. 2014. *Policy brief – mining and water resources in Botswana*. Department of Water Affairs and the Centre for Applied Research.

EPA. 2005. *Argyle Diamond Mine – underground project 110 km south of Kununurra, East Kimberly.* Report and Recommendations of the Environmental Protection Authority. Perth, Australia. Bulletin 1205, November 2005. Available at: https://www.epa.wa.gov.au/sites/default/files/EPA_Report/2152_B1205.pdf.

Exigo3. 2019. *Lucara Botswana - Karowe Diamond Mine: Lugeon (packer) testing and analysis.* Technical Report: HG-P-18-064-V3.

Jeffay J. 2021. *Third time lucky: Firestone finally sells Botswana operation*. Newsroom Full Article. IDEX July 5, 2021. Available at: https://www.idexonline.com/FullArticle?id=46834.

Galli, N., Chiarelli, D. D., D'Angelo, M., and Rulli, M. C. 2020. *Environmental impacts of diamond mining in the Democratic Republic of Congo*. EGU General Assembly 2020, Online, 4–8 May 2020, EGU2020-20634. DOI: https://doi.org/10.5194/egusphere-egu2020-20634.

Geoflux. 2007. *Environmental Impact Assessment for the Proposed AK06 Diamond Mine*. EIA Report. Volume 1 Main Report. Boteti Exploration (Pty) Ltd.

GGF. 2017. *Water over diamonds: a landmark ruling in Zimbabwe*. Global Greengrants Fund. Available at: https://www.greengrants.org/2017/08/02/zimbabwe/.

GMS. 2019. *Borehole geophysics siting for dewatering, Karowe Diamond Mine*. Enquiry No. BOT/PROC/TENDERS/2019/0147. Final Report.

HCI. 2007. *Initial three-dimensional ground-water flow model of Damtshaa Mine and predicted ground-water conditions during mining.* Damtshaa Mine. HCI-1821.

IEMA. 2005. *Public watchdog for environmental management at the Ekati Diamond Mine*. Presentation to Western Mining Action Network, October 2005 – IEMA. Available at:

https://monitoringagency.net/wpcontent/uploads/legacy/IEMA%20%28KOR%20Pres%20to%20WMAN%20Oct%202005%29.pdf.

Itasca. 2015. *Karowe Mine groundwater flow model and predictive dewatering simulations*. Technical Memorandum 4016. Boteti Mining.

Itasca. 2020. *Karowe groundwater model.* Prepared for Lucara Diamond Mine. SA-187.

JDS. 2019. *Karowe Mine underground feasibility study: technical report*. JDS Energy and Mining Inc. Botswana. Report Date: December 16, 2019.

Karmakar, H.N. and Das, P.K. 2012. *Impact of mining on ground and surface water*. Central Mine Planning and Design Institute Ltd., R.I-II, Koyla Bhawan Complex, Dhanbad -826005, Bihar, India. International Mine Water Association 2012. Available at: https://www.imwa.info/docs/imwa_1991/IMWA1991_Karmakar_187.pdf.

KDM. 2019. *Annual groundwater monitoring report. Volume 7.* Ref: LUC/2019/01 Lucara Botswana.

KDM. 2023. *Annual groundwater monitoring report*. *Volume 11*. Ref: LUC/2024/01 Lucara Botswana.

Keller, P.C. and Guo-dong, W. 1986. *The Changma Diamond District, Mengyin, Shandong Province, China*. Available at: https://www.gia.edu/doc/The-Changma-Diamond-District-Mengyin-Shandong-Province-China.pdf.

KLMCS. 2006. *AK06 Project – Preliminary Hydrogeological Conceptual Model*. De Beers Geotechnical Department. October 2006.

KLMCS. 2007a. *AK6 dewatering project pre-feasibility study*. De Beers Geotechnical Department. June 2007.

KLMCS. 2007b. *Initial groundwater flow model of AK6 pit and recommendations for dewatering*. July 2007

KLMCS. 2010. *AK6 Mine Feasibility Study Project* – Hydrogeological Evaluation Report. ON P1228-F- PPM – AK6-010 DP017. PPM Projects

KLMCS. 2011. *AK6 Drilling and Aquifer Testing Report*. *AK6 Mine Pit Groundwater Dewatering Study*. Boteti Mining. Botswana.

KLMCS. 2014. *Karowe Mine Groundwater Modelling Review. Final Report 2014.*

KLMCS. 2017. *Karowe Mine conceptual model to 720 mbgl*. Report by KLM Consulting Services. Boteti Mining, Karowe Diamond Mine Site. December 2017.

KLMCS. 2018. *Karowe Mine Numerical Modelling Report*. Boteti Mining, Karowe Diamond Mine Site. Order No. Z4345, November 2017.

Lekula, M. and Lubczynski, M. 2019. *Use of remote sensing and long term in-situ time series data in an integrated hydrological model of the Central Kalahari Basin, Southern Africa*. Hydrogeology Journal 27 : 1541–1562. DOI : https://doi.org/10.1007/s10040-019-01954-9.

Maguwu, F. 2019. M*arange Diamond Mines pollute rivers, Zimbabwe.* Available at: https://www.ejatlas.org/print/marange-diamond-mines-pollute-rivers-zimbabwe.

Matthews, H. undated. *Diamond mining in South Africa*. Available at: https://hayleymatthews-diamondmining-southafrica.weebly.com/mining-in-kimberley.html [Accessed 12 March 2023].

Maydan M.V. 2015. *Diamond mining in the Democratic Republic of Congo: the effects of the Kimberly Certification Process Scheme*. Available at: https://www.grin.com/document/452243 [Accessed 26 September 2023].

MCDF. 2021. *Large scale diamond mining in Lesotho: unpacking its impact on adjacent communities*. Available at: https://www.kpcivilsociety.org.

Mills, M. 2019. *Geochemical study for the Karowe Diamond Mine*. Prepared by Mills Water - September 2019.

Mindat. 2024. *Dingjigang Mine, Yuan River placers (Yuanjiang placers), Dingcheng District, Changde, Hunan, China*. Available at: https://www.mindat.org/loc-185573.html.

Minerals Council. 2022. Mining for Schools. Available at: https://www.miningforschools.co.za/lets-explore/diamond/environment [Accessed 27 September 2023)

Mining Technology. 2013. *Venetia Mine*. Available at: https://www.mining-technology.com/projects/de_beers/ [Accessed 28 September 2023].

Morton K. and Muller S., 2003. *The hydrogeology of Venetia Diamond Mine, South Africa*. Geological Society of South Africa. Available at: https://www.researchgate.net/publication/250085280_Hydrogeology_of_the_Venetia_Diamond_Mine_South_Africa [Accessed on 27 September 2023].

NMJD. 2021. *The challenges characterizing Sierra Leone's artisanal diamond mining sector and why the sector should be formalized*. Network Movement for Justice and Development. Kimberly Process Civil Society Coalition. Sierra Leone. Available at : https://www.kpcivilsociety.org/publication/coalition/grassroots-research-on-local-diamond-mining-impacts/sierra-leone/.

Obakeng, T.O. 2007. *Soil moisture dynamics and evapotranspiration at the fringe of the Botswana Kalahari, with emphasis on deep rooting vegetation*. ITC dessertation number 141. ITC. The Netherlands.

O'Connell, J. 2022. *The impact of diamond mining in DRC*. The Borgen Project. Available at: https://borgenproject.org/diamond-mining-in-drc/.

Olson, S. 2023. *9 biggest mining companies in China*. Investopedia. Available at: https://www.investopedia.com/insight/chinese-mining-companies/ [Accessed 20 November 2024].

Oluleye, G. 2021. *Environmental impacts of mined diamonds*. Center for Environmental Policy, Imperial College London. Available at: http://www.imperial-consultants.co.uk/wp-content/uploads/2021/02/Final-report-Environmental-Impacts-of-Mined-Diamonds.pdf [Accessed 31 August 2022].

Petra Diamonds. 2009. *Sustainable development report 2009*. Available at: https://files.investis.com/petradiamonds/sdr2009/environment.html.

Rao, D.K., Panchaksharjah, S., Pati, B.N., Narayana, A. and Raiker, D.L.S. 1982. *Chemical composition of irrigation waters from selected parts of Bijapur District Karnataka, Mysore*. Research Journal of Agriculture and Biological Sciences 16(4): 426–432.

Rastogi, V. 2023. *RMSE and MAE*. Available at: https://medium.com/@vaibhav1403/rmse-and-mae-415470f52b58.

Rentmeesters, K. 2021. *About that diamond mine in China. Let's talk facts*. Available at: https://www.linkedin.com/pulse/diamond-mine-china-lets-talk-facts-karen-rentmeesters/.

Rio Tinto, 2023. *Sustainability report. Surface water allocation*. Available at: https://experience.arcgis.com/experience/6c146e9361814524bb0926ce2871b471.

SADC-GMI. 2020. *Transboundary diagnostic analysis of the Eastern Kalahari-Karoo Basin aquifer system*. SADC-GMI report: Bloemfontein, South Africa.

Selaolo, E.T. 1998. *Tracer studies and groundwater recharge assessment in the Eastern Fringe of Botswana Kalahari*. PhD thesis, Vrije Universiteit, Amsterdam, The Netherlands, 229 p

Statistics Botswana. 2017. *Annual agricultural survey report 2017.* Revised Version. Published by Statistics Botswana. Gaborone, Botswana.

SRK. 2019. *Update of the AK6 geological model in support of a mineral update for the 2019 Karowe Underground Feasibility Study*. Project 2CL026.003.

Trucost. 2019. *The socioeconomic and environmental impact of large-scale diamond mining.* Diamond Producers Association. Available at: https://lucaradiamond.com/site/assets/files/4832/the-socioeconomic-and-environmental-impact-of-large-sca.pdf.

UNEP. 2017. *UNEP study – catastrophes et conflicts*. Available at: https://www.unep.org/fr/node/848.

WSB. 2007. *AK06 wellfield investigation study* -Enquiry No 0614-E8162.Project Number AK06-15COR-0228. De Beers Prospecting (Pty) Ltd. Final Report July 2007.

WSB. 2008. *AK06 wellfield investigation study* – Ref: purchase order C2737/DH/DRAAF/001. De Beers Prospecting (Pty) Ltd. Final Report January 2008.

WSB. 2013. *Wellfield 7 groundwater development project*. Water Surveys Botswana. Draft Final Report Volume 1 – Main Volume.

WCS. 2001. *EIA for DiamondEx Botswana Limited. Martin's Drift Diamond Project, Central District, Botswana*. Wellfield Consulting Services.

World Bank. 2010. *Botswana: enhancing environmental sustainability in the implementation of the NDP1*0. Draft Policy Note. Report No: XXXXX-XX, Draft – October 2010. Available at: https://www.car.org.bw/wp-content/uploads/2016/06/Botswana-Environment-Policy-Note-October2010-final.pdf.

Yakovleva, P.N., Alabaster, T. and Petrova, G.P. 2000. *Natural resource in the Russian north: a case study of diamond mining in the Republic of Sakha*. Available at: https://www.researchgate.net/publication/235311727_Natural_resource_use_in_the_Russian_North_a_case_study_of_diamond_mining_in_the_Republic_of_Sakha.

ABSTRACT

Lucara Botswana operates Karowe Diamond Mine (KDM, formerly known as the AK6 kimberlite pipe) which occurs in the Boteti region. The mine is situated within an agricultural zone where groundwater is the main source of water supply. The mine was commissioned in July 2012 as an open pit mine (JDS, 2019). The life of mine for the open pit is expected to extend to 2025 upon which underground operations will start.

Open pit mining excavations at KDM have extended below the groundwater table. Groundwater is removed through dewatering boreholes to lower the phreatic surface to allow for a safe mining environment. The large volumes of water extracted are pumped for use in ore processing, while the slimes from the process plant are deposited in a tailings facility. The main existing and potential impacts from mining are therefore twofold: 1) impacts on groundwater quantity because of depletion of the aquifer system due to mine dewatering, and 2) impacts on groundwater quality from the open pit, waste rock dump, plant, and tailings facility.

While mining operations abstract water from deeper saline aquifer system, private farmers tap the shallow fresh basalt waters. This study aims to investigate the impacts that open pit mining will have on the water resources in the vicinity of KDM.

The data used for the research study was collected through literature review, hydrocensus activities, and groundwater monitoring (water level, abstraction and water quality). Water samples were collected from both KDM and farm boreholes for analysis and the results were interpreted to determine water quality changes. Water levels and abstraction data were measured from KDM boreholes. Water level and abstraction data from farm boreholes were not available to be used in the research study.

Three different aquifer systems exist in the research area. The basalt aquifer is characterised by TDS < 1000 mg/L, sandstone aquifer at TDS between 1500 – 4500 mg/L and the granite system at TDS >10,000 mg/L. Water quality analysis revealed that two types of water exist in the research area, Na-Cl and Na-HCO_3-Cl/Na (Mg/Ca)-HCO_3-Cl types. The most dominant ions are Na^+ and Cl^-. The slimes dams were identified as the main source of groundwater pollution. Slurry water that is not recycled back to the plant infiltrates into the subsurface and forms a perched aquifer system within the weathered basalt. Over time, the concentration of salts at the slimes dams increases and high salinity seepage from this will ultimately alter the quality of water in the basalt system.

The numerical groundwater flow model was developed and calibrated for both steady state and transient conditions. For steady-state simulation, a specified head was assigned to the southeastern and northwestern model boundary. Internal partial barrier boundaries were represented by SE-NW

faults and dykes. The SE–NW fracture zone is the main conduit that brings water into the pit. For transient simulations, no flow boundaries were changed to reflect pumping conditions in the model. Recharge was estimated at 0.05% MAP. The accuracy of the simulated results was assessed by evaluating the differences between the simulated and actual groundwater levels (referred to as errors). For the simulated groundwater levels, an MAE of 0.73 and an RMS of 0.86 were estimated from the 25 groundwater level pairs (measured and modelled). A correlation coefficient of 0.82 was estimated, indicating a strong linear relationship between the model calculated values and the actual data.

The impact of pumping on water levels in 2010 is not well established because there were only four active boreholes at the time. The water level around the pit averaged 977 mamsl. Farther away from the pit, conditions changed slightly. Water levels around the slimes dams increased from 968 mamsl to 1006 mamsl. The increase was caused by seepage water coming from slurry deposition at the slimes dams. In 2013, the number of active pit dewatering boreholes was increased to 16, resulting in the expansion of the cone of depression. In 2015, the water level 5 km from the pit perimeter was 960 mamsl compared to 964 mamsl in 2009. Water levels changed by <1 m some 10 km from the pit perimeter.

The period from 2018 to 2022 experienced the implementation of an accelerated dewatering program. KDM increased the number of pit dewatering by nine. The maximum simulated drawdown in the pit is to an elevation of 777 mamsl by end of open pit mining in 2025. Water levels are drawn down to within the Tlhabala mudstone. The dewatering program will depressurise Ntane sandstone aquifer by 2025 and all water supply requirements will come from the lower Mosolotsane sandstone aquifer.

The simulated drawdowns at neighbouring farm boreholes ranged 3.23 m to 99.04 m by 2025. The most impacted farm borehole belongs to Mokgalo at a drawdown of 99.04 m by 2025. Boreholes along the SE-NW fracture zone are the most impacted with a drawdown >10 m by 2025. Kabakae and Oitsile are the least impacted boreholes with a drawdown of 3.23 m and 5.72 m respectively. Eleven farm boreholes will record a drawdown between 11.12 m and 19.08 m.

In 2012, eight dewatering boreholes produced 4105 m^3/day. The amount abstracted from boreholes was determined by the need to dewater the open pit and mine wide water requirements. Boreholes increased from 16 in 2013 and to 31 in 2021. The volumes abstracted from pit dewatering increased to 5775 m^3/day in 2013 to 7060 m^3/day in 2016. The volume abstracted had decreased to 5381 m^3/day by 2023. The decrease was caused by decaying borehole yields and low borehole efficiency. The average total simulated, and actual discharge were 5861 m^3/day and 5801 m^3/day, respectively, for the period 2009 to 2025.

APPENDIX A

WATER QUALITY CHANGES OVER TIME

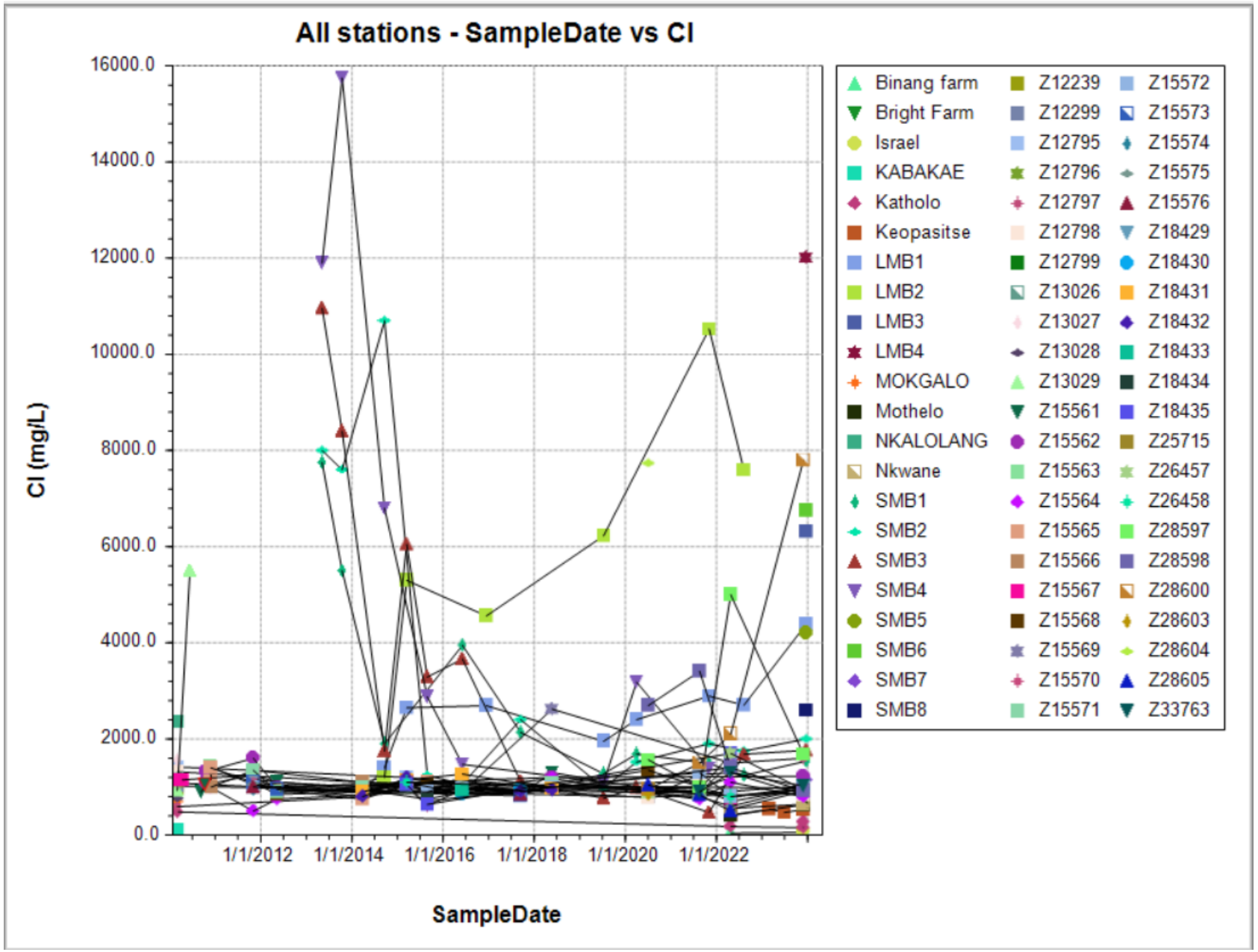
All stations - SampleDate vs Cl
Cl (mg/L)
16000.0
14000.0
12000.0
10000.0
8000.0
6000.0
4000.0
2000.0
0.0
1/1/2012
1/1/2014
1/1/2016
1/1/2018
1/1/2020
1/1/2022
SampleDate
Binang farm
Bright Farm
Israel
KABAKAE
Katholo
Keopasitse
LMB1
LMB2
LMB3
LMB4
MOKGALO
Mothelo
NKALOLANG
Nkwane
SMB1
SMB2
SMB3
SMB4
SMB5
SMB6
SMB7
SMB8
Z12239
Z12299
Z12795
Z12796
Z12797
Z12798
Z12799
Z13026
Z13027
Z13028
Z13029
Z15561
Z15562
Z15563
Z15564
Z15565
Z15566
Z15567
Z15568
Z15569
Z15570
Z15571
Z15572
Z15573
Z15574
Z15575
Z15576
Z18429
Z18430
Z18431
Z18432
Z18433
Z18434
Z18435
Z25715
Z26457
Z26458
Z28597
Z28598
Z28600
Z28603
Z28604
Z28605
Z33763

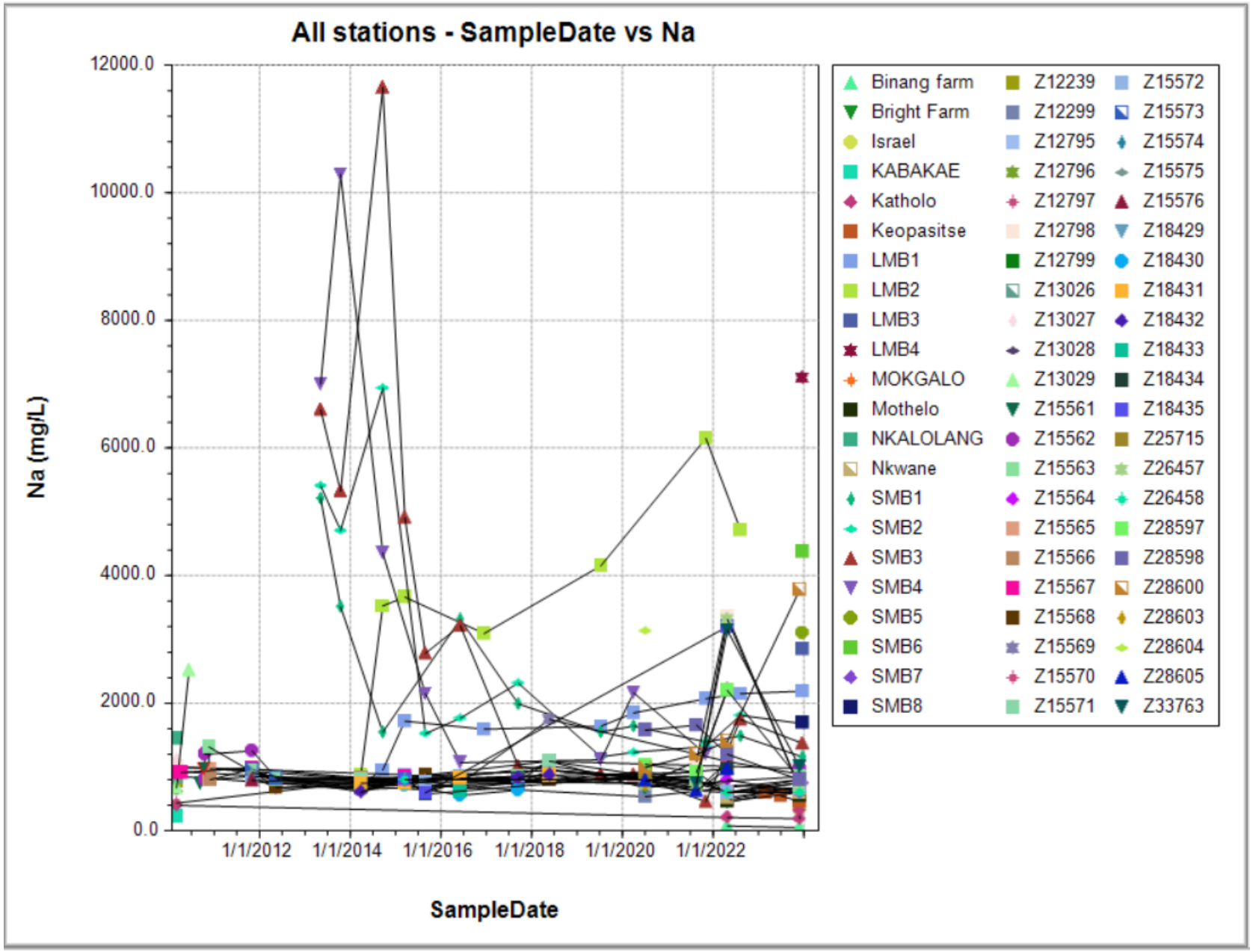
All stations - SampleDate vs Na
Na (mg/L)
12000.0
10000.0
8000.0
6000.0
4000.0
2000.0
0.0
1/1/2012
1/1/2014
1/1/2016
1/1/2018
1/1/2020
1/1/2022
SampleDate
Binang farm
Bright Farm
Israel
KABAKAE
Katholo
Keopasitse
LMB1
LMB2
LMB3
LMB4
MOKGALO
Mothelo
NKALOLANG
Nkwane
SMB1
SMB2
SMB3
SMB4
SMB5
SMB6
SMB7
SMB8
Z12239
Z12299
Z12795
Z12796
Z12797
Z12798
Z12799
Z13026
Z13027
Z13028
Z13029
Z15561
Z15562
Z15563
Z15564
Z15565
Z15566
Z15567
Z15568
Z15569
Z15570
Z15571
Z15572
Z15573
Z15574
Z15575
Z15576
Z18429
Z18430
Z18431
Z18432
Z18433
Z18434
Z18435
Z25715
Z26457
Z26458
Z28597
Z28598
Z28600
Z28603
Z28604
Z28605
Z33763

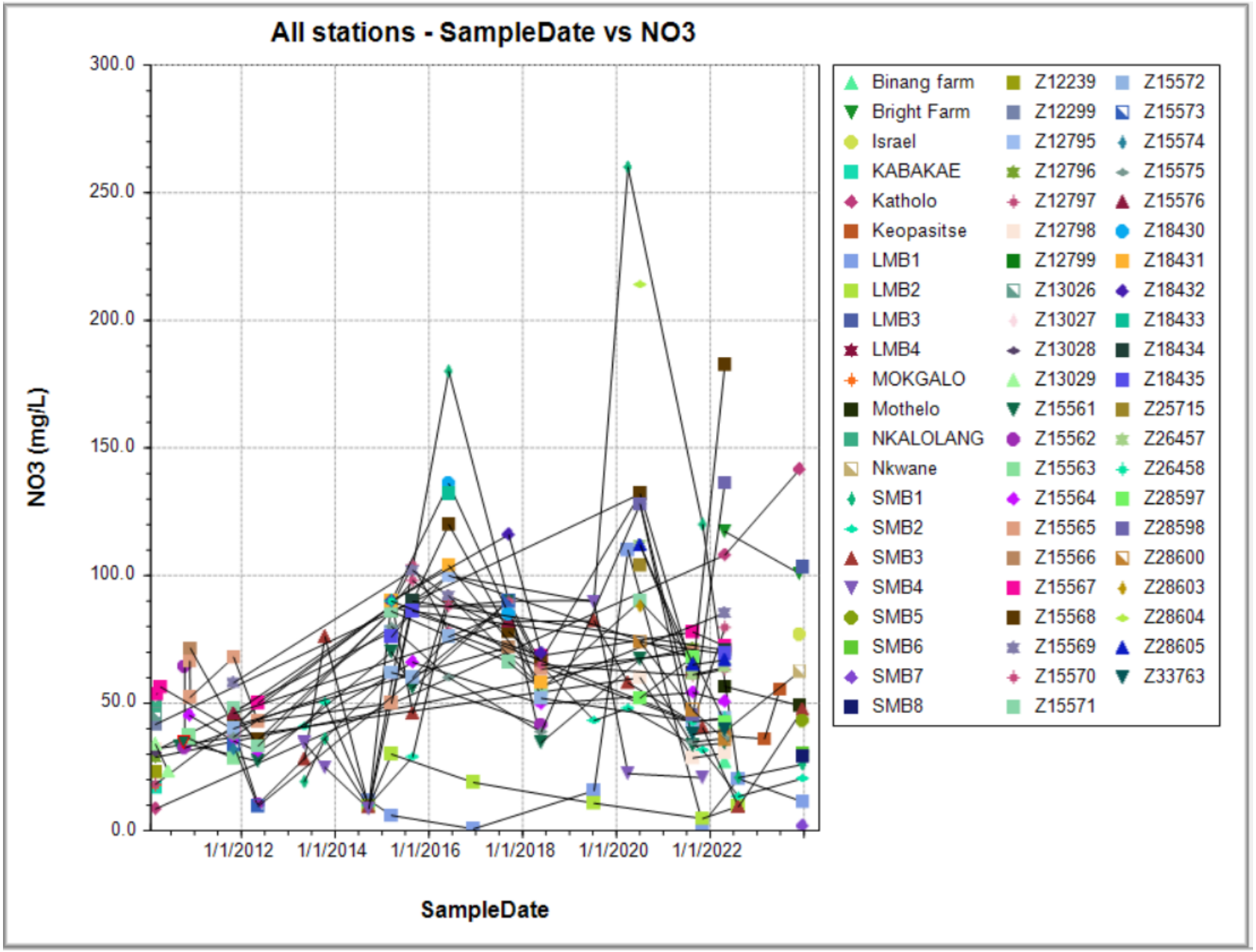
All stations - SampleDate vs NO3
NO3 (mg/L)
300.0
250.0
200.0
150.0
100.0
50.0
0.0
1/1/2012
1/1/2014
1/1/2016
1/1/2018
1/1/2020
1/1/2022
SampleDate
Binang farm
Bright Farm
Israel
KABAKAE
Katholo
Keopasitse
LMB1
LMB2
LMB3
LMB4
MOKGALO
Mothelo
NKALOLANG
Nkwane
SMB1
SMB2
SMB3
SMB4
SMB5
SMB6
SMB7
SMB8
Z12239
Z12299
Z12795
Z12796
Z12797
Z12798
Z12799
Z13026
Z13027
Z13028
Z13029
Z15561
Z15562
Z15563
Z15564
Z15565
Z15566
Z15567
Z15568
Z15569
Z15570
Z15571
Z15572
Z15573
Z15574
Z15575
Z15576
Z18430
Z18431
Z18432
Z18433
Z18434
Z18435
Z25715
Z26457
Z26458
Z28597
Z28598
Z28600
Z28603
Z28604
Z28605
Z33763

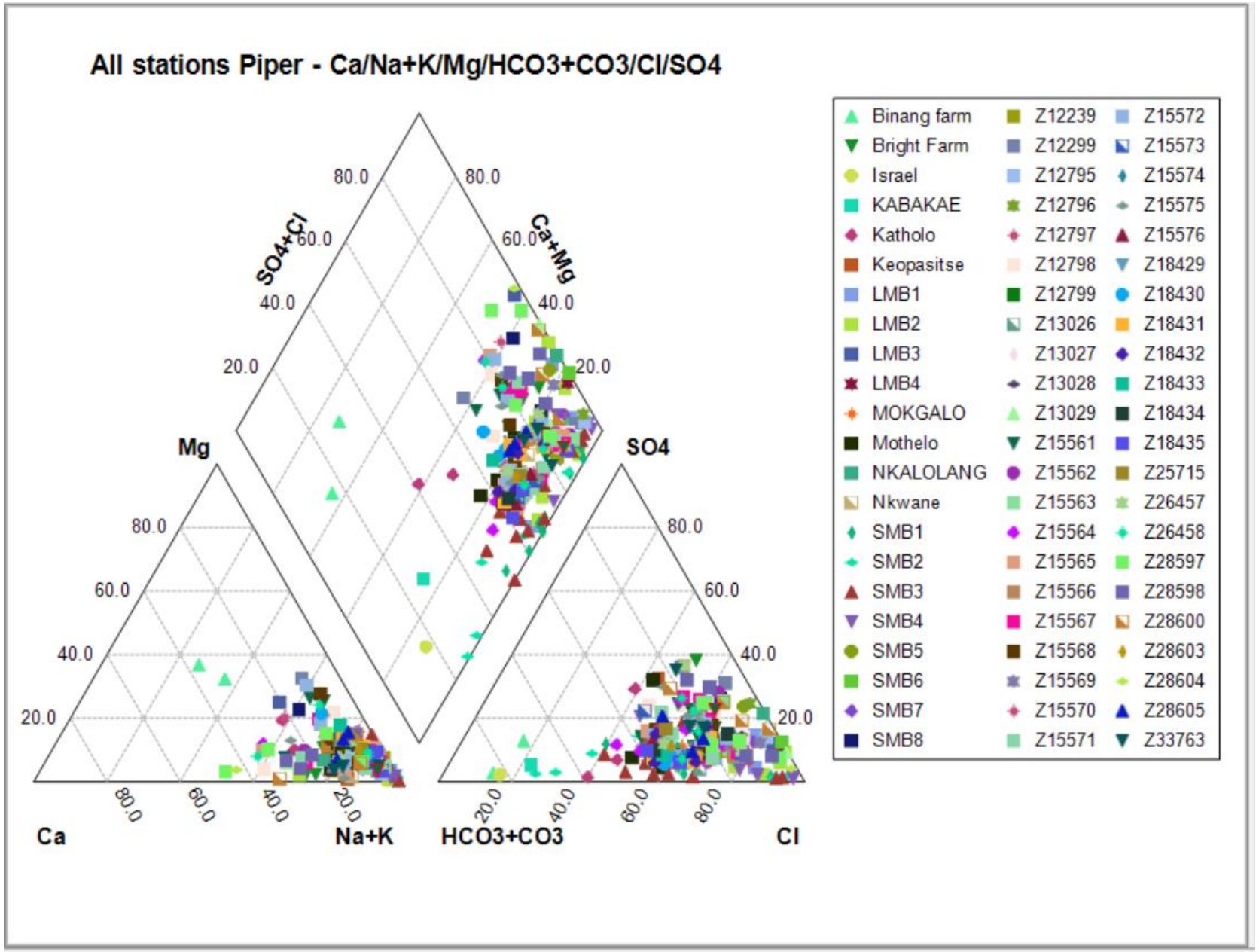
All stations Piper - Ca/Na+K/Mg/HCO3+CO3/Cl/SO4
SO4+Cl
Ca+Mg
Mg
SO4
Ca
Na+K
HCO3+CO3
Cl
80.0
60.0
40.0
20.0
Binang farm
Bright Farm
Israel
KABAKAE
Katholo
Keopasitse
LMB1
LMB2
LMB3
LMB4
MOKGALO
Mothelo
NKALOLANG
Nkwane
SMB1
SMB2
SMB3
SMB4
SMB5
SMB6
SMB7
SMB8
Z12239
Z12299
Z12795
Z12796
Z12797
Z12798
Z12799
Z13026
Z13027
Z13028
Z13029
Z15561
Z15562
Z15563
Z15564
Z15565
Z15566
Z15567
Z15568
Z15569
Z15570
Z15571
Z15572
Z15573
Z15574
Z15575
Z15576
Z18429
Z18430
Z18431
Z18432
Z18433
Z18434
Z18435
Z25715
Z26457
Z26458
Z28597
Z28598
Z28600
Z28603
Z28604
Z28605
Z33763

APPENDIX B

TRANSIENT CALIBRATION

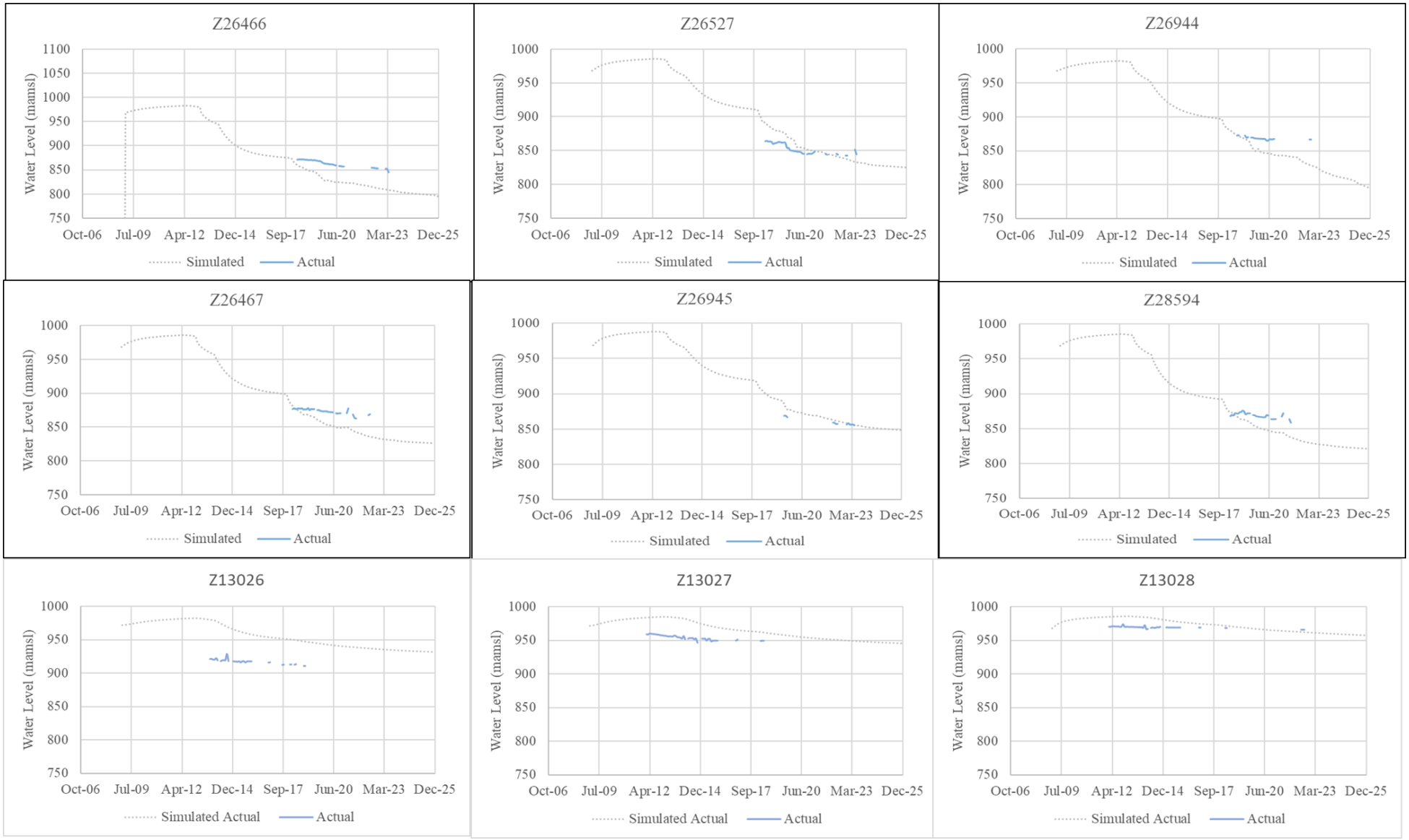
Z26466
Water Level (mamsl)
1100
1050
1000
950
900
850
800
750
Oct-06 Jul-09 Apr-12 Dec-14 Sep-17 Jun-20 Mar-23 Dec-25
Simulated
Actual
Z26527
Water Level (mamsl)
1000
950
900
850
800
750
Oct-06 Jul-09 Apr-12 Dec-14 Sep-17 Jun-20 Mar-23 Dec-25
Simulated
Actual
Z26944
Water Level (mamsl)
1000
950
900
850
800
750
Oct-06 Jul-09 Apr-12 Dec-14 Sep-17 Jun-20 Mar-23 Dec-25
Simulated
Actual
Z26467
Water Level (mamsl)
1000
950
900
850
800
750
Oct-06 Jul-09 Apr-12 Dec-14 Sep-17 Jun-20 Mar-23 Dec-25
Simulated
Actual
Z26945
Water Level (mamsl)
1000
950
900
850
800
750
Oct-06 Jul-09 Apr-12 Dec-14 Sep-17 Jun-20 Mar-23 Dec-25
Simulated
Actual
Z28594
Water Level (mamsl)
1000
950
900
850
800
750
Oct-06 Jul-09 Apr-12 Dec-14 Sep-17 Jun-20 Mar-23 Dec-25
Simulated
Actual
Z13026
Water Level (mamsl)
1000
950
900
850
800
750
Oct-06 Jul-09 Apr-12 Dec-14 Sep-17 Jun-20 Mar-23 Dec-25
Simulated Actual
Actual
Z13027
Water Level (mamsl)
1000
950
900
850
800
750
Oct-06 Jul-09 Apr-12 Dec-14 Sep-17 Jun-20 Mar-23 Dec-25
Simulated Actual
Actual
Z13028
Water Level (mamsl)
1000
950
900
850
800
750
Oct-06 Jul-09 Apr-12 Dec-14 Sep-17 Jun-20 Mar-23 Dec-25
Simulated Actual
Actual

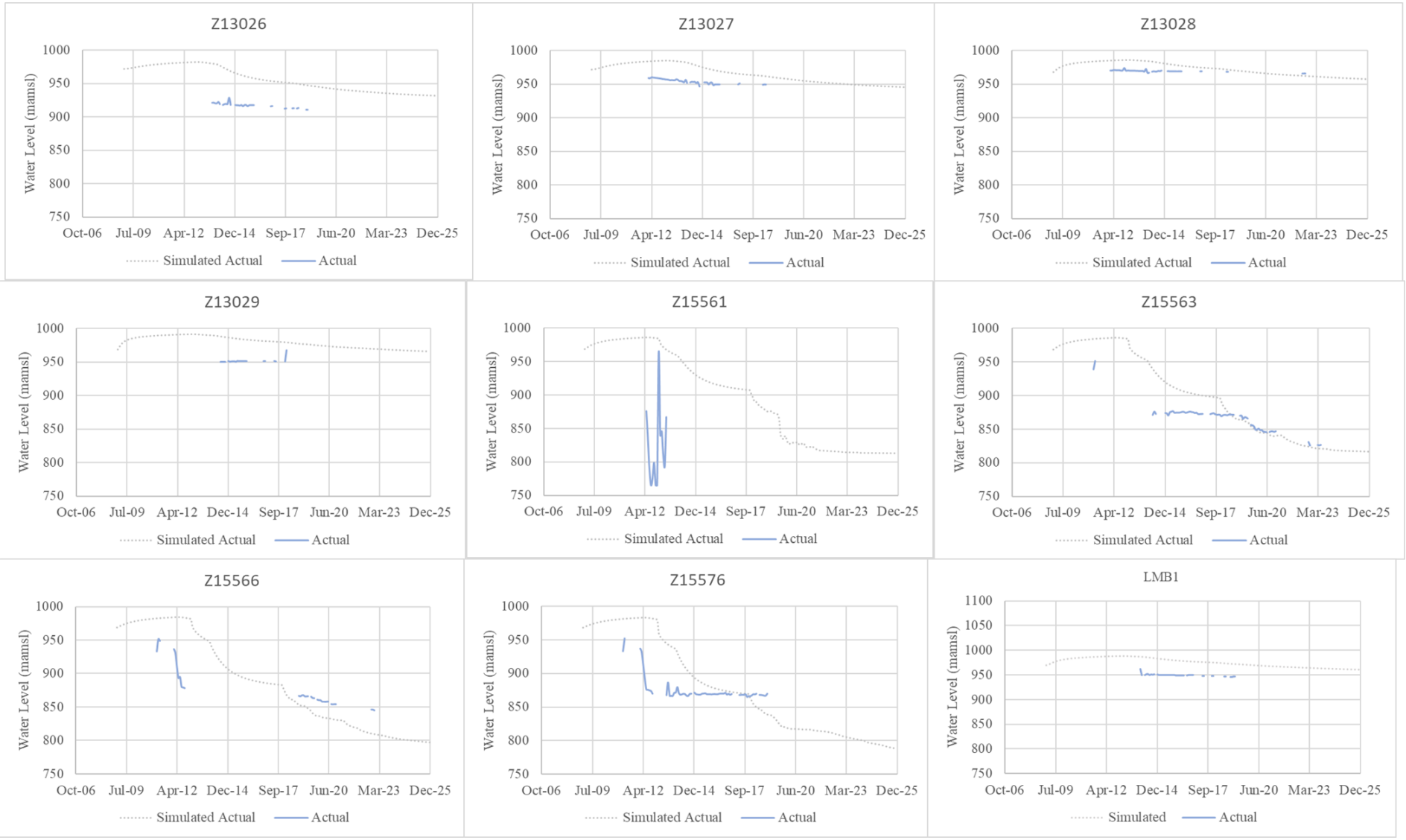
Z13026
Z13027
Z13028
Z13029
Z15561
Z15563
Z15566
Z15576
LMB1
Water Level (mamsl)
Oct-06 Jul-09 Apr-12 Dec-14 Sep-17 Jun-20 Mar-23 Dec-25
Simulated Actual
Actual
Simulated